

การป้องกันไฟโดยแผ่นยับซึมสำหรับแผ่นพื้นคอนกรีตเสริมกำลังด้วยพอลิเมอร์เสริมเส้นใย



นางสาวเฟรสก้า อีวีต้า อายุรานานดา

ศูนย์วิทยุทรัพยากร

วิทยานิพนธ์นี้เป็นส่วนหนึ่งของการศึกษาตามหลักสูตรปริญญาวิศวกรรมศาสตรมหาบัณฑิต

สาขาวิชาวิศวกรรมโยธา ภาควิชาวิศวกรรมโยธา

คณะวิศวกรรมศาสตร์ จุฬาลงกรณ์มหาวิทยาลัย

ปีการศึกษา 2552

ลิขสิทธิ์ของจุฬาลงกรณ์มหาวิทยาลัย

GYPSON-BOARD FIRE PROTECTION FOR FIBER REINFORCED POLYMER
STRENGTHENED CONCRETE SLABS



Ms. Frieska Evita Ayurananda

A Thesis Submitted in Partial Fulfillment of the Requirements
for the Degree of Master of Engineering Program in Civil Engineering

Department of Civil Engineering

Faculty of Engineering


Chulalongkorn University

Academic Year 2009

Copyright of Chulalongkorn University

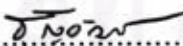
Thesis Title GYPSUM-BOARD FIRE PROTECTION FOR FIBER REINFORCED
POLYMER STRENGTHENED CONCRETE SLABS
By Ms. Frieska Evita Ayurananda
Field of study Civil Engineering
Thesis Advisor Associate Prof. Thanyawat Pothisiri, Ph.D.


Accepted by the Faculty of Engineering, Chulalongkorn University in Partial
Fulfillment of Requirements for the Master's Degree


..... Dean of the Faculty of Engineering
(Associate Professor Boonsom Lardhirunwong, Dr.Ing.)

THESIS COMMITTEE


..... Chairman
(Professor Thaksin Thepchatri, Ph.D.)


..... Thesis Advisor
(Associate Professor Thanyawat Pothisiri, Ph.D.)


..... Examiner
(Assistant Professor Naret Limsamphancharoen, Ph.D.)

เฟสเก่า อีวีดีอา อายุรานานคา : การป้องกันไฟโดยแผ่นยิปซัมสำหรับแผ่นพื้นคอนกรีตเสริมกำลังด้วยพอลิเมอร์เสริมเส้นใย. (GYPSUM-BOARD FIRE PROTECTION FOR FIBER REINFORCED POLYMER STRENGTHENED CONCRETE SLABS) อาจารย์ที่ปรึกษา: รองศาสตราจารย์ ดร.ธัญวัฒน์ โพธิศิริ, 93 หน้า.

พอลิเมอร์เสริมเส้นใย (Fiber reinforced polymer: FRP) ได้มีการใช้งานอย่างแพร่หลายในการเสริมกำลังโครงสร้างคอนกรีต อย่างไรก็ตามเนื่องจากอุณหภูมิแปรสภาพแก้วของ FRP ที่มีค่าต่ำ ซึ่ง ณ อุณหภูมิดังกล่าววัสดุจะเริ่มอ่อนตัวและสูญเสียกำลังในการส่งผ่านแรงสู่เส้นใยเสริมกำลัง จึงส่งผลให้เกิดการสูญเสียความสามารถในการรับน้ำหนักบรรทุกอย่างมีนัยสำคัญและอาจนำไปสู่การวิบัติของโครงสร้าง ดังนั้นการใช้งาน วัสดุดังกล่าวจึงจำเป็นต้องได้รับการป้องกันจากสภาพอุณหภูมิสูง เช่น กรณีเพลิงไหม้ เพื่อให้เกิดความปลอดภัย

การศึกษานี้ทำการทดสอบการป้องกันไฟของ FRP โดยระบบฝ้าเพดานแผ่นยิปซัมแบบแขวนซึ่ง ประกอบด้วยชั้นของแผ่นยิปซัม และใยหิน รวมทั้งโครงเคร่าโลหะ โดยดำเนินการทดสอบภายใต้ความสัมพัทธ์อุณหภูมิ-เวลา มาตรฐาน ISO 834 และนำผลการทดสอบมาเปรียบเทียบกับผลการวิเคราะห์เชิงตัวเลขด้วยระเบียบวิธีไฟไนต์เอลิเมนต์ เพื่อกำหนดรูปแบบของระบบฝ้าเพดานแผ่นยิปซัมแบบแขวนซึ่งมีอัตราการทนไฟ 2 ชั่วโมง ตามข้อกำหนดของกระทรวงฉบับที่ 60 พ.ศ.2529 โดยในการประเมินความสามารถในการทนไฟอาศัยโปรแกรมไฟไนต์เอลิเมนต์เชิงพาณิชย์ Abaqus/CAE

การทนไฟของระบบป้องกันไฟพิจารณาจากความเป็นฉนวน โดยใช้ค่าอุณหภูมิที่ผิวของ FRP เป็นเกณฑ์ ซึ่งพบว่าอัตราการทนไฟของระบบฝ้าเพดานที่ทดสอบ คือ 104 นาที และ 83 นาที สำหรับระบบที่ 1 และ 3 ตามลำดับ ทั้งนี้สำหรับระบบที่ 2 อาจถือได้ว่ามีอัตราการทนไฟสูงสุดหากระหว่างการทดสอบไม่เกิดความผิดพลาดในการทำงานของอุปกรณ์

จากการเปรียบเทียบระหว่างผลจากแบบจำลองและผลการทดสอบ พบว่าแบบจำลองโดย Abaqus/CAE สามารถทำนายอุณหภูมิภายในระบบฝ้าเพดานระหว่างการทดสอบได้ค่อนข้างแม่นยำ เมื่อกำหนดค่าคุณสมบัติของวัสดุที่ถูกต้องและแผ่นยิปซัมรวมทั้งวัสดุฉนวนยังคงอยู่ในที่

สาขาวิชา..... วิศวกรรมโยธา ลายมือชื่อนิสิต
ปีการศึกษา..... 2552 ลายมือชื่ออาจารย์ที่ปรึกษา

##4970727021: MAJOR CIVIL ENGINEERING

KEYWORDS : FIBER REINFORCED POLYMER/HEAT TRANSFER/FINITE
ELEMENT MODEL/ABAQUS/GYPSUM BOARD/LIGHT FRAME
CONSTRUCTION

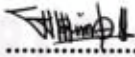
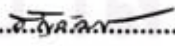
FRIESKA EVITA AYURANANDA: GYPSUM-BOARD FIRE
PROTECTION FOR FIBER REINFORCED POLYMER STRENGTHENED
CONCRETE SLABS. THESIS ADVISOR: ASSOC. PROF. THANYAWAT
POTHISIRI, Ph.D., 93 pp.

Fiber reinforced polymer (FRP) has been widely used for strengthening concrete structures. However, the glass transition temperature of FRP is low at which point the material may begin to soften and lose its capability to transfer loads to the fiber reinforcement. This can result in a significant deterioration of the structural load-bearing capacity which may lead to the structural failure. It is therefore essential to protect the material against the high-temperature conditions, e.g. fire, to ensure safety.

In this research, a series of fire tests are conducted on the gypsum-board suspended ceiling systems, which consist of gypsum-board and rock wool layers as well as metal frame sections, for FRP protection. The tests are conducted in accordance with the ISO 834 standard time-temperature relationship. The test results are compared with the numerical results obtained from the finite-element analysis to determine a 2-hr fire rated gypsum-board suspended ceiling system required by the Ministry of Interior Regulation 60, B.E. 2549. The fire resistance capability of the tested configurations of the gypsum-board fire protection systems for FRP material subjected to the time-temperature relationship according to ISO 834 was assessed by using a commercially available finite element computer program, Abaqus/CAE.

The fire resistance of the fire protection systems is assessed based upon their insulation by using temperatures on the FRP surface as the criteria. It was found that the fire resistance ratings for the tested gypsum board assemblies were 104 minutes and 83 minutes for assembly 1 and assembly 3, respectively. It is also reasonable to state that if there was no equipment malfunction during the fire test of assembly 2, the assembly would have the best fire rating.

Based on the comparison between the modeling results and the experimental results, it was found that the Abaqus/CAE model could predict the temperatures within the gypsum board assemblies during the fire test with reasonable accuracy, when the correct material properties were used and when the gypsum boards and insulation material remained in place.

Department: Civil Engineering Student's Signature 
Field of Study: ... Civil Engineering Advisor's Signature 
Academic Year: . 2009

ACKNOWLEDGEMENTS

Firstly, I would like to thank my advisor, Associate Professor Thanyawat Pothisiri, Ph.D. He always made his time available for me to discuss my research. Working with him has been an exhilarating experience. I also thank him for his constant guidance, help, and support in my academic life during my study at Chulalongkorn University. I consider it my great fortune and privilege to have the opportunity to work with him and to have excellent research environment.

I also express thanks to Professor Thaksin Thepchatri, Ph.D., and Assistant Professor Naret Limsamphancharoen, Ph.D. for being my examination committee. Their inputs, helpful suggestions, and comments on the proposal exam as well as on the thesis exam are invaluable for the next step of my research.

My thanks go to all lecturers in Department of Civil Engineering Chulalongkorn University, all my classmates, all Indonesian students in Thailand, my friends in Suksitnives International House, especially Cheryl Lyne Capiz my roommate, my friends under AUN/Seed-Net Scholarship, Indonesian people in Thailand, and all of my friends in Indonesia for their support, care, discussion and friendship. I also thank all officers working in Chulalongkorn University, especially in International School of Engineering for their kindness and help during my study. Many lecturers in the Department of Civil Engineering at Gadjah Mada University kindly helped me for coming to Chulalongkorn University. In this, I am especially thankful to Dr. Iman Satyarno and Dr. Djoko Sulistyono. My study at Chulalongkorn was partially supported by AUN/SEED-NET scholarship, which is gratefully acknowledged.

I am indebted and deeply thanks to my parents, Lilik Hermanto and Tutik Darmiati, my beloved brother and sister, Rezha Suryendra Kurniawan and Widha Rinjani Ajeng Kusuma, my cousins especially Dian Martha Indarti, my niece and nephews, for their years of unflinching love, caring and support. It is to them that I dedicate this thesis. Finally, I am foremost grateful to Allah SWT for this wonderful, magnificent, and amazing life; that He is the One who always accompanies me whenever I am down and loose my way.

CONTENTS

	Page
Abstract (Thai)	iv
Abstract (English)	v
Acknowledgements	vi
Contents	vii
List of Tables	x
List of Figures	xi
CHAPTER I INTRODUCTION	1
1.1 Background	1
1.2 Problem Statement.....	2
1.3 Objective of the Research.....	4
1.4 Scope of the Research	4
CHAPTER II LITERATURE REVIEW.....	5
2.1 Strengthening of Structures using Fiber Reinforced Polymer (FRP).....	5
2.1.1 Externally Bonded Reinforcement (EBR)	5
2.1.2 Externally Bonded Fiber Reinforced Polymer.....	6
2.2 Behaviour of FRP Strengthened Structures during Fire	7
2.2.1 The Effect of Elevated Temperatures on the Structural Strength and Bond between FRP and Concrete	8
2.2.2 Structural Behaviour of FRP Strengthened Structures Subjected to Standard Fire Tests	12
2.3 Fire Protection Schemes for FRP Strengthened Structures	13
2.3.1 Intumescent Coatings	13
2.3.2 Spray-on Systems	13
2.3.3 Board Systems	15
2.4 Gypsum Board Assemblies as Fire Protection Systems	16
2.4.1 Effect of Number and Thickness of Gypsum Boards	16
2.4.2 Effect of Insulations in the Cavity	17
2.4.3 Effect of Stud Type	17
2.4.4 Effect of Gypsum Boards Fall-off on the Fire Resistance Rating 17	17
2.5 Heat Transfer Finite Element Modeling of the Gypsum Board Assemblies.....	18
CHAPTER III COMPUTATIONAL MODEL.....	21

3.1	Computer Program.....	21
3.2	Modeling of the Geometry.....	23
3.3	Meshing (Discretization)	24
3.4	Material Properties.....	24
	3.4.1 Gypsum Plasterboard.....	25
	3.4.2 Steel Stud (Primary and Secondary Channels).....	29
	3.4.3 Insulation Material (Rock wool).....	31
	3.4.4 Summary of the Thermal Properties Used.....	31
3.5	Analysis Procedures and Boundary Conditions	35
	3.5.1 Heat Transfer Mechanism on Exposed and Unexposed Side	37
	3.5.2 Heat Transfer Mechanism on Cavity.....	38
	3.5.3 Heat Transfer through the Assembly.....	39
3.6	Post Processing and Results	39
CHAPTER IV EXPERIMENTAL INVESTIGATION		40
4.1	Specimen Description	40
	4.1.1 Reinforced Concrete Slabs	40
	4.1.2 FRP Strengthening System	41
	4.1.3 Gypsum Board Fire Protection System	43
	4.1.4 Summary of Specimens Tested	48
4.2	Testing Equipment.....	49
	4.2.1 Instrumentation.....	49
	4.2.2 Furnace	54
4.3	Testing Procedures.....	55
	4.3.1 Fire Exposure	55
	4.3.2 Performance Criteria.....	56
4.4	Observations after the Fire Tests	56
	4.4.1 Specimen-1.....	57
	4.4.2 Specimen-2.....	59
	4.4.3 Specimen-3.....	60
CHAPTER V RESULTS AND DISCUSSION.....		61
5.1	Experimental Results.....	61
	5.1.1 Thermocouples at level 1.....	61
	5.1.2 Thermocouples at level 2.....	64
	5.1.3 Thermocouples at level 3.....	66
	5.1.4 Thermocouples at level 4.....	68
	5.1.5 Thermocouples at level 5.....	70
	5.1.6 Thermocouples at level 6.....	73
	5.1.7 Thermocouples at all levels	75
5.2	Computer Modeling Results	77
5.3	Parametric study	81
	5.3.1 Effect of gypsum board conductivity	81
	5.3.2 Effect of convective coefficient.....	82
	5.3.3 Effect of the gap radiation.....	83
5.4	Conclusions and Recommendations.....	85

References 88

Biography 93



ศูนย์วิทยทรัพยากร
จุฬาลงกรณ์มหาวิทยาลัย

LIST OF TABLES

	Page
Table 3.1 Assemblies used in the computational model	24
Table 3.2 Gypsum board thermal properties.....	33
Table 3.3 Steel thermal properties	34
Table 3.4 Rock wool thermal properties.....	35
Table 4.1 Components of the gypsum board assembly	46
Table 4.2 Details of the tested gypsum board assemblies.....	48



ศูนย์วิทยทรัพยากร
จุฬาลงกรณ์มหาวิทยาลัย

LIST OF FIGURES

	Page
Figure 2.1 Relative strength variation of CFRP/epoxy bond with epoxy temperature (Gamage <i>et al.</i> 2005)	10
Figure 3.1 Phases in Abaqus/CAE finite element modeling (Abaqus Analysis User's Manual 2008).....	22
Figure 3.2 Description of the model assembly	23
Figure 3.3 Finite element used in Abaqus/CAE	25
Figure 3.4 Density of gypsum plasterboards relative to the ambient density vs. temperature.....	26
Figure 3.5 Thermal conductivity of gypsum plasterboards reported by various studies	27
Figure 3.6 Specific heat of gypsum plasterboard reported by various studies..	28
Figure 3.7 Thermal conductivity of steel as a function of temperatures.....	30
Figure 3.8 Specific heat of steel as a function of temperatures	31
Figure 3.9 Comparison of results from the computational model using various material properties and the experiment.....	32
Figure 3.10 Process in Abaqus/Standard in finding the solution of nonlinear problems.....	36
Figure 4.1 Cross section of the slab	41
Figure 4.2 Steel reinforcements on the slab	41
Figure 4.3 Wet Lay-Up GFRP strengthening system	43
Figure 4.4 Isometric view of the ProLine MAX concealed ceiling system (Siam Gypsum Industry Co., Ltd.).....	44
Figure 4.5 Bottom view of the specimen.....	45
Figure 4.6 Cross section I-I of the gypsum board assembly	45
Figure 4.7 Details of the fasteners used in the gypsum board assembly	46
Figure 4.8 Locations of thermocouples at the unexposed face of the gypsum board assembly.....	49
Figure 4.9 Locations of thermocouples within the cross section A-A.....	50

Figure 4.10	Locations of thermocouples within the cross section B-B	50
Figure 4.11	Locations of thermocouples within the cross section 1-1	51
Figure 4.12	Locations of thermocouples within the cross section 2-2	51
Figure 4.13	Locations of thermocouples at the FRP surfaces.....	52
Figure 4.14	Locations of thermocouples at the hanging rods	52
Figure 4.15	Specimen-1 with the thermocouples attached	53
Figure 4.16	Specimen prior to the fire test.....	53
Figure 4.17	Top view of the furnace	54
Figure 4.18	Furnace cross section.....	55
Figure 4.19	Standard Time-Temperature Curve (ISO 834 2002)	56
Figure 4.20	Actual time-temperature curves during the tests vs.....	57
Figure 4.21	Specimen-1 after the fire test	58
Figure 4.22	The GFRP strengthening system in specimen-1 after the fire test..	58
Figure 4.23	Specimen-2 after the fire test	59
Figure 4.24	Specimen-3 after the fire test	60
Figure 5.1	Time-temperature relationship at the surface of the exposed gypsum board facing cavity (T1) of assembly 1 during the fire test.....	63
Figure 5.2	Time-temperature relationship at the surface of the exposed gypsum board facing cavity (T1) of assembly 2 during the fire test.....	63
Figure 5.3	Time-temperature relationship at the surface of the exposed gypsum board facing cavity (T1) of assembly 3 during the fire test.....	64
Figure 5.4	Time-temperature relationship at the interface between the secondary channel and the primary channel (T2) of assembly 1 during the fire test.....	65
Figure 5.5	Time-temperature relationship at the interface between the secondary channel and the primary channel (T2) of assembly 2 during the fire test.....	65
Figure 5.6	Time-temperature relationship at the interface between the secondary channel and the primary channel (T2) of assembly 3 during the fire test.....	66

Figure 5.7	Time-temperature relationship at the interface between the primary channel and the unexposed gypsum board (T3) of assembly 1 during the fire test	67
Figure 5.8	Time-temperature relationship at the interface between the primary channel and the unexposed gypsum board (T3) of assembly 2 during the fire test	67
Figure 5.9	Time-temperature relationship at the interface between the primary channel and the unexposed gypsum board (T3) of assembly 3 during the fire test	68
Figure 5.10	Time-temperature relationship at the top of the unexposed gypsum board (T4) of assembly 1 during the fire test.....	69
Figure 5.11	Time-temperature relationship at the top of the unexposed gypsum board (T4) of assembly 2 during the fire test.....	69
Figure 5.12	Time-temperature relationship at the top of the unexposed gypsum board (T4) of assembly 3 during the fire test.....	70
Figure 5.13	Time-temperature relationship at the surface of GFRP (T5) of assembly 1 during the fire test	71
Figure 5.14	Time-temperature relationship at the surface of GFRP (T5) of assembly 2 during the fire test	72
Figure 5.15	Time-temperature relationship at the surface of GFRP (T5) of assembly 3 during the fire test	72
Figure 5.16	Time-temperature relationship at the hanging rod (T6) of assembly 1 during the fire test	73
Figure 5.17	Time-temperature relationship at the hanging rod (T6) of assembly 2 during the fire test	74
Figure 5.18	Time-temperature relationship at the hanging rod (T6) of assembly 3 during the fire test	74
Figure 5.19	Time-temperature relationship at all levels on assembly 1 during the fire test	75
Figure 5.20	Time-temperature relationship at all levels on assembly 2 during the fire test	76
Figure 5.21	Time-temperature relationship at all levels on assembly 3 during the fire test	76
Figure 5.22	Temperature distribution across the gypsum board assembly of computational model 1 at the end of the fire test.....	78

Figure 5.23 Comparison of results from the experiment and the computational model of assembly 1.....	78
Figure 5.24 Temperature distribution across the gypsum board assembly of computational model 2 at the end of the fire test.....	79
Figure 5.25 Comparison of results from the experiment and the computational model of assembly 2.....	79
Figure 5.26 Temperature distribution across the gypsum board assembly of computational model 3 at the end of the fire test.....	80
Figure 5.27 Comparison of results from the experiment and the computational model of assembly 3.....	80
Figure 5.28 Comparison of results from the experiments, the computational model (J1) and computational model-2 (J2) of assembly 1.....	81
Figure 5.29 Comparison of results from the experiments, the computational model (J1) and computational model-3 (J3) of assembly 1.....	82
Figure 5.30 Comparison of results from the computational model-3 (J3) vs. the computational model-4 (J4).....	83
Figure 5.31 Comparison of results from the experiment (exp), from the computational model that incorporated gap conduction only (J1) and from the computational model that incorporated gap conduction and gap radiation (J4).....	85

CHAPTER I

INTRODUCTION

1.1 Background

Deterioration of structures, particularly reinforced concrete structures, can generally be classified as natural deteriorations, accidental deteriorations or structural disorders. Examples of natural deteriorations are ageing of structures, corrosion of steel reinforcements, spalling of concrete, chemical aggressions, etc. The accidental deteriorations can be due to fires, impacts, explosions, overloads, earthquakes or other natural disasters while the structural disorders maybe the results of poor initial design, bad workmanship, change of service conditions (i.e. increase in loads) and change in regulations (the regulations may change due to the recent phenomena e.g. earthquake, tsunami, etc). Deteriorated structures can be structurally or functionally deficient.

In order to maintain the safety standards, one needs to either demolish the structures and construct new ones, restrict the use of the structures through limiting the imposed loads and continuously monitoring the structures, or strengthen or upgrade the structures. Strengthening or upgrading the structures can be advantageous compared to the other two choices since it is frequently more cost-effective and time-efficient to strengthen than to rebuild. Due to the increase in economical and environmental concerns, the current trend is to upgrade deteriorated and obsolete structures rather than replacing them with new buildings (Perera *et al*, 2006).

Structural strengthening is the process of upgrading the structural system of an existing building to improve its performance under existing loads or to increase the strength of structural components to carry additional loads (Alkhrdaji & Thomas, 2004). There are many techniques to strengthen existing buildings, such as span shortening, externally bonded reinforcement, external post-tensioning systems, section enlargement, etc. One of the most widely used techniques is externally bonded reinforcement. This technique was developed in 1967 by L'Hermite and Bresson using steel plates as external reinforcement (Tan, 2003). The externally-bonded steel plate technique is considered simple and economical since it provides minimal disruption of normal operation of the structures during ongoing construction work (Tan, 2003). However, the susceptibility of steel plates to corrosion and the difficulties of installing heavy steel plates particularly in confined space have been known as major drawbacks for this technique.

In 1987, the Swiss Federal Laboratories for Materials Testing and Research (EMPA) proposed partial substitution of externally bonded steel plates with fiber

reinforced polymer (FRP) strips. By the end of the 1980's, the externally bonded FRP systems had been used to strengthen and retrofit existing concrete structures around the world (Tan 2003). Fiber reinforced polymers are composite materials comprising a polymer matrix reinforced with glass or carbon fibers that were previously known mainly as the materials used in the automotive and aerospace industries. FRPs have several advantages over the traditional construction materials including very low self weight but high strength-to-weight ratio and also good corrosion resistance.

A rapid growth in the use of FRP systems for strengthening applications is followed by the need of the design guidelines in this area. The design codes and the guidelines for the field application of externally bonded FRP systems have been developed in Europe, Japan, Canada and the United States. Within the last 10 years, the Japan Society of Civil Engineers (JSCE), the Japan Concrete Institute (JCI) and the Railway Technical Research Institute (RTRI) published several documents related to the use of FRP materials in concrete structures (Tan 2003). In Europe, the Task Group 9.3 of the International Federation for Structural Concrete (FIB) published a bulletin on the design guidelines for externally bonded FRP reinforcement for reinforced concrete structures (FIB Bulletin 14, 2001). In Canada, Section 16 on "Fiber Reinforced Concrete" of the Canadian Highway Bridge Design Code was completed in 2000 (CSA S806-02) whereas the Canadian Standard Association (CSA) approved the code "Design and Construction of Building Components with Fiber Reinforced Polymers" (CSA S806-02). In the United States, the ACI 440.22R-02 Guide for the Design and Construction of Externally Bonded FRP Systems for Strengthening Concrete Structures was published in 2002 (Setunge *et.al*, 2002).

1.2 Problem Statement

Fiber reinforced polymers have been proved effective as alternative to steel plates for externally bonded flexural reinforcement of various concrete structures (Kachlakev *et al.* 2000; Tan 2003; Enochsson *et al.* 2006; Hosny *et al.* 2006; and Benjeddou *et al.* 2006). Nonetheless, the application of FRP strengthening systems to date has been limited only to the cases in which either fire resistance considerations are not critical factors in design or the existing structures are capable of supporting service loads without FRP during a fire event (ACI, 2002). This is because FRP composites are known for the low resistance against elevated temperatures.

The strength and stiffness properties of FRPs can degrade rapidly with the increasing temperatures. According to Saafi (2002), the tensile strength of the glass fibers, which is part of the FRP composite, at a temperature of 500 °C is reduced to about half of its value at room temperature; while the tensile strength of the carbon fibers seems to be unaffected by the elevated temperature up to about 1000 °C. However, the strength of the epoxy, which is the matrix of the FRP composite, decreases significantly when its temperature rises to the glass transition temperature,

T_g – the temperature below which the physical properties of amorphous materials vary in a manner similar to those of a crystalline phase (glassy state) and above which amorphous materials behave like liquids (rubbery state). As such, bonding within the FRP composites as well as bonding between concrete and the FRP composites, which rely on the shear properties of the epoxies, can be expected to be severely reduced at temperatures exceeding the glass transition temperatures.

Based on the experimental results published in the literature (William *et al.*, 2005; Aguiar *et al.*, 2007; and Gamage *et al.*, 2005), above the glass transition temperature, the structural performance of the FRP composites degrades rapidly. According to ACI (2002), the glass transition temperature (T_g) depends on the specific polymer matrix constituents, typically varying from 65 to 82 °C. Aguiar *et al.* (2007) and Gamage *et al.* (2005) showed that the T_g values for FRP composites with epoxy as polymer matrix range between 60 to 70 °C.

According to the experiments conducted by Gamage *et al.* (2005), without any fire protection system on the FRP strengthening structure the carbon fiber reinforced polymer (CFRP) strengthened concrete can only last for approximately 5.5 – 6 minutes. Once the average temperature within the epoxy adhesive reaches 70 °C, the bond between externally glued CFRP and concrete was lost and the CFRP strengthening system was no longer effective. Thus, to maintain the integrity between CFRP strengthening system and concrete, fire protection system must be designed to keep the epoxy temperature under 70 °C.

William *et al.* (2005) have conducted an experimental and numerical study on fire protection for FRP strengthening slab exposed to fire. Various combinations of cementitious spray-applied plaster and intumescent coating are used as fire protection systems for FRP strengthened slabs. The experimental results show that a 38 mm thick fire protection system yields a 43-minute fire resistance rating. It has also been concluded from the numerical study that a 50 mm thick fire protection system would give a 90-minute fire resistance rating. Since the insulation thickness greater than 50 mm is impractical in many field applications, the maximum fire resistance rating that can be achieved using this fire protection system is only 90 minutes. Kexu *et al.* (2007) and Gamage *et al.* (2005) have used a 50 mm thick cementitious spray-applied fire protection system and achieved a 70-minute fire resistance rating.

According to the regulations of Thailand's Ministry of Interior (Thailand's Ministry of Interior, 2006), the required fire resistance ratings are generally between 2 and 3 hours for building components, depending upon the structures' use and occupancy. Thus far, there have not been any fire protection systems that can ensure these periods of integrity for FRP strengthening system during the event of fire.

1.3 Objective of the Research

The objective of this research is to determine the most effective configuration of gypsum-board fire insulation systems for FRPs that can satisfy a 2-hour fire resistance rating through numerical and experimental studies.

1.4 Scope of the Research

For the preliminary study, the heat transfer analysis for various gypsum-board fire insulation systems subjected to the ISO 834 standard fire curve is conducted using a commercial finite element program ABAQUS. The criterion used to determine the fire resistance rating is expressed in terms of a critical temperature at the epoxy adhesive to maintain the effectiveness of the FRP strengthening system. Based on the experimental works of Gamage *et al.* (2005), the critical temperature for determining the fire resistance rating in this research is set to 70 °C, the temperature at which the epoxy adhesive starts to debond.

To investigate the actual thermal insulation of the gypsum-board fire protection systems, a series of non-loadbearing fire tests is conducted. The slab specimens are designed based on the minimum requirements to ACI 318 and ACI 216, with the dimensions based on the dimension of the furnace being used. The glass fiber reinforced polymer (GFRP) sheets are installed to the soffit of the slab using the wet lay up method. Note that for the economic reason GFRP is selected for the current study over CFRP since our primary focus is on the thermal behaviour, rather than the structural behaviour, of the system. The gypsum-board steel-stud assemblies used as the fire protection systems for the tests are designed with the configurations of the gypsum boards that have been identified to be able to achieve a fire resistance rating of at least 2 hours based on the results from the preliminary analysis using ABAQUS.

CHAPTER II

LITERATURE REVIEW

2.1 **Strengthening of Structures using Fiber Reinforced Polymer (FRP)**

The load-carrying capacity and serviceability of structures tend to diminish with time due to structural deteriorations. Financial-wise, strengthening or upgrading structures is usually a more preferable choice compare with complete replacement in order to maintain the safety standards of the structures. There are many techniques to strengthen existing buildings; one of the most widely used techniques is the externally bonded reinforcement.

2.1.1 Externally Bonded Reinforcement (EBR)

Externally bonded reinforcement, developed in the late 1960's, is a strengthening technique where epoxy-bonded steel plates are attached to the tension face of the deteriorated structures in order to increase the load bearing capacity. This technique was first used to strengthen concrete beams in an apartment complex in Durban, South Africa, in 1964, where part of the reinforcing steel in the building had been accidentally omitted during construction (Tan 2003). The strengthening or upgrading of reinforced concrete beams using bonded steel plates has since been proven in the field to increase the load-carrying capacity of the members under service loads for ultimate conditions and also to control flexural deformations and crack widths (Hollaway and Leeming 2001). It is recognized to be a simple and rapid strengthening technique because it provides minimal disruption of normal operation of the facility during ongoing construction work. When completed, the changes to the overall dimensions of the structural sizes are negligible (Tan 2003).

Despite the fact that the externally bonded steel plate has been shown to be a successful strengthening technique in practice, it has some drawbacks. One is that the steel plates are often heavy to mount at work sites. When the bonding is done upside down, external pressure must be applied on the steel plates and scaffolding must be installed during the curing of the adhesive. Another drawback is the risk of corrosion of the steel plates used. Furthermore steel plates might need lapped butt joints due to limited transportation length and may be difficult to apply to the curved surfaces (Carolin 2003). These drawbacks have prompted engineers to search for a better material that has the same or better strengthening specifications as steel but without the problems inherent. Recently, fiber reinforced polymer (FRP) composites have been considered as a contender to replace steel (Tan 2003).

2.1.2 Externally Bonded Fiber Reinforced Polymer

Fiber reinforced polymer (FRP) is a composite, heterogeneous, and anisotropic material which is formed through the physical combination of two major components, fiber reinforcements and resin. The fibers provide strength and stiffness to the composite and act as the main load carrying component, while the resin binds the fibers into a firm matrix, protects fibers from environmental and mechanical damage, and distributes the load among them. The most commonly used fibers in the construction industry are the carbon, aramid and glass fibers. The resin material is generally a polymer, such as polyester, vinyl ester or epoxy. FRP composite materials date back to the early 1940s, in the defense industry, particularly for use in aerospace and naval applications. In the mid-1950, FRP composite products were used to reinforce concrete structures and since then the composite has gained popularity and is considered as an alternative construction material (Tang, 1997).

The application of FRP materials for retrofitting and strengthening existing structures have been rapidly growing all around the world. The externally bonded FRP system was first investigated at the Swiss Federal Laboratory for Material Testing and Research (EMPA) in 1984 through testing of flexural strengthened reinforced concrete (RC) beams. Numerous experimental studies have been conducted by researchers worldwide ever since. Due to the results from those extensive researches, the strengthening technique using adhesive bonded FRPs has been established as an effective method applicable to many types of concrete structures such as columns, beams, slabs, and walls (Carolin 2003). FRPs can be adhered to the tension side of structural members (e.g. slabs or beams) to provide additional flexural strength (Hutchinson 1998; Alkhrdaji and Nanni 1999; Kachlakev and McCurry 2000; Mosallam and Mosalam 2003; Tan 2003; Benjeddou *et al.* 2006; and Enochsson *et al.* 2007). FRPs can also be adhered to web sides of joists and beams or wrapped around columns to provide additional shear strength (Kachlakev and McCurry 2000). Wrapping FRP systems completely around certain types of compression members can confine those members, leading to increases in axial compression strengths (Al-Salloum and Almusallam 2002).

The FRP strengthening technique poses a number of potential advantages over steel, such as:

- *High strength:* FRP composites have higher ultimate strengths compared to steel. The tensile strength of FRP can exceed 3000 MPa while the tensile strength of reinforcing steel is only up to 400 MPa.
- *Handling and transportation:* The FRP composite materials used for strengthening are very light and easy to handle. In comparison to steel plate bonding where plates no longer than 2-3 meters can be handled, almost infinitely long plates or sheets of FRPs can be handled. In addition, no overlap plating is

necessary. Also, compared to traditional concrete overlays or shotcrete, much less material has to be transported when the FRP strengthening system is used.

- *Durability and maintenance:* FRP composites have especially exceptional durability, long term fatigue properties, and do not normally need to be maintained over time due to the corrosion resistance feature.
- *Thin strengthening layer:* In many situations, thin strengthening layers can be advantageous. Thin layers will not change the dimension of the existing structure and can also be combined with thin concrete overlays or surface-protecting materials.
- *Construction time:* Time is always a critical factor in the construction industry. If time can be reduced, money can be saved. FRP strengthening systems can often be installed during short periods without stopping the traffic or closing the buildings, and little time is needed for hardening of the bonding agents.
- *Pre-stressing possibilities:* During the last few years, FRP products have been introduced to the market that can be pre-stressed in combination with bonding. This gives a higher utilization of the strengthening products, at the same time reducing cracks, and increasing the yield load of the existing steel reinforcement. It is also possible to use pre-stressing to increase the shear capacity of concrete structures.
- *Design:* The possibility to optimize the FRP materials in the direction most needed is a benefit for design. FRP composites can be formed into complex, desirable shapes.
- *Cost:* Even though the cost of the FRP material is higher than those of conventional materials, but for application in the strengthening of the structures where the material cost is but one consideration and may be only a small portion of the total cost including labour cost and loss due to interruptions to services, FRP composites often provide the most cost-effective solution overall (Hollaway and Leeming 1999).

With all those benefits FRPs have over steel, it is not surprising that the interest in FRPs as externally bonded reinforcement has been considerably increased. Even though so, the majority of field applications of this system have been only in bridges and other exterior structures. One of the impediments to the use of FRP composites in all construction area is their susceptibility to degradation due to exposure to elevated temperatures.

2.2 Behaviour of FRP Strengthened Structures during Fire

To date, FRP reinforcement and strengthening systems have been used predominantly in structures either where fire resistance considerations are typically

not critical factors in design or where the existing structure is capable without FRPs on supporting design loads during a fire event. In case where strict fire code regulations apply, FRP systems are not being used to their full potential or their structural effectiveness should be ignored during fire (ACI 440 2002).

As mentioned previously, the FRP composites consist of two different elements: fiber reinforcement and resins. The fiber reinforcements are manufactured by heat treatment processes called carbonization and graphitizing. In carbonization, the fibers are heated up to 1500-2000°C to obtain high tensile strength, while in graphitizing the fibers are heated up to 2500-3000°C to obtain high modulus of elasticity. Due to the manufacturing process, the fiber reinforcement itself has no problem withstanding high temperatures. On the other hand, the resin behavior in high temperatures depends on the glass transition temperature (T_g). T_g is the temperature at which resins will soften and lose its ability to transfer shear loads among the fibers and subsequently between the FRP composites and concrete surface. The glass transition temperature (T_g) of thermoset resins; the type of resin that is usually used in construction, is determined by its cure temperature. Epoxy resins used in strengthening systems is usually cured in ambient temperature, and has T_g approximately 140°F (60°C). At elevated temperatures (i.e., above the T_g of the polymer matrix/adhesive) the mechanical properties of the polymer matrix will reduce, which leads to a reduction in the ability of the matrix to transfer forces between the fibers. Consequently, the externally-bonded FRP materials can be expected to display severe reductions in strength, stiffness, and bond properties at elevated temperatures. In order to understand this topic better, brief explanations from some previous research works on the behavior of FRP strengthened structures exposed to fire loading are presented below.

2.2.1 The Effect of Elevated Temperatures on the Structural Strength and Bond between FRP and Concrete

Epoxy adhesives used to form the bond between FRP and concrete are highly sensitive to temperature variations. Exposure to elevated temperatures will lead to rapid and severe deterioration of the FRP-concrete bond, resulting in delamination of the FRP sheet and loss of its effectiveness. There is only a few data available in the literature about the variation of thermal and mechanical properties of FRP-epoxy bond on concrete under elevated temperatures.

Gamage *et al.* (2005) have conducted single shear tests under transient heat on nine carbon-fiber reinforced polymer (CFRP) strengthened concrete specimens in order to study the influence of temperature on the bond strength between CFRP and concrete. The main outcome of this series of tests was the variation of failure loads at different epoxy temperatures. The relative bond strength variation with the epoxy temperature can be seen in Figure 2.1. The epoxy relative strength is expressed as a

ratio of the epoxy strength at the testing temperature to that at the room temperature. Besides the failure load of the specimens, the failure mechanisms are also observed in these tests. It has been observed that at low temperatures (epoxy temperature $<50^{\circ}\text{C}$), CFRP strengthened concrete specimens failed at similar loads as in room temperature and the combination of concrete rupture and adhesive failure has been noted as the failure mechanism. This indicates that the adhesive bond strength between the CFRP sheet and the concrete is not adversely affected by the temperature as long as the epoxy temperature is maintained below 50°C . From the experimental results it can also be seen that when the epoxy temperature exceeds 50°C the bond strength of CFRP strengthened concrete member can be adversely affected by the increase in the epoxy temperature and rapid strength loss appears when the epoxy temperature ranges between 60°C and 70°C . It has also been observed that when the epoxy temperature exceeds 60°C , the failure mechanism changed to the peeling off of the CFRP sheet.

Aguiar *et al.* (2007) have tested CFRP strengthened RC beams and reference (unstrengthened) RC beams. The specimens were subjected to either three-point bending tests or compressive shear tests. From the three-point bending test results, it can be noted that with the increase in temperature, the bending moment vs. deformation curves of the strengthened beams became closer to the curves of the beams without strengthening systems which means that the flexural load capacity of the CFRP strengthened beams decreased with the increase of the severity of the thermal exposure and that the efficiency of the CFRP strengthening system tended to vanish. It is also observed that when the specimens were exposed to the temperatures below T_g ($<60^{\circ}\text{C}$), the CFRP strengthened beams exhibited delamination caused by failure of the cover concrete. But when the aggressiveness of the thermal exposition was near or exceeded T_g , debonding occurred at the concrete-adhesive interfaces was observed. From the compressive shear test results, it can be stated that the epoxy resin maintained all of its properties up until the temperature reached T_g . As the temperature exceeded T_g , the failures occurred predominantly at the adhesive and the failure stress decreased significantly. The shear strength of the specimens after exposure to 60°C ($T_g = 60^{\circ}\text{C}$) was 61% of that obtained at 40°C while the shear strength of the specimens after exposure to 80°C ($>T_g$) was 30% of that obtained at 40°C . Based on the results obtained, it is possible to conclude that the epoxy adhesive bond properties deteriorate rapidly with exposure to high temperatures especially when it exceeds T_g of the adhesive.

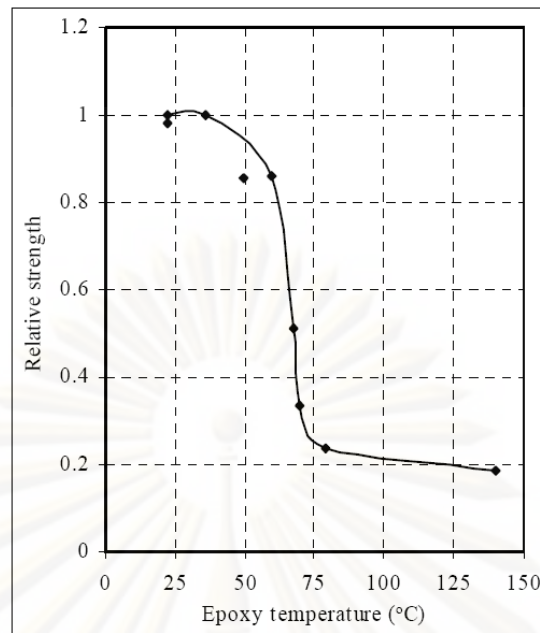


Figure 2.1 Relative strength variation of CFRP/epoxy bond with epoxy temperature (Gamage *et al.* 2005)

Klamer *et al.* (2008) have presented the experimental results of Blontrock (2003) in order to study the effect of temperature on concrete structures strengthened with externally bonded FRPs. Klamer *et al.* (2008) mentioned that Blontrock (2003) investigated the effect of temperature on concrete specimens strengthened with externally bonded CFRP laminates by carrying out double-lap shear tests. From the experimental results, it was found that the increasing temperature up to T_g of the adhesive resulted in the increase in the failure load. But further increasing the temperature resulted in a decrease of the failure load and a changed type of failure. Around the temperature value of T_g , the failure mode changed from failure in the concrete adjacent to the concrete-adhesive interface to failure exactly at the interface, without leaving any concrete attached to the adhesive after debonding. The change in failure mode was expected to be the main cause of the decrease in the failure load above the glass transition temperature. Klamer *et al.* (2008) have also investigated the influence of temperature on full-scale beams strengthened with externally bonded CFRP. The beams were tested at three different temperatures; at 20°C as a reference, at 50°C, which was below the glass transition temperature of the adhesive ($T_g = 62^\circ\text{C}$) and at 70°C, which was above T_g of the adhesive. From the experimental results it was found that for all the beams tested at 50°C, no change in the type of debonding was observed compared to the beams tested at 20°C. The failure load was also not significantly affected at 50°C, compared to the room temperature. At 70°C, the type of failure changed from bond failure in the concrete to failure where significantly less concrete remained attached to the adhesive (failure at the adhesive). The failure load at 70°C was significantly lower compared to that at room temperature. Klamer *et al.* (2008) recommended that there is no need to take the effect of the temperature into

account for the design of a FRP-strengthened structure as long as the temperature stays below 50°C ($\approx T_g - 10^{\circ}\text{C}$). Strengthening of structures at temperatures above this temperature should be avoided, due to the possible change in the type of bond failure and the corresponding reduced bond strength. At these temperatures, extra precautions should be taken to avoid premature debonding.

Leone *et al.* (2009) have conducted double face shear tests on FRP strengthened concrete members under varying temperatures in order to determine the effect elevated service temperatures have on the bond performance of the structure. From the experimental results obtained at $T=20^{\circ}\text{C}$, $T=65^{\circ}\text{C}$ and $T=80^{\circ}\text{C}$ for the different types of FRP strengthening systems, it can be concluded that in all cases a decrease of the bond strength can be observed for elevated temperatures beyond T_g . In particular, at 80°C the bond strength decreases by 54% in the case of specimens strengthened with CFRP sheets, 72% for GFRP sheets and 25% for CFRP laminates with respect to that at the room temperature. It was also shown that the type of failure changed with the increasing test temperature. Specimens tested at $T = 50^{\circ}\text{C}$ showed cohesion failure within the concrete, while at the $T = 80^{\circ}\text{C}$ an adhesion failure at the interface was observed. The reason for this change, according to Leone *et al.* (2009), is that at temperatures similar or higher than T_g the adhesion strength drops below that of the concrete, causing the bond failure at the FRP-adhesive interface.

From these researches, it can be concluded that the flexural strength and the shear strength of the FRP strengthened structures are adversely affected by the increasing temperature and that the magnitude of the strength loss is governed by the temperature of the adhesive. As long as the adhesive temperature is less than its glass transition temperature (T_g), the strength (failure load) is not significantly affected by the elevated temperatures. But when the adhesive temperature exceeds its T_g , rapid strength loss will be observed. It can also be concluded that there are two types of failure mechanism; failure within the concrete and failure in adhesive. Failure within the concrete, either flexural failure or shear failure, is quite similar to the failure of unstrengthened RC members, taking the FRP as additional reinforcement into account. Failure in the adhesive, also called the bond failure at the FRP-adhesive interface, is due to the fact that the adhesion strength drops below that of the concrete. When the adhesive temperature is less than T_g , the FRP strengthened structure usually exhibit delamination caused by failure within the concrete. When the temperature exceeds T_g , the failure mode changes to that at the FRP-adhesive interface. Overall, it can be concluded that the adhesive temperature, especially its glass transition temperature (T_g), has an important role in determining the failure modes and also the failure loads of the FRP strengthened structures subjected to elevated temperatures. According to ACI 440 (2002), the value of the glass transition temperature can vary depending on the polymer chemistry, but a typical range for field-applied resins and adhesives is 140°F to 180°F (60°C to 82°C).

2.2.2 Structural Behaviour of FRP Strengthened Structures Subjected to Standard Fire Tests

Very few test results on the structural behaviour of concrete members strengthened with externally bonded FRP materials during fire are available in the literature. According to ACI 440 (2007), the initial research in this area was performed in Europe by Deuring (1994), who demonstrated the extreme susceptibility of externally bonded FRP flexural strengthening systems to fire.

More recently, Barnes and Fidell (2006) have tested RC beams and CFRP strengthened RC beams by either four-point bending or cellulosic fire and four-point bending. A visual examination of the specimens showed that the adhesive and the resin component of the CFRP plate had been destroyed by the fire although the carbon fibers were still intact. From the experimental results it can be concluded that after being exposed to cellulosic fire, the CFRP strengthened RC beams had effectively the same average strength as the control (unstrengthened) beams. This means that the CFRP strengthening system is no longer effective after the structures were exposed to cellulosic fire. From observations it can also be concluded that the plane of failure is within the concrete cover, which is reasonable since the CFRP strengthening system deteriorated after the structure was exposed to fire.

The National Research Council Canada (NRCC) has investigated the behavior of FRP wrapped RC columns subjected to a standard time-temperature fire curve and concentric axial loading, as prescribed by ASTM E119 (Chowdhury *et al.* 2007). The experimental results showed that the failure loads of the FRP strengthened RC columns are similar to that of the unstrengthened ones. It was also observed that the unprotected FRP strengthening system burned within minutes of fire exposure and completely debonded from the column in less than 30 minutes. From the literature it can be concluded that the FRP strengthening system will be destroyed within minutes once they are exposed to fire, leading to the ineffectiveness of the FRP strengthening system during fire.

From the literature review, we have learned that the FRP strengthening system is susceptible against elevated temperatures and when leaving unprotected, it will be destroyed within minutes in the early event of fire. We have also learned that the most sensitive part of the FRP strengthening system is the adhesive/epoxy. The effectiveness of the FRP strengthening system is governed by the temperature of the adhesive/epoxy, particularly its glass transition temperature (T_g). Thus, to ensure the effectiveness of the FRP strengthening system, throughout the event of fire, fire protection systems must be applied to restrain the epoxy temperature from exceeding its T_g .

2.3 Fire Protection Schemes for FRP Strengthened Structures

Since there has not been any passive fire protection system that is specifically designed to protect the adhesive temperature, the researchers try to incorporate steel fire protection systems for this purpose. There are many passive fire protection systems available to reduce the rate of temperature increase in the steel structures exposed to fire. Some of the commonly used fire protection methods are briefly described below.

2.3.1 Intumescent Coatings

Intumescent coating is a special paint material that swells up into a thick charry mass when it is heated (Buchanan 2001). When temperatures reach about 200°C, the paint will swell to black foam about 2.5 cm thick, containing millions of tiny closed, fire-resistant cells forming a barrier to retard rapid heating of the material's surface. This method does not increase the overall dimensions of the member, can be applied quickly, and allow the protected members to be seen directly without any covering other than the paint. But these types of coatings require blast cleaned surface, a priming coat and are more expensive compared to other passive fire protection systems.

Stratford *et al.* (2009) have investigated the performance of an externally bonded CFRP plate strengthened concrete ceiling, protected using an intumescent coating and subjected to real compartment fires. After the tests it was observed that the FRP strengthening system had completely separated from the concrete and the matrix polymer had burnt away, leaving exposed concrete on the ceiling and a bundle of exposed fibers on the floor. The FRP strengthening system debonded from the ceiling around 10 minutes after the start of the fire. Stratford *et al.* (2009) concluded that the intumescent coating fire protection system was ineffective due to its activation temperature (the temperature at which it expands to form an insulating layer) that is higher than the glass transition temperature of the adhesive. The intumescent coating can be more useful if it is used with other fire protection systems, such as spray-on systems.

2.3.2 Spray-on Systems

Spray-on materials are usually cement-based with some form of glass or cellulosic fibrous reinforcement to hold the material together (Buchanan 2001). This form of passive fire protection is generally applied directly to the surface of the structure. This is a relatively low cost system and can be applied rapidly. However due to its undulating finish, it is usually preferred to be applied on surfaces which are hidden from the view. Briefly described below are some researches that tried to use the spray-on system as the fire protection method for FRP strengthened structures.

Gamage *et al.* (2005) have used a spray-on fire resistance coating, called Vermitex-TH, as the passive fire protection system on CFRP strengthened concrete blocks. The failure temperature of epoxy (73.6°C) was taken from the previous shear test results of the non-insulated identical specimens tested under uniformly increasing temperatures. Based on the experimental results, failure times under the experimental temperature conditions were finalized at 67.8 minutes and 70 minutes for the two specimens tested. Gamage *et al.* (2006) have used the strand7 finite element analysis program to develop a numerical model for heat transfer analysis using data from these experiments. The parametric studies performed using this program showed that the 2-hour and 3-hour fire resistance ratings can be achieved using 55-mm and 77-mm thick Vermitex-TH layers, respectively. But these results are inefficient since the insulation thickness greater than 50- mm is considered impractical in many field applications.

Barnes and Fidell (2006) have insulated CFRP strengthened concrete beams with a proprietary cementitious fire protection of between 15 and 20 mm thickness with supplemental bolt fasteners. The beams were placed in a furnace such that the beam soffits formed the roof of the furnace, were subjected to cellulosic fire for a time period of 1 hour and were loaded after the fire test. The temperature at the concrete-CFRP interface reached a maximum of 140°C, well above the T_g value of 81°C, although not sufficiently high to destroy the adhesive, as determined by visual inspection. Even though most of the fire protection had dropped off, the CFRP plate remained bonded to the beam along half of the beam length. Based on the four-point bending test results, it was shown that the fire protected unbolted CFRP strengthened beams had effectively the same average strength as the unstrengthened beam, showing that although the CFRP appeared to be intact but the bond was destroyed and no strength benefit was obtained. This means that the fire protection schemes used is not sufficient. However when comparing the midspan deflection of protected and unprotected beams, the fire protection appeared to provide a slight increase in stiffness.

Kexu *et al.* (2007) have protected CFRP strengthened RC beams using 50 mm thick fire resistance coating. Based on the experimental result, with the critical temperature to be regarded as 100°C, it was concluded that the proposed fire protection system could protect the adhesive only up to 73 minutes.

Other proprietary systems have been developed to protect the externally bonded FRP strengthening systems and have been tested on columns, beams and slabs (Bisby *et al.* 2005; Williams *et al.* 2006; Kodur *et al.* 2007). The researchers used the combination of cementitious spray-on materials and intumescent coatings. The glass transition temperature (T_g) used are 71°C and 93°C, depending on the type of the adhesives. The best fire resistance rating, using T_g as the failure temperature, for the columns, beams and slabs are 118 minutes, 52 minutes and 104 minutes, respectively.

2.3.3 Board Systems

The boards that are used as the fire protection system are available in vermiculite, mineral wool, calcium silicate, plasterboards or combinations of those materials. The boards are cut and fitted to the structures on site using mechanical methods such as screws, straps and lightweight angles or are glued and pinned. The board systems have the advantages that they are easy to install in a dry process, and easy to finish with decorative materials. The number and thickness of layers can be easily adapted to the particular application (Buchanan 2001). Briefly described below are some of the previous researches on the FRP strengthened structures protected using the boards systems.

Blontrock *et al.* (2001) have conducted fire tests on concrete slabs strengthened with FRP sheets and protected with a variety of gypsum board and mineral wool insulation schemes. The slabs were held under constant load in the furnace. As the temperature increased, central deflection was monitored and where a sudden increase in deflection occurred it was assumed that the interaction between the FRP sheet and the concrete was lost. According to the experimental results, this occurred at time periods ranging from 24 to 55 minutes, when the temperature of the adhesive reached a value between 47°C and 69°C. It was concluded that the application of thermal protection for the externally strengthening system was needed to maintain the interaction between the externally strengthening system and the concrete.

Stratford *et al.* (2009) have investigated the performance of an externally bonded CFRP plate strengthened concrete ceiling subjected to real compartment fires. The FRP was protected using gypsum boards, alongside the FRP that was left unprotected. After the tests it was observed that the gypsum-board protection was still fully intact, with no visible holes in the protection or signs that the fire had penetrated it and the CFRP plate was found to be fully bonded to the concrete and there was no visual damage to either the plate or the adhesive. For the unprotected specimen, the FRP strengthening system had completely separated from the concrete and the matrix polymer had burnt away, leaving exposed concrete on the ceiling and a bundle of exposed fibers on the floor. In all cases the adhesive temperature rapidly exceeded its T_g (65°C, as given by the manufacturer) in less than a minute after flashover, with the gypsum board protected specimen having the longest time. This means that the gypsum boards can protect the FRP strengthened structures, even though for only few minutes.

Under Thailand's Ministry of Interior regulations (Thailand's Ministry of Interior, 2006), the required fire resistance ratings are generally between 2 and 4 hours for building components, depending upon the structures' use and occupancy.

Thus far, there has not been any fire protection system that can ensure these periods of integrity for FRP strengthening systems during the event of fire. In this research, we attempt to use the gypsum board system as the fire protection method for FRP strengthened slabs due to the flexibility of the drywall construction. The type and thickness of the gypsum boards and the framing (stud) configurations can be modified in order to achieve specific performance requirements.

2.4 Gypsum Board Assemblies as Fire Protection Systems

Gypsum boards have been used in the building industry worldwide (Wakili *et al.*, 2007) because of the ease of fabrication and application, environmental friendliness and the energy consuming (endothermic) dehydration process taking place when subjected to fire. A common fire barrier system, usually referred to as the drywall construction, consists of two or more gypsum boards fixed on one or two sides of the lightweight construction such as steel studs or wood studs, while the cavity in between is filled with insulation materials or left empty. The drywall construction is an efficient and cost effective method of achieving a flexible fire protection system within commercial or residential buildings. The flexibility of the drywall construction is its ability to specify the type and thickness of the linings and the framing configuration in order to achieve specific performance requirements, such as appearance of the finished structure, impact resistance, water resistance, sound control or fire resistance rating, while maintaining a light form of construction (Jones 2001). In order to design the best drywall construction configuration that can protect the adhesive temperature during the event of fire, we need to understand several parameters influencing the fire resistance rating of the gypsum board assemblies

2.4.1 Effect of Number and Thickness of Gypsum Boards

Several researchers have investigated the effect of number of gypsum boards on the fire resistance rating of the assemblies (Sultan and Kodur 2000; Sakumoto *et al.* 2003; Benichou and Sultan 2003; Benichou and Sultan 2004). These studies concluded that increasing the number of the gypsum boards or the thickness of the gypsum boards resulted in the increase in fire resistance rating. Benichou and Sultan (2003) have reported that increasing the number of gypsum boards, from one to two layers, would increase the fire resistance rating for wood joist and wood I joist by 78% and 71%, respectively. Sultan and Kodur (2000) have similarly reported that adding one more layer of gypsum boards on the exposed side can increase the fire resistance rating of the assembly by 55%. Sultan and Kodur (2000) have also reported that the thickness of the gypsum boards did not play a significant role in the fire resistance rating. Elewini *et al.* (2007) have concluded that adding a second layer of

gypsum board increased the protection time of the time, causing the increase in the fire resistance rating.

2.4.2 Effect of Insulations in the Cavity

The effect from the installation of insulation materials in the cavity of the gypsum board assembly is inconclusive. Benichou and Sultan (2003) and Sultan *et al.* (1998) have reported that the installation of glass fiber on floor assemblies reduced the fire resistance rating by 8% but when installed on wall assemblies, it had no effect on the fire resistance rating. Meanwhile the installation of rock fiber increased the fire rating by 54% but the installation of cellulose (wet sprayed on the exposed gypsum board surface facing cavity) decreased the fire rating by 8%. Elewini *et al.* (2007) have reported that the installation of either glass fiber, rock fiber or cellulose insulation on the floor assemblies accelerated the fall-off time of the gypsum board assemblies which resulted in the reduction of the fire resistance rating. These various results from the effect of the installation of insulation materials in the cavity prompt for further investigation.

2.4.3 Effect of Stud Type

Benichou and Sultan (2003) have reported that the type of studs, either wood or steel, is insignificant for assemblies with 2 layers of gypsum boards on each side. Also the effect of stud joist spacing on the fire resistance rating is insignificant.

2.4.4 Effect of Gypsum Boards Fall-off on the Fire Resistance Rating

Sakumoto (2003) has stated that the fire resistance rating of walls and floors thermally insulated by gypsum boards is largely affected by the falling off of the gypsum boards. Once the gypsum boards fall off, the temperature of light gauge steel increases abruptly, resulting in the failure of wall and floor assemblies in an extremely short time. Elewini *et al.* (2007) have reported that for the assemblies without insulation materials installed in its cavity, the fire resistance rating correlates well with the fall-off time of the gypsum boards. But for the assemblies with insulation materials installed in the cavity, the experimental results are scattered and inconclusive.

Taking into account all the parameters above, current study aims to find the gypsum board assemblies that can restrain the adhesive temperature below T_g during the event of fire for a specific time period. The fire tests under standard time-temperature furnace conditions are needed in order to determine the fire resistance rating of the gypsum board assemblies. But since the full-scale tests to measure the fire resistance of the assemblies are expensive and time consuming, validated

analytical models have been adopted as a way to predict the performance of the gypsum board assemblies.

2.5 Heat Transfer Finite Element Modeling of the Gypsum Board Assemblies

For many years, researchers have conducted heat transfer analyses, either using mathematical models or general finite element packages, to simulate the behavior of the gypsum board-steel stud assemblies in fire. Briefly explained below are some of the previous works done on this subject.

Gerlich (1995) has used a commercially available computer program, Temperature Analysis of Structures Exposed to Fire (TASEF), to predict heat transfer through steel frame walls exposed to fire. Three fire tests were performed to evaluate the performance of the wall assemblies. Two assemblies were subjected to the furnace time-temperature conditions in accordance with the standard ISO 834 fire curve and one assembly was subjected to “real” fire, with a relatively slow start and rapid acceleration to temperatures significantly higher than the ISO 834 conditions after about 8 minutes.

TASEF temperature predictions were non conservative (i.e., too low) compared to the measured temperatures from the “real” fire test. This was due to the fact that TASEF was unable to account for the mass loss during fire conditions, degradation of joints opening, cracking and ablation of fire-exposed gypsum plasterboard linings. However, when compared to the experimental results from the standard ISO 834 fire resistance tests, the model showed 80% - 90% accuracy.

Sultan (1996) has developed a one dimensional mathematical model to predict the temperature history across steel-stud, non-insulated and unloaded gypsum plasterboard protected wall assemblies. To predict the temperature history across the wall assembly, a finite difference method was used. In this method, the gypsum board layers on the fire exposed and unexposed sides were divided into a number of elementary layers. A heat transfer equation was written for each elementary region to calculate the temperature history for each element. Using these equations, the temperature of each element was successively evaluated for any time. Two non-insulated steel stud wall assembly arrangements were constructed and tested in accordance with CAN/ULC-S101-M89 to validate the mathematical model.

The comparison between the measured and the predicted temperatures showed that the model provided reasonably conservative fire resistance predictions, approximately 3% lower than the experimental measured values, especially at the initial stage of the tests, when the temperature was less than 100°C, and at the last stage, when the temperature was above 600°C. The conservative prediction at the initial stage was probably caused by the furnace flame impinging on the wall during the initial fast temperature rise required by the time temperature relationship. For this

case, force heat convection mechanism must be considered instead of natural heat convection as assumed in the model. The conservative prediction at the last stage was due to the assumption that the gypsum board remained in place for the entire model simulation. In the fire tests, when the free and molecular water was driven off, the gypsum board temperature increased rapidly until it reached 600°C. At this temperature the gypsum board on the fire exposed side lost its integrity and either cracked and partially fell off or completely fell off. At this point in the test, the temperature of the gypsum board on the exposed side facing the cavity was more or less equal to the furnace temperature.

Cooper (1997) has developed a methodology and an associated FORTRAN subroutine, GYPST, to simulate the thermal response of fire exposed steel-stud gypsum plasterboard wall assemblies. GYPST calculates time dependent temperatures through the thickness of the panels at equidistant sets of node points. Two full-scale steel-stud gypsum plasterboard wall assemblies were tested in accordance with ASTM E119 standard to validate the model predictions. The comparison of the model predictions and the experimental results showed good agreement.

Alfawakhiri and Sultan (2000) have conducted retrospective numerical simulations of temperature histories using the computer program TRACE (Temperature Rise Across Construction Elements), which employs an explicit integration algorithm (Sultan 1966) to solve one-dimensional transient heat transfer equations. A large number of numerical trial runs were conducted to achieve thermal properties that can produce a reasonable agreement of simulated and measured temperature histories at all tests. These apparent thermal properties implicitly accounted for physical phenomena other than heat transfer, such as mass transfer, phase change, etc. TRACE also models the spalling of gypsum board by removing it from the simulation at user-specified time. Six wall assemblies, insulated and non-insulated, were tested in accordance with CAN/ULC-S101-M89 to validate the model predictions. Based on the comparison between the experimental results and the model predictions, the predicted failure time is in good agreement with the measured failure time.

Jones (2001) has used a commercially available finite element program, SAFIR, to predict the behavior of various gypsum plasterboard assemblies. Five pilot-scale furnace tests, one was subjected to the standard ISO 834 fire resistance test and four were subjected to the “real” fire test, were performed to provide an insight into the behavior of these systems exposed to non-standard conditions, and also to validate predictions from the model. The result from the standard ISO 834 fire resistance test was used to calibrate the finite element (SAFIR) model, by manipulating the thermal properties of the gypsum plasterboards. The model calibrated using the results from the standard ISO 834 fire test provided reasonable predictions of temperatures within the assemblies exposed to a moderate fire.

However, the computer model (SAFIR) predictions for heat transfer through light steel frame gypsum plasterboard systems exposed to fire conditions that are more severe than the standard ISO 834 fire curve are relatively poor. This problem was viewed probably due to the inability of the SAFIR program to model moisture movement, ablation, and shrinkage of plasterboard linings.

Feng *et. al.* (2003) have used a commercially available finite element program Abaqus to simulate the temperature distribution through the cold-formed thin-walled steel panel systems under the standard fire conditions. Abaqus was also used to carry out a parametric study to investigate the thermal performance of these systems with different number of gypsum boards on the exposed and unexposed sides and that of cassette systems.

In the experimental study, fire tests were conducted on eight steel stud panels with different types of steel section, different number of gypsum boards and either with or without interior insulation. The eight panels were subjected to time-temperature conditions in accordance with BS 476 Part 20- cellulosic fire curve. The experimental results were then used to validate the finite element model. It was concluded that the finite element model Abaqus can be used to simulate detailed temperature distributions in cold formed thin walled steel systems under the standard fire condition, including cavity radiation, provided there was no integrity failure of the gypsum boards and the appropriate thermal boundary conditions and material thermal properties were adopted.

Sharp (2008) has used a finite element analysis software package TASEF (Temperature Analysis of Structure Exposed to Fire) to simulate the performance of non-loadbearing gypsum protected steel stud walls in the furnace tests. Three wall assemblies were tested according to ASTM E119 standard. The predicted failure time calculated by TASEF was 56.5 minutes while the measured failure time was 63 minutes. The thermal conductivity of the model was then varied to bring the calculation in line with the measurements. Even though the failure point was the same, TASEF did not do a very good job at predicting the temperature plateau around 100°C that was observed in the experimental data. This plateau was explained to be due to calcinations of the gypsum boards and moisture evaporation.

With a significant number of research and model development in this field, modeling the behaviour of gypsum boards assemblies has been proven a powerful tool for the prediction of the fire resistance rating, with several limitations of the modeling parameters such as the difficulty to model the calcinations, moisture evaporation and the ablation of the gypsum board assemblies. The current study intends to develop a finite element model that can be used to evaluate the performance of the fire protection system for FRPs using the glass transition temperature as the failure criterion.

CHAPTER III

COMPUTATIONAL MODEL

The behaviour of a phenomenon in a system depends upon the geometry or domain of the system, the properties of the material, the boundary, initial and loading conditions. For an engineering system, the geometry or domain can be very complex. Further, the boundary and initial conditions can also be complicated. It is therefore, in general, very difficult to solve the governing differential equation via analytical means. In practice, most of the problems are solved using numerical methods such as the finite element method. Realistic finite element problems might consist of up to hundreds of thousands, and even several millions, of elements and nodes, and therefore they are usually solved in practice using commercially available software packages (Liu and Quek, 2003).

3.1 Computer Program

The computer program employed to predict the heat transfer of the tested gypsum board assemblies in this study is Abaqus/CAE Version 6.8. Abaqus is a suite of engineering simulation programs, based on the finite element method, which can solve problems ranging from simple linear analyses to the more challenging non-linear simulations. Abaqus contains a library of elements that can model almost any geometry, and an extensive list of material models. Designed as a general-purpose simulation tool, Abaqus can be used to study structural (stress/displacement) problems as well as to simulate heat transfer problems (Abaqus Analysis User's Manual 2008).

The Abaqus finite element system consists of Abaqus/Standard, a general-purpose finite element program; Abaqus/Explicit, an explicit dynamics finite element program; Abaqus/CAE; and Abaqus/Viewer. The process of running an analysis using Abaqus consists of three phases, as illustrated in Figure 3.1. In the first phase, called preprocessing phase, the user defines the model of the physical problem and creates an Abaqus input file (.inp). The model is usually created graphically using Abaqus/CAE, or created directly using a text editor. The second phase is simulation phase, which can be done either using Abaqus/Standard or Abaqus/Explicit analysis tool. The analysis tool performs the analysis on the input file from the previous phase; send information to Abaqus/CAE, allowing user to monitor the progress of the job; and generates an output database. Since the type of analysis performed in this study is uncoupled heat transfer analysis, Abaqus/Standard is chosen as the analysis tool. The last phase is post processing, which is usually done using a post processor such as

Abaqus/Viewer to read the output database and show the results of the analysis graphically (Abaqus Analysis User's Manual 2008).

First phase of the Abaqus/CAE finite element modeling which is called preprocessing phase, can generally be divided into four steps:

- Modeling of the geometry
- Meshing (discretization)
- Specification of material properties, and
- Specification of boundary, initial, and loading conditions.

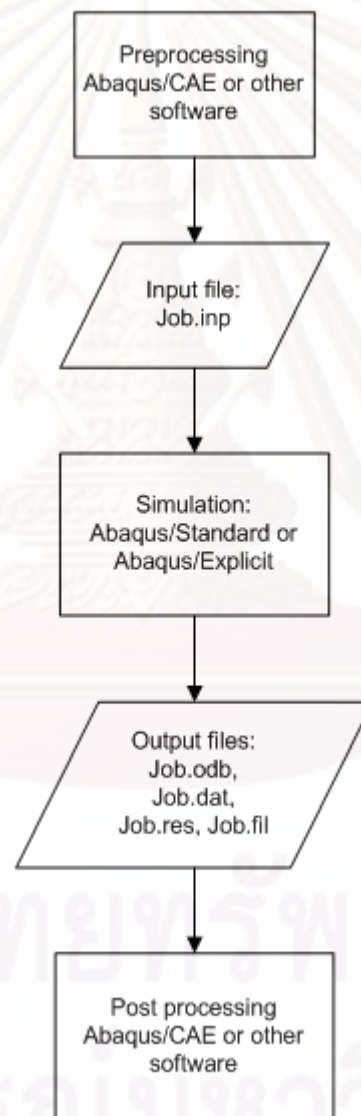


Figure 3.1 Phases in Abaqus/CAE finite element modeling (Abaqus Analysis User's Manual 2008)

3.2 Modeling of the Geometry

The first step in the preprocessing phase is creating a model which is done graphically using Abaqus/CAE. The model consists of parts which must be put together to create an assembly. The system then writes this data as part of the model data and saves it in the .cae file.

The assemblies used in the experiments are proprietary systems available from Siam Gypsum Industry Co., Ltd., called Proline MAX. It is a concealed ceiling system utilizing double-layer steel studs; primary channels and secondary channels, as frame and gypsum boards as lining material. The heat transfer across the gypsum board assembly is considered a two-dimensional problem. The assemblies for the computational model consist of; two 64 x 34 x 0.52 mm thick steel channel combined together acting as a primary channel; one 34 x 15 x 0.52 mm thick steel channel as a secondary channel; and 15-mm thick Type X gypsum boards lining extending 100 mm to either side of the stud centerline, as shown in Figure 3.2. As in the experimental studies, there are three configurations of gypsum board assemblies to be modeled; 2x1-w, 3x1-w, and 3x1-wo. The detailed information about all these assemblies can be seen in Table 3.1.

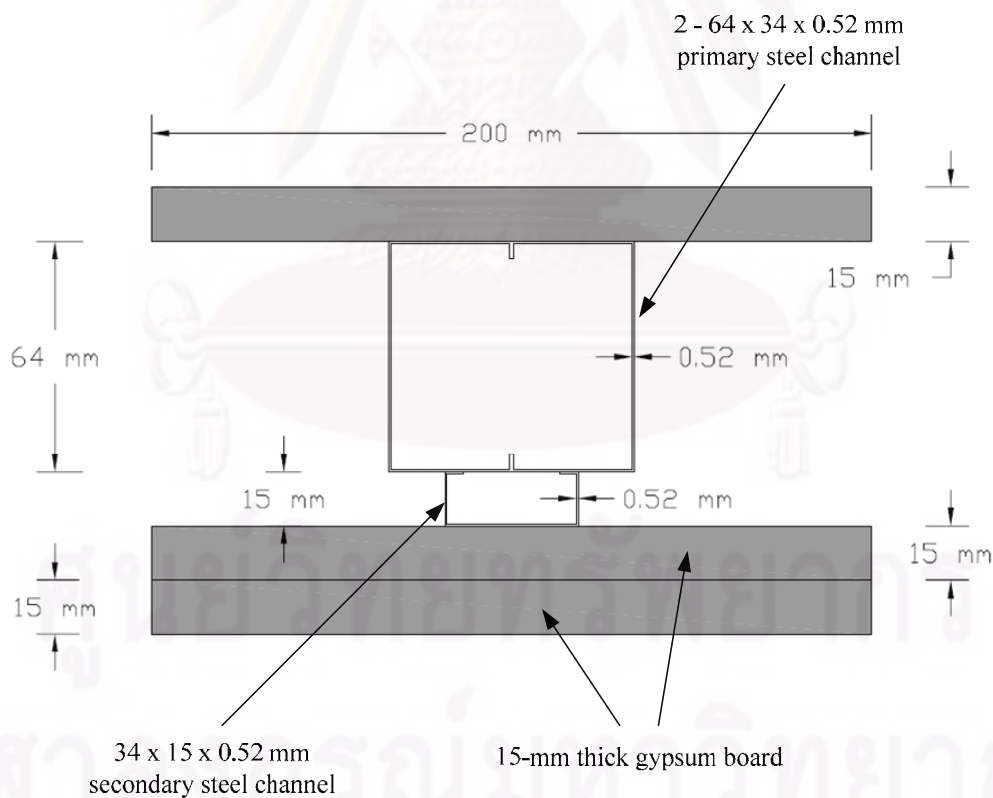


Figure 3.2 Description of the model assembly

Table 3.1 Assemblies used in the computational model

Assembly	Number of gypsum board on the exposed side	Number of gypsum board on the unexposed side	Insulation material within the cavity
2x1-w	2	1	Yes
3x1-w	3	1	Yes
3x1-wo	3	1	No

3.3 Meshing (Discretization)

The basic idea of the finite element method is to discretize the geometry created into small pieces called elements which is connected by nodes, in order to obtain an approximate solution. For uncoupled heat transfer analysis, Abaqus/Standard suggests using the diffusive heat transfer element which allow for heat storage (specific heat and latent heat effects) and heat conduction. In the heat transfer analysis, the diffusive elements have only temperature degrees of freedom. The diffusive elements use either first-order (linear) interpolation or second-order (quadratic) interpolation. The first-order heat transfer element uses a numerical integration rule while the second-order heat transfer element uses conventional Gaussian integration. For two dimensional analyses the Abaqus/Standard provides two types of elements: triangular and quadrilaterals. Triangular elements are geometrically versatile and are used in many automatic meshing algorithms. However, a good mesh of hexahedral elements usually provides a solution of equivalent accuracy at less cost. Moreover, quadrilateral elements have better convergence rate than triangles and sensitivity to mesh orientation in regular meshes is not an issue (Abaqus Analysis User's Manual 2008). Thus, for this study the first-order quadrilateral diffusive heat transfer elements (DC2D4) were chosen as the element type of the computational model. Figure 3.3 shows the mesh configuration for one of the assembly; 2x1 gypsum board configurations with insulation material installed in the cavity.

3.4 Material Properties

The gypsum board assemblies consist of gypsum plasterboards, steel sections, and insulation material (rock wool). In transient heat transfer analysis, the material properties that must be specified in the input file are the density, the thermal conductivity, and the specific heat. The values of these thermal properties for each of the material mentioned previously are obtained from the literature.

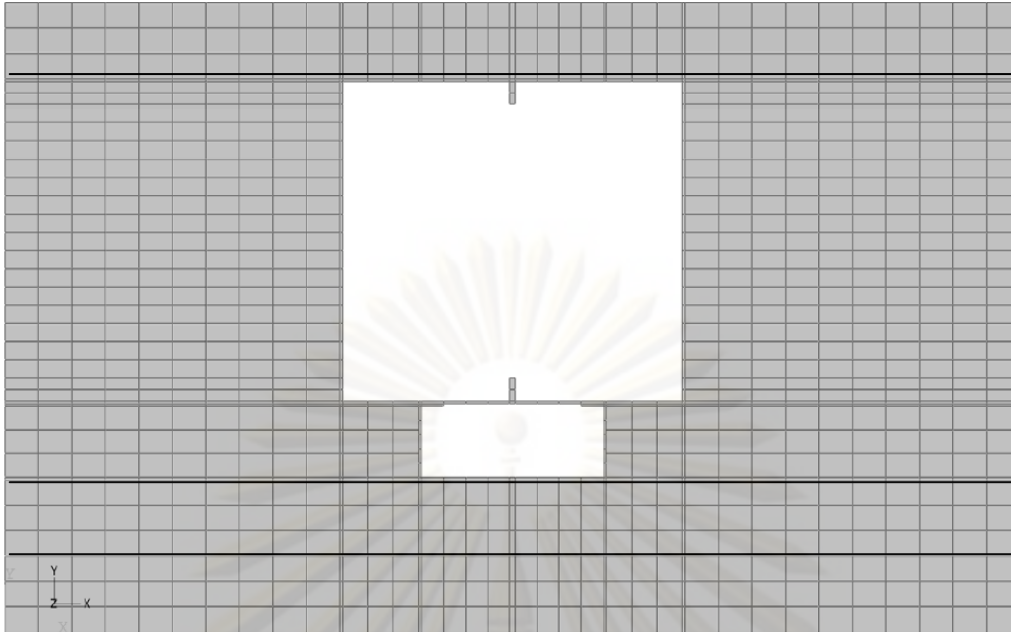


Figure 3.3 Finite element used in Abaqus/CAE

3.4.1 Gypsum Plasterboard

The type of gypsum boards used in the experiments is the type X gypsum boards. Type X board is the generic term used to designate the gypsum board with a specially formulated core that provides a greater fire resistance compared to a regular gypsum board of the same thickness (Sultan 1996).

3.4.1.1. Density

The density of a material is defined as its mass per unit volume. In heat transfer problems, the density works with the specific heat to determine how much energy a body can store per unit increase in temperature. Increasing the temperature generally decreases the density, but for gypsum boards the decrease in density is not always in linear configuration with the increase in temperature. Sultan (1996); Cooper (1997); Jones (2001); Sharp (2008); and Rahmanian and Wang (2009) reported the variation of the density of gypsum plasterboards due to the effect of elevated temperatures. The variation of the density of gypsum plasterboards relative to the ambient density during elevated temperatures is illustrated in Figure 3.4.

จุฬาลงกรณ์มหาวิทยาลัย

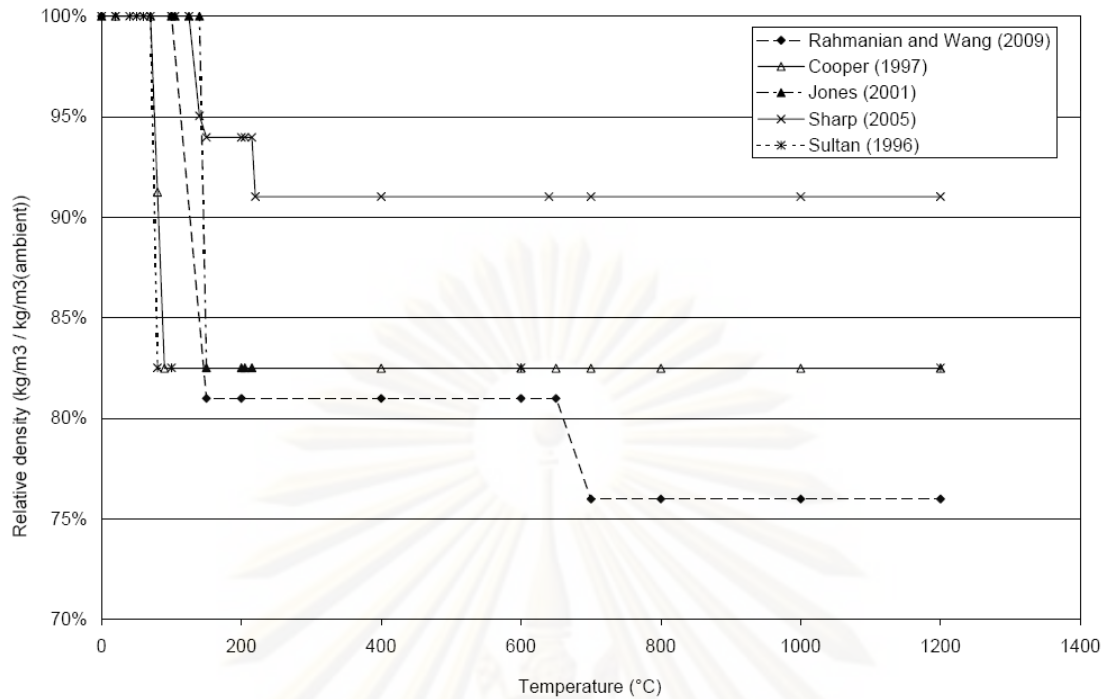


Figure 3.4 Density of gypsum plasterboards relative to the ambient density vs. temperature

According to Rahmanian and Wang (2009), the decrease in the density of gypsum boards with respect to the increasing temperature is due to the evaporation of water. Pure gypsum consists of calcium sulphate with free water at equilibrium moisture content of approximately 3% and chemically combined water of crystallization, approximately 20% (Gerlich, 1995). Its chemical formula is $\text{CaSO}_4 \cdot 2\text{H}_2\text{O}$ (calcium sulphate di-hydrate). When the gypsum plasterboard is heated during a fire, its temperature on the exposed surface will increase steadily until about 100°C . Until this time, the density of the gypsum board remains the same as the one at ambient temperature because no water had been driven off. From this time there will be a delay in the evolution of the temperature through the gypsum core because the water inside the gypsum board (the water of crystallization) starts being driven off. As the heating continues, the 100°C temperature plateau will progress slowly through the board, until the entire board has been dehydrated. The dehydration reaction on the gypsum plasterboard occurs at approximately 100°C – 120°C , indicated by the rapid reduction of density during that time, as can be seen in Figure 3.4. Rahmanian and Wang (2009) have also reported the influence of the second dehydration reaction, which occur approximately at 700°C , on the reduction of relative density.

3.4.1.2. Thermal Conductivity

Thermal conductivity is the property of a material that indicates its ability to conduct heat. It describes the rate at which heat flows within a body for a given temperature difference. The thermal conductivity of gypsum plasterboards reported by various studies can be seen in Figure 3.5. Cooper (1997) defined the default values for thermal conductivity of gypsum boards within the SAFIR software, originated from the work of Sultan (1996) on Type X and Type C boards. Rahmanian and Wang (2009) derived an equation to calculate the gypsum board conductivity based on the theory that since gypsum is a porous material, heat transfer through gypsum is a combination of all three modes: conduction through the solid, convection and radiation through the pores. Therefore the proposed equation to calculate the effective thermal conductivity of gypsum included these effects.

As shown in Figure 3.5, there is consistent agreement among researchers that the thermal conductivity is constant up to 90°C-100°C. This is due to the fact that the dehydration reaction on the gypsum plasterboard has not happened yet. After the temperature reaches 100°C, the dehydration process initiates which cause the moisture to be trapped within a gypsum board and change its thermal behaviour at elevated temperatures considerably. It is a well-known fact that heat transfer in moist material is influenced significantly by moisture content. Moisture can increase the thermal conductivity and heat capacity of composites due to the fact the water is a better heat conductor than air and that additional heat can be transferred by the migration of moisture. Also, during heating of the material, a process of vaporization of moisture takes place. For the moisture to be evaporated, a certain amount of energy is needed, and the absorption of this energy retards its temperature rise.

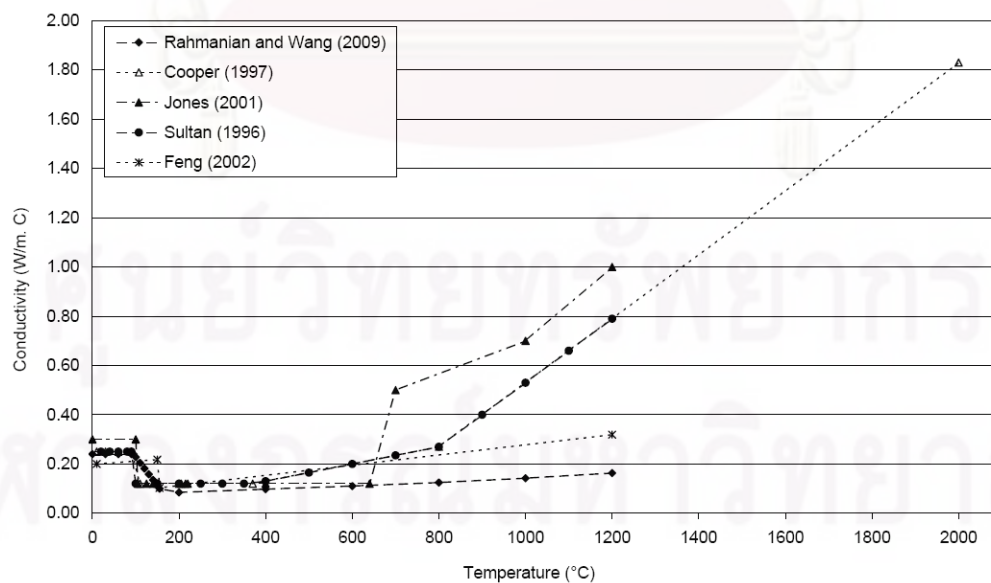


Figure 3.5 Thermal conductivity of gypsum plasterboards reported by various studies

3.4.1.3. *Specific Heat*

Specific heat is the measure of heat or thermal energy required to increase the temperature of a unit quantity of a substance by one unit. In heat transfer problems, the density works with the specific heat to determine how much energy a body can store per unit increase in temperature. The temperature-dependent specific heat of gypsum corresponding to the two dehydration reactions of gypsum, thus experiences two peaks. These peaks represent the energy consumed to dissociate and evaporate water and include the water movement and recondensation of water in cooler region of gypsum (Rahmanian and Wang 2009).

Similar to the change in density with temperature, there is a large variation between the reported values of specific heat with temperature from different studies of similar gypsum boards. Figure 3.6 shows that there is a good agreement amongst researchers that the first dehydration reaction occurs at approximately 100°C – 120°C when the calcium sulphate di-hydrate is converted to calcium sulphate hemihydrates. However, as can be seen in Figure 3.6, there are some discrepancies on where the second dehydration reaction occurs. The second dehydration reaction occurs when calcium sulphate hemihydrates is converted to calcium sulphate anhydrate.

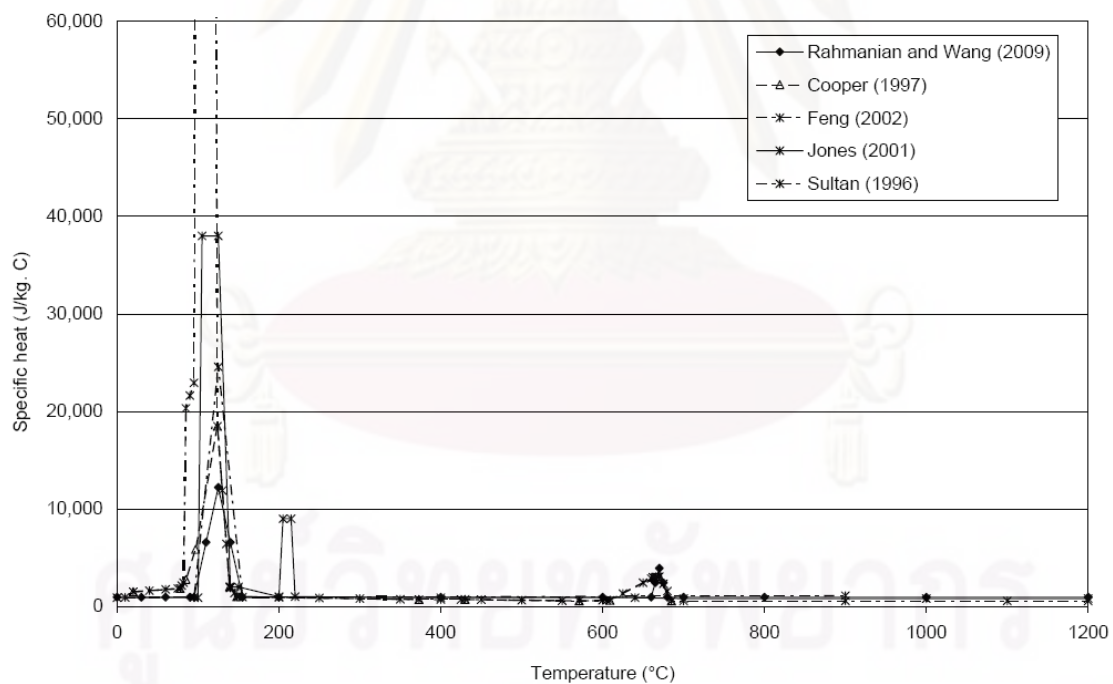


Figure 3.6 Specific heat of gypsum plasterboard reported by various studies

3.4.2 *Steel Stud (Primary and Secondary Channels)*

The temperature rise of a steel member is a function of the thermal conductivity and specific heat of the material. The accuracy in the determination of the thermo-physical properties of steel, such as specific heat and thermal conductivity, has little influence on the thermal modeling of the gypsum board assembly exposed to fire because steel framing plays a minor role in the overall heat transfer mechanism of the assembly (Alfawakhiri *et al* 1999). Specific heat and conductivity of steel are affected by changes in temperature. The properties of steel used in this study are derived from those described in the Eurocodes (EC 1995).

3.4.2.1. Density

The ambient density of steel is typically taken as 7850 kg/m^3 (Buchanan 2000), which remains essentially constant with increasing temperature.

3.4.2.2. Thermal Conductivity

The variation of thermal conductivity with temperature for steel can be expressed as (see Figure 3.7):

For $20^\circ\text{C} \leq \theta_a \leq 800^\circ\text{C}$

$$\lambda_a = 54 - 3.33 \times 10^{-2} \theta_a \text{ (W/m. K)} \quad (3.1)$$

For $800^\circ\text{C} \leq \theta_a \leq 1200^\circ\text{C}$

$$\lambda_a = 27.3 \text{ (W/m. K)} \quad (3.2)$$

where λ_a and θ_a are the thermal conductivity and temperature of steel, respectively.

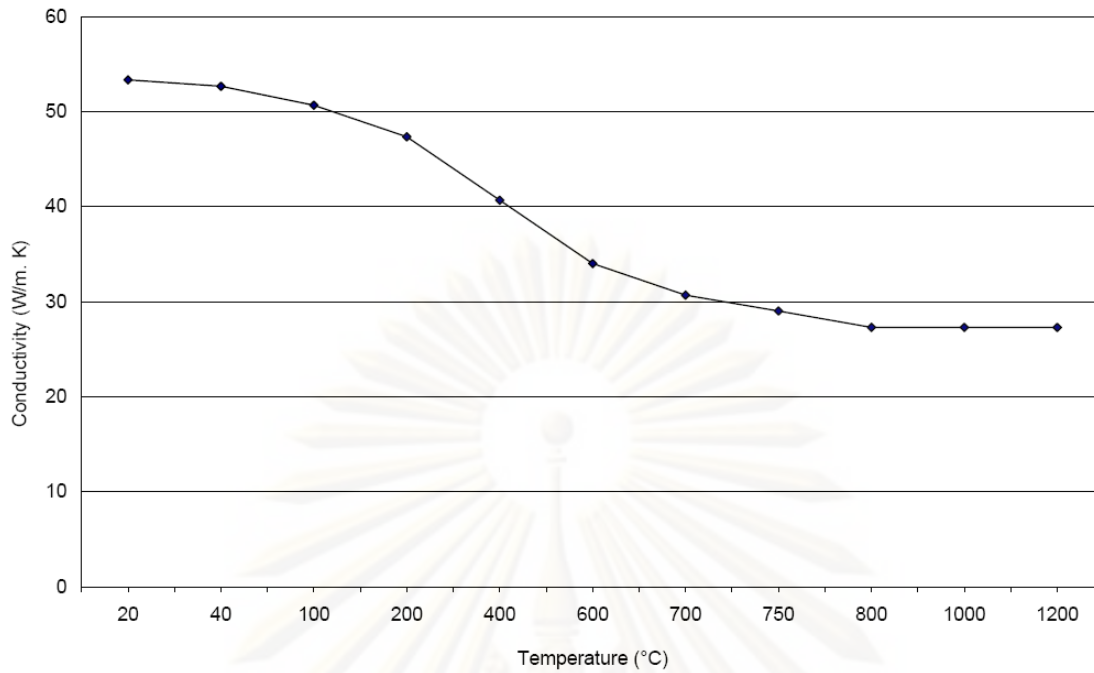


Figure 3.7 Thermal conductivity of steel as a function of temperatures

3.4.2.3. Specific Heat

The specific heat of steel varies with temperature as shown in Figure 3.8, where the peak results from a metallurgical change at about 730°C. The following equations define the relationship shown in Figure 3.8 and have been adopted from EC3 (1995).

For $20^{\circ}\text{C} \leq \theta_a \leq 600^{\circ}\text{C}$

$$C_a = 425 + 7.73 \times 10^{-1} \theta_a - 1.69 \times 10^{-3} \theta_a^2 + 2.22 \times 10^{-6} \theta_a^3 \quad (\text{J/kg. K}) \quad (3.3)$$

For $600^{\circ}\text{C} \leq \theta_a \leq 735^{\circ}\text{C}$

$$C_a = 666 + 13002 / (738 - \theta_a) \quad (\text{J/kg. K}) \quad (3.4)$$

For $735^{\circ}\text{C} \leq \theta_a \leq 900^{\circ}\text{C}$

$$C_a = 545 + 17820 / (\theta_a - 731) \quad (\text{J/kg. K}) \quad (3.5)$$

For $900^{\circ}\text{C} \leq \theta_a \leq 1200^{\circ}\text{C}$

$$C_a = 650 \quad (\text{J/kg. K}) \quad (3.6)$$

where C_a and θ_a are the specific heat and temperature of steel, respectively.

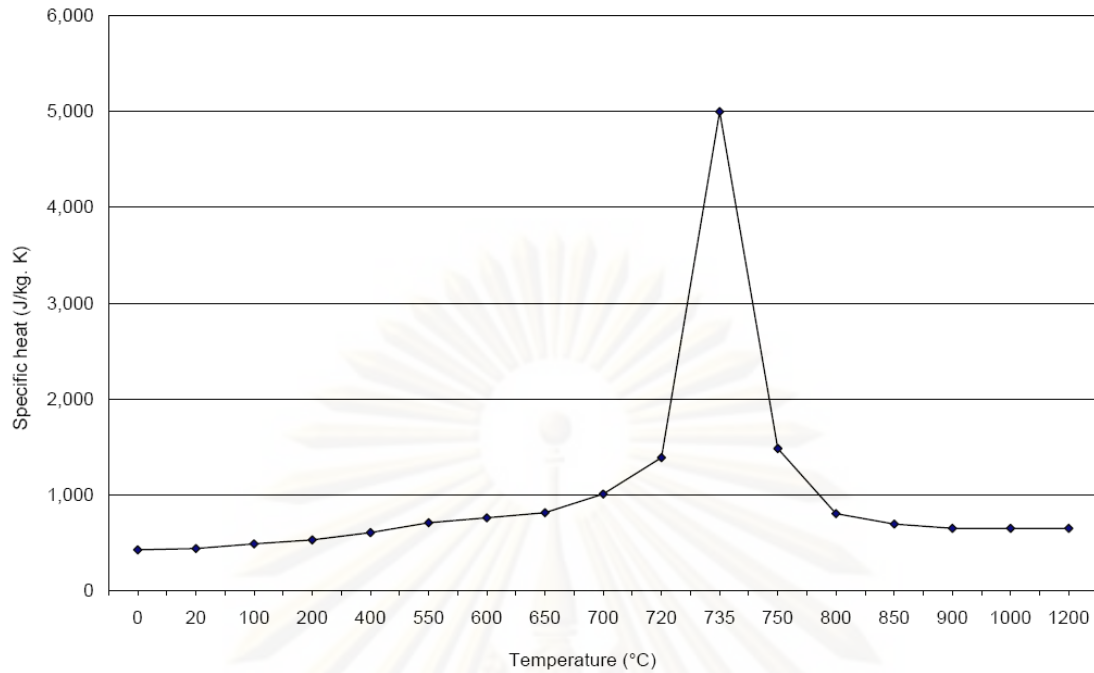


Figure 3.8 Specific heat of steel as a function of temperatures

3.4.3 Insulation Material (Rock wool)

The thermal properties of the insulation material are adopted from the experimental results of Benichou *et al* (2001). Since the actual thermal properties of the insulation material used in the current study are unknown, it is decided to use the thermal material properties from previous researches that are assumed to be testing a similar type of material. Benichou *et al* (2001) have conducted a set of tests on several kinds of insulation materials such as; cement board, rock wool, and glass fiber insulation, to determine their thermal properties. Since the insulation material used in our experiments is rock wool, the thermal properties from the tests on rock wool insulation as reported by Benichou (2001) are being used in the model. The values of the thermal conductivity, density, and specific heat of rock wool are summarized in Table 3.4.

3.4.4 Summary of the Thermal Properties Used

To develop an accurate heat transfer model, it is important to choose the correct thermal properties of the building materials. Since direct laboratory testing for determining the thermal properties of materials is not possible at this time, a sensitivity analysis based on the literature review is done instead. Different sets of thermal properties based on the works reported by various researchers are incorporated into the computational model. The results from these models are then compared with the experimental results. Figure 3.9 shows the comparison between the results from the computational model utilizing the material properties from

various researches and the results from our experiment. The comparison is done for the assembly 2x1-w considering the temperature on the unexposed side.

From Figure 3.9, it can be concluded that the material properties reported by Jones (2001) yield the best-fit results. As such, the material properties used in this study are adopted from Jones (2001). The values of the thermal properties for the gypsum board, steel and insulation material are summarized in Table 3.2, Table 3.3 and Table 3.4, respectively.

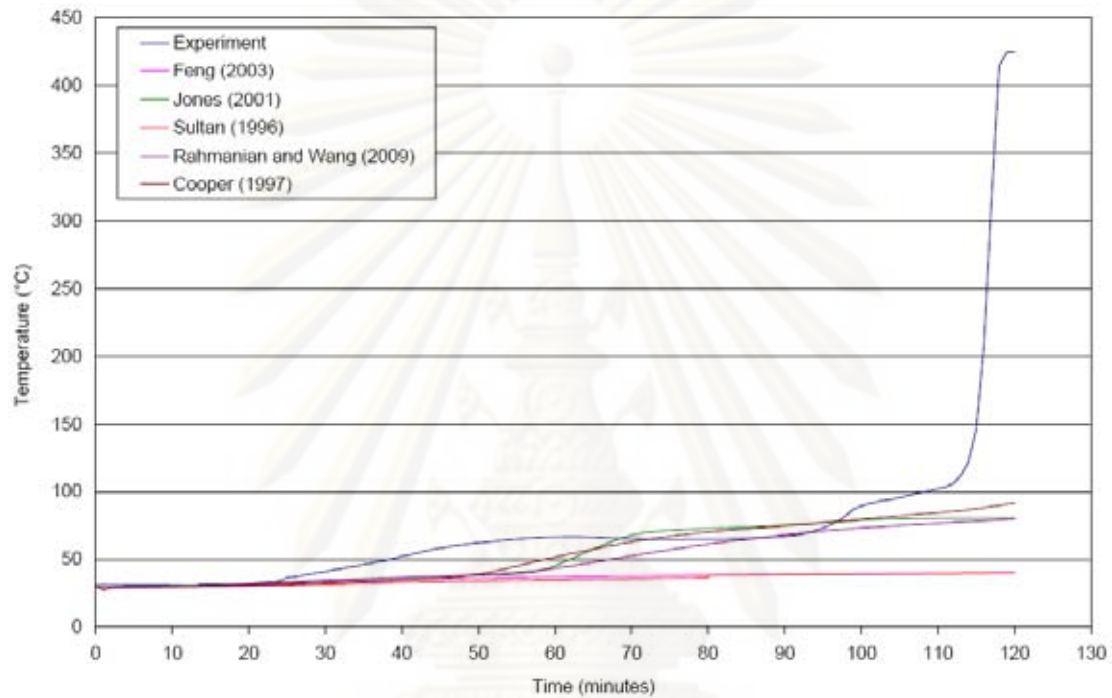


Figure 3.9 Comparison of results from the computational model using various material properties and the experiment

Table 3.2 Gypsum board thermal properties

Temperature (°C)	Density (kg/m ³)	Conductivity (W/m. °C)	Specific heat (J/kg. °C)
0	747	0.30	900
100	747	0.30	900
105	747	0.12	38000
125	747	0.12	38000
140	710	0.12	2000
150	702	0.12	2000
200	702	0.12	1000
205	702	0.12	9000
215	702	0.12	9000
220	680	0.12	1000
400	680	0.12	900
640	680	0.12	900
700	680	0.50	800
1000	680	0.70	800
1200	680	1.00	800

ศูนย์วิทยทรัพยากร
จุฬาลงกรณ์มหาวิทยาลัย

Table 3.3 Steel thermal properties

Temperature (°C)	Conductivity (W/m. °C)	Temperature (°C)	Specific heat (J/kg. °C)
20	53.334	0	425.00
40	52.668	20	439.80
100	50.67	100	487.62
200	47.34	200	529.76
400	40.68	400	605.88
600	34.02	550	708.28
700	30.69	600	760.22
750	29.025	650	813.75
800	27.3	700	1008.16
1000	27.3	720	1388.33
1200	27.3	735	5000.00
-	-	750	1482.89
-	-	800	803.26
-	-	850	694.75
-	-	900	650.00
-	-	1000	650.00
-	-	1200	650.00

ศูนย์วิทยทรัพยากร
จุฬาลงกรณ์มหาวิทยาลัย

Table 3.4 Rock wool thermal properties

Temperature (°C)	Conductivity (W/m. °C)	Temperature (°C)	Specific heat (J/kg. °C)
25	0.026	40	631.90
101	0.036	60	691.60
194	0.054	80	698.80
297	0.076	100	707.70
396	0.119	150	771.90
501	0.166	200	859.00
602	0.202	250	901.00
724	0.207	300	780.80
856	0.229	350	474.40
959	0.278	400	81.70
1066	0.352	600	681.60
-	-	650	611.10
-	-	690	755.50

3.5 Analysis Procedures and Boundary Conditions

For the current study, the problem of heat transfer across the gypsum board assemblies is modeled as a two-dimensional heat transfer problem. Since the temperature field is calculated without consideration of the stress/deformation or the electrical field in the bodies being studied, this problem can be considered as an uncoupled heat transfer problem. The uncoupled heat transfer analysis is intended to model solid body heat conduction with general, temperature-dependent conductivity; internal energy (including latent heat effects); and quite general convection and radiation boundary conditions (Abaqus theory manual). The heat transfer problem in this study is also considered a nonlinear problem because the material thermal properties are temperature-dependent and the radiation effect is being considered. To solve a nonlinear heat transfer problem, Abaqus suggests using Abaqus/Standard as the analysis tool. The Abaqus/Standard uses the iteration scheme which employs the Newton method to solve nonlinear equations. The general process of the iteration scheme can be illustrated in Figure 3.10.

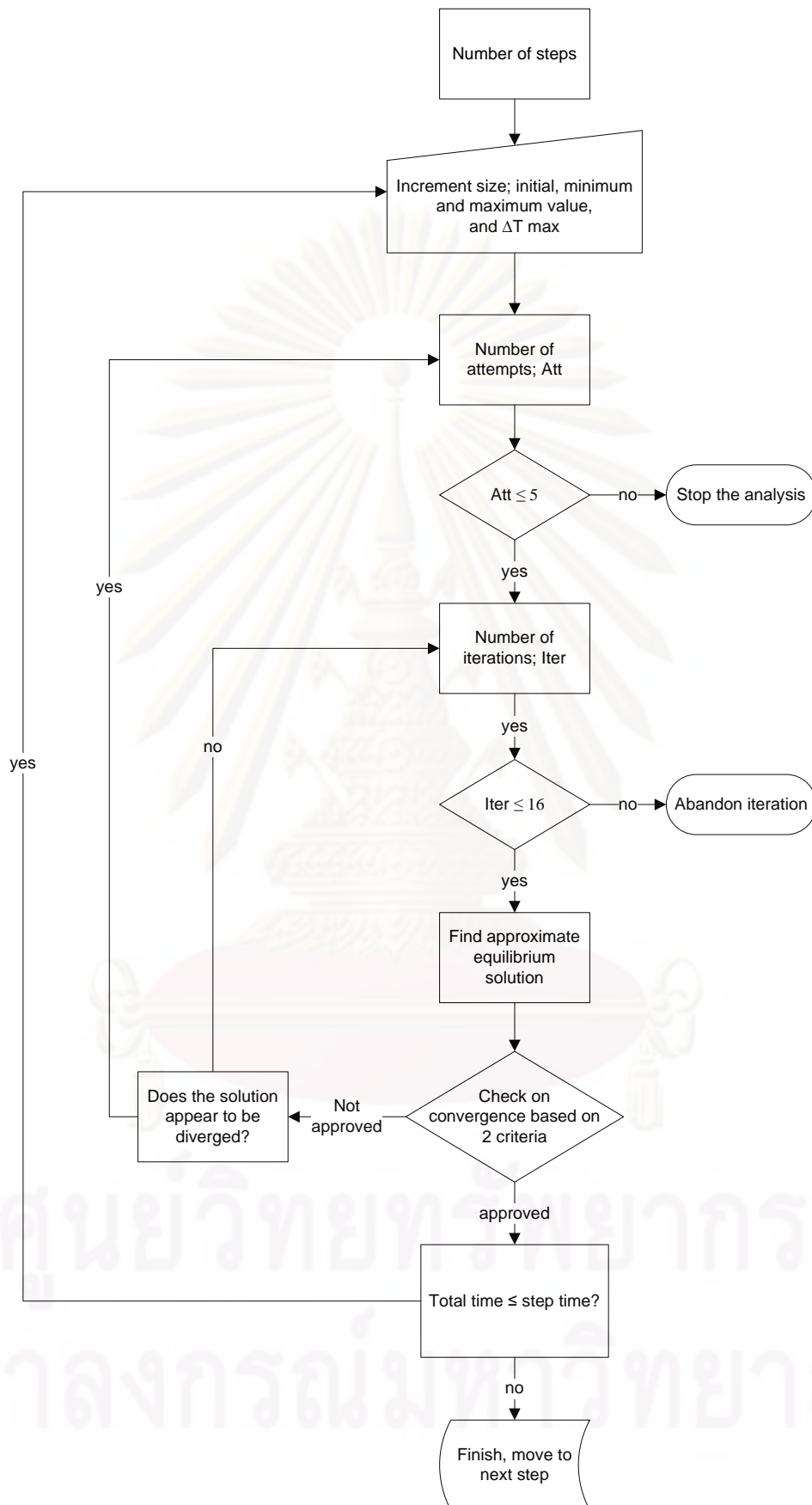


Figure 3.10 Process in Abaqus/Standard in finding the solution of nonlinear problems

The time history for a simulation consists of one or more steps, in which different loads, boundary conditions, analysis procedures, and output requests can be defined. In a nonlinear analysis the solution cannot be calculated by solving a single system of linear equations, as would be done in a linear problem. Instead, the solution is found by specifying the loading as a function of time and incrementing time to obtain the nonlinear response. Abaqus /Standard subdivide the nonlinear analysis in each step into increments so that the nonlinear solution path can be followed. Users input the size of the initial increment, and Abaqus/Standard automatically chooses the size of the subsequent increments. At the end of each increment the structures is in (approximate) equilibrium and the results are available for writing to the output database files.

In this study, the simulation time history is divided into 30 steps based on the time temperature curve. The first 15 minutes of the ISO time temperature curve are divided into steps with 1-minute step time each, the next 45 minutes of the curve are divided into steps with 5-minute step time each, and the last 1 hour of the curve are divided into steps with 10-minute step time each. The boundary conditions and loading are prescribed for each step. The boundary, initial and loading conditions play a decisive role in solving the simulation (Liu and Quek, 2003). Thus understanding these topics before inputting the data to the model would help making a better model.

According to Sultan (1996), the heat transfer mechanism through the gypsum board assembly exposed to fire can be divided into:

- Heat transfer from the fire to the exposed surface by radiation and convection;
- Heat transfer through the gypsum board on the exposed side by conduction;
- Heat transfer from the cavity to the unexposed side by conduction; and
- Heat transfer from the gypsum board on the unexposed surface to ambient by convection and radiation.

3.5.1 Heat Transfer Mechanism on Exposed and Unexposed Side

As mentioned before, the heat transfer mechanisms on the exposed and unexposed sides are convection and radiation. According to the Abaqus theory manual, for the uncoupled heat transfer analysis, the boundary convection and radiation can be specified as:

- Surface convection

$$q = h (\theta - \theta^0), \quad (3.7)$$

where: $h = h(x, t)$ is the film coefficient, and

$\theta^0 = \theta^0(x, t)$ is the sink temperature

- Radiation

$$q = \xi \times \sigma \times \left\{ (\theta - \theta^Z)^4 - (\theta^0 - \theta^Z)^4 \right\}, \quad (3.8)$$

where: ξ = surface emissivity,

σ = Stefan-Boltzmann constant = $5.67 \times 10^{-8} \text{ W m}^{-2} \text{ K}^{-4}$, and

θ^Z = the absolute zero on the temperature scale used = -273.15°C

The sink temperature for the gypsum board assembly exposed to the standard cellulosic fire on the exposed side is $\theta^0 = 345 \log 10(8t+1) + 20$ (ISO834 2002), while on the unexposed side $\theta^0 = 30^\circ\text{C}$ (ambient temperature). The values of film coefficient (h) for the exposed and unexposed sides are $25 \text{ W/m}^\circ\text{C}$ and $12 \text{ W/m}^\circ\text{C}$, respectively (Jones 2001). The surface emissivity for the gypsum board, at the unexposed and exposed surfaces, is taken as $\xi = 0.8$.

3.5.2 Heat Transfer Mechanism on Cavity

In Abaqus when the surfaces are separated by a narrow gap, the heat transfer is modeled using gap heat transfer. The gap heat transfer mechanism can be specified as gap conductance, gap radiation, and gap heat generation. Abaqus assumes that radiative heat transfer between closely spaced contact surfaces occurs in the direction of the normal between the surfaces and radiative heat transfer is defined as a function of clearance between the surfaces through the effective view factor. Abaqus states that normally the heat flux from conduction is much larger than the radiative heat flux so the radiative heat flux only causes a minor inaccuracy. Due to this reason, in the current study it is assumed that gap radiation is being neglected.

According to Abaqus/Standard, the conductive heat transfer between the contact surfaces is assumed to be defined by

$$q = k(\theta_A - \theta_B) \quad (3.9)$$

where q is the heat flux per unit area crossing the interface from point A on one surface to point B on the other, θ_A and θ_B are the temperatures of the points on the surfaces, and k is the gap conductance. Point A is a node on the slave surface and point B is the location on the master surface contacting the slave node or, if the surfaces are not in contact, the location on the master surface with a surface normal that intersects the slave node. In Abaqus/CAE the input data to define the gap conductance k can be created using a tabular data, as a function of the gap clearance d

3.5.3 Heat Transfer through the Assembly

As mentioned previously, the model analyzed in Abaqus is called the assembly which is built from one or more part instances. Abaqus/CAE considers that the mere physical proximity of two surfaces in an assembly is not enough to indicate any type of interactions between the surfaces. Thus to ensure the heat transfer continuity through the gypsum board assembly, the interaction between part instances must be specified. For heat transfer analysis Abaqus/Standard suggests using tie constraint to connect two adjacent parts together, so that each of the nodes on the slave surface will have the same temperature value as the point on the master surface.

Once all the tasks involved in defining a model (such as defining the geometry of the model, assigning section properties, and defining contact) have been finished, the model is ready to be analyzed. Abaqus then submits the input file for analysis to Abaqus/Standard. The progress of the analysis can be monitored in Abaqus/CAE.

3.6 Post Processing and Results

The last phase of the computational procedure using Abaqus finite element software called post processing is done using Abaqus/Viewer post processor which can be accessed through the Visualization module in Abaqus/CAE. The Visualization module, which reads the neutral binary output database file, has a variety of options for displaying the results, including color contour plots, animations, deformed shape plots, and X-Y plots. The results from the computational model can be seen in the next chapter.

CHAPTER IV

EXPERIMENTAL INVESTIGATION

To investigate the performance of the gypsum board assemblies in protecting the glass fiber reinforced polymer (GFRP) strengthened concrete slab exposed to fire, three furnace tests were carried out at the Fire Safety Research Center of Chulalongkorn University, Thailand. The results from these fire tests are used to validate the Abaqus/CAE computational models described in the previous chapter.

4.1 Specimen Description

Each of the test specimens in this study consists of a reinforced concrete slab, the GFRP strengthening system, and the gypsum board fire protection system. The GFRP was installed on the soffits of the reinforced concrete slab which was then fire protected using the gypsum board assembly.

4.1.1 Reinforced Concrete Slabs

The dimension of the slab was designed based on the dimension of the furnace, which is 1500 x 2900 mm. The entire slab was cast with ready mix concrete and reinforced with deformed steel bars. The slab was reinforced with eight 10 mm-diameter deformed steel bars spaced at 350 mm center-to-center in the longitudinal direction and with four 10 mm-diameter deformed steel bars spaced at 350 mm center-to-center in the transverse direction. The reinforcement details and the concrete cover correspond to the minimum reinforcement and minimum concrete cover as specified by ACI 318 (2005) and ACI 216 (2006). Details of the cross section and steel reinforcement of the slab are shown in Figure 4.1 and Figure 4.2, respectively.

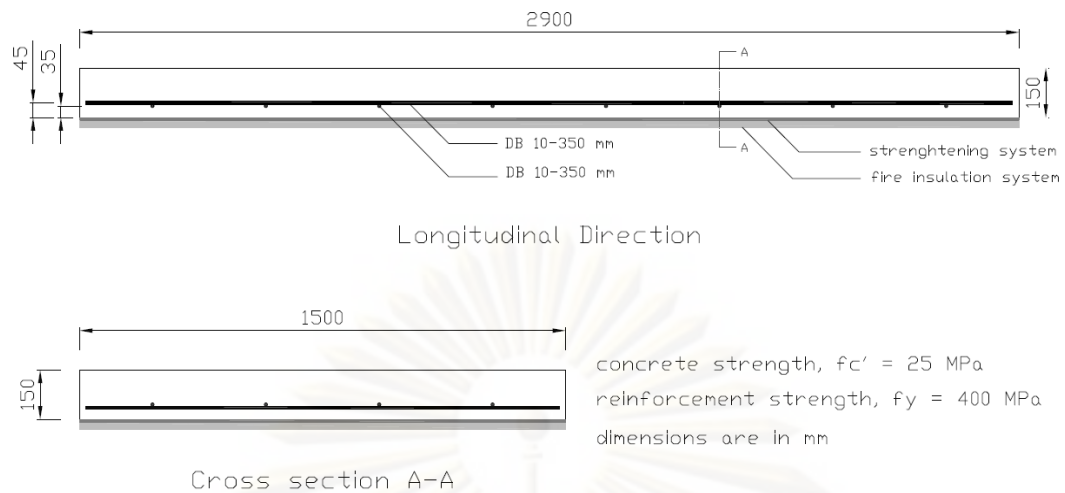


Figure 4.1 Cross section of the slab

4.1.2 FRP Strengthening System

The strengthening system used in this study is the glass fiber reinforced polymer (GFRP) strengthening system which is supplied by Nontri Co., Ltd. (Thailand). The GFRP strengthening system is applied using the wet lay-up process. In the wet lay-up process there are roughly two steps that must be undertaken: preparation and FRP bonding.

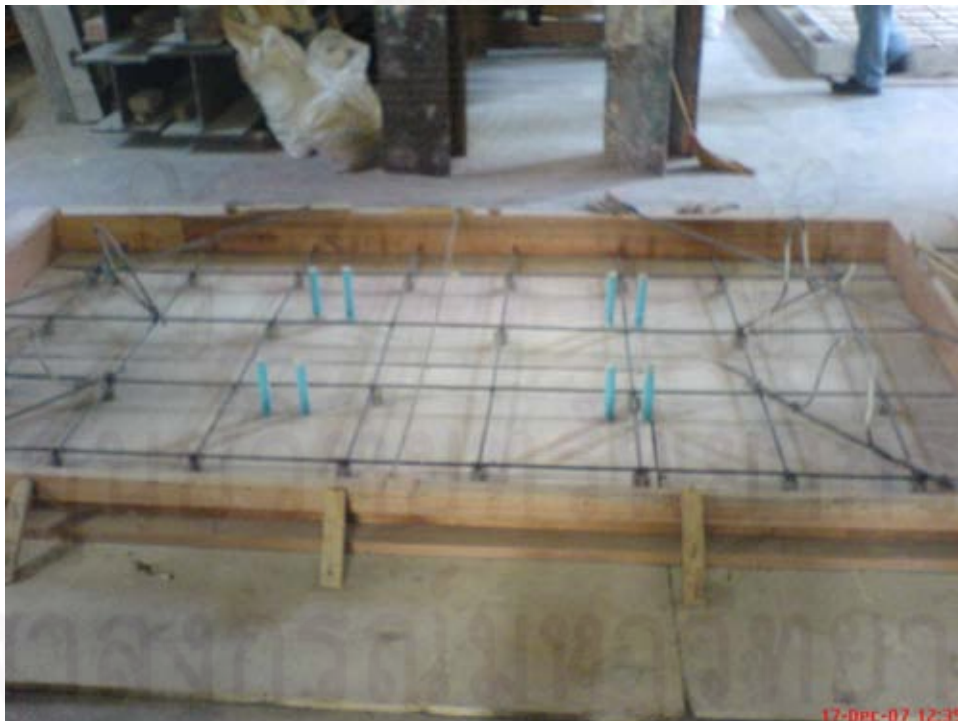


Figure 4.2 Steel reinforcements on the slab

The wet lay-up process started by removing oils, grease, dust or any loose material from the soffit of the slab using compressed air or vacuum cleaner. After that a primer for the strengthening system, called MBrace[®] Primer, was applied and allowed to harden. MBrace[®] Primer is a low viscosity epoxy primer that can penetrate concrete pore structures. In wet lay-up systems the application of a primer prior to FRP bonding is necessary in order to prevent the epoxy from being absorbed by the concrete, instead of wetting the fibers. And since the primer penetrates the concrete via the pores, it also enhances the bond for the fibers (Carolin 2003). After the MBrace[®] Primer was hardened, MBrace[®] Putty which acts as the leveling mortar for a flat surface was applied. The MBrace[®] Primer and MBrace[®] Putty were quickly and easily applied to the concrete with a brush or a soft roller, as seen in Figure 4.3.

After the preparation was completed, the strengthening system was applied. In the wet lay-up process the strengthening work started with applying adhesive, MBrace[®] Saturant, to the prepared surface using a roller as can be seen in Figure 4.3. A single layer of GFRP sheet was cut into the design length and pressed down to eliminate the trapped air and impregnate the fiber sheet with the saturant. To obtain the complete impregnation prior to curing of the first layer of adhesive, the second layer of adhesive was applied 30 minutes after the previous layer. The complete procedures for the wet lay-up process of the GFRP strengthening systems are illustrated in Figure 4.3.

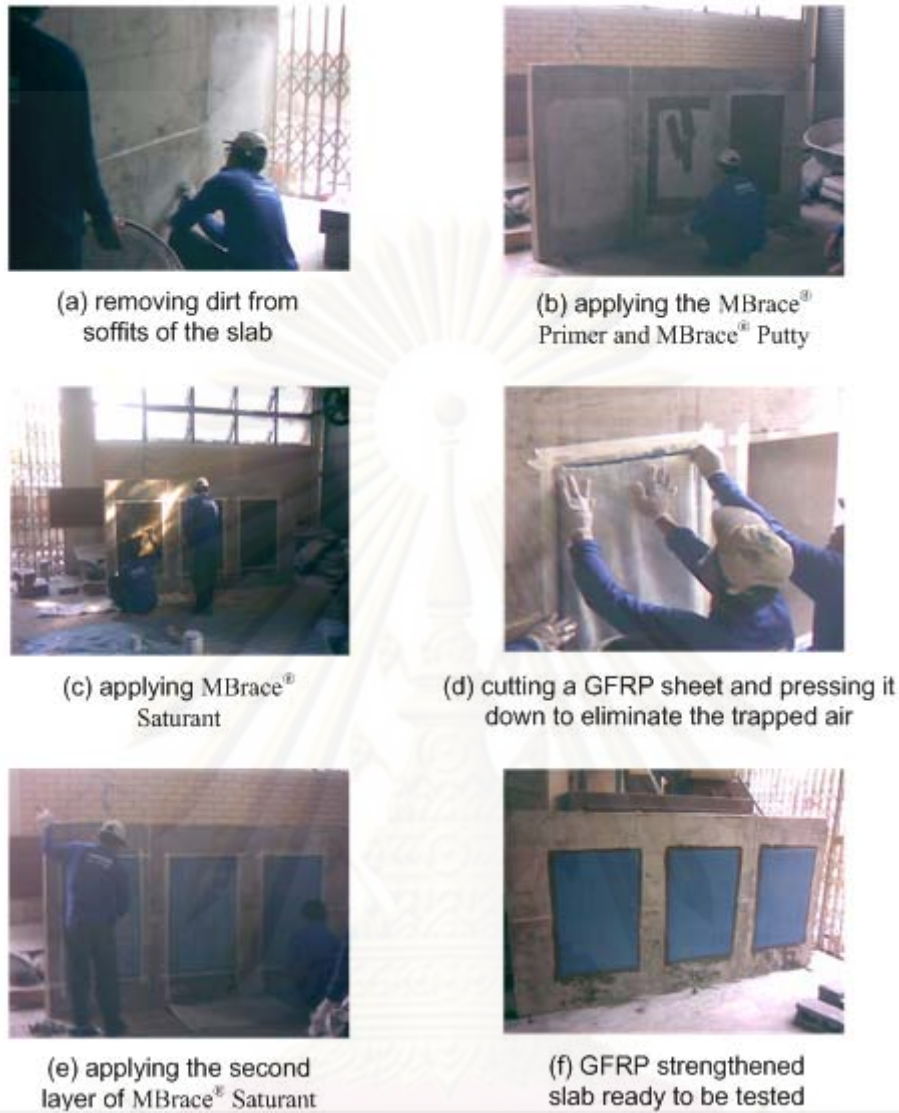


Figure 4.3 Wet Lay-Up GFRP strengthening system

4.1.3 Gypsum Board Fire Protection System

The fire insulation system used in this study is the gypsum board assembly called ProLine MAX, a proprietary system from the Siam Gypsum Industry Co., Ltd., Thailand. This gypsum board assembly is installed onto the soffit of the slab and acts as the fire protection system as well as the ceiling system. The ProLine MAX concealed ceiling system consists of double-layer steel studs, primary and secondary channels, as frames and gypsum boards as linings. The gypsum board fire protection system is illustrated in Figure 4.4.

The primary channels were constructed using two 0.52-mm thick ProWall C64 steel stud made of galvanized steel attached together using Pro MAX connecting clips. The secondary channels were 0.52-mm thick Pro C-line steel studs. The primary channels were placed at the top of the secondary channels, using Pro MAX

connecting clips or 10-mm truss head screws. The first layer of the gypsum board was then fixed to the secondary channels using 3-cm or 7-cm nails. The system was then attached to the soffit of the slab using Pro Max rigid hangers, steel thread rods and drop in anchors. The configurations of the gypsum board assembly are illustrated in Figure 4.4 – Figure 4.7

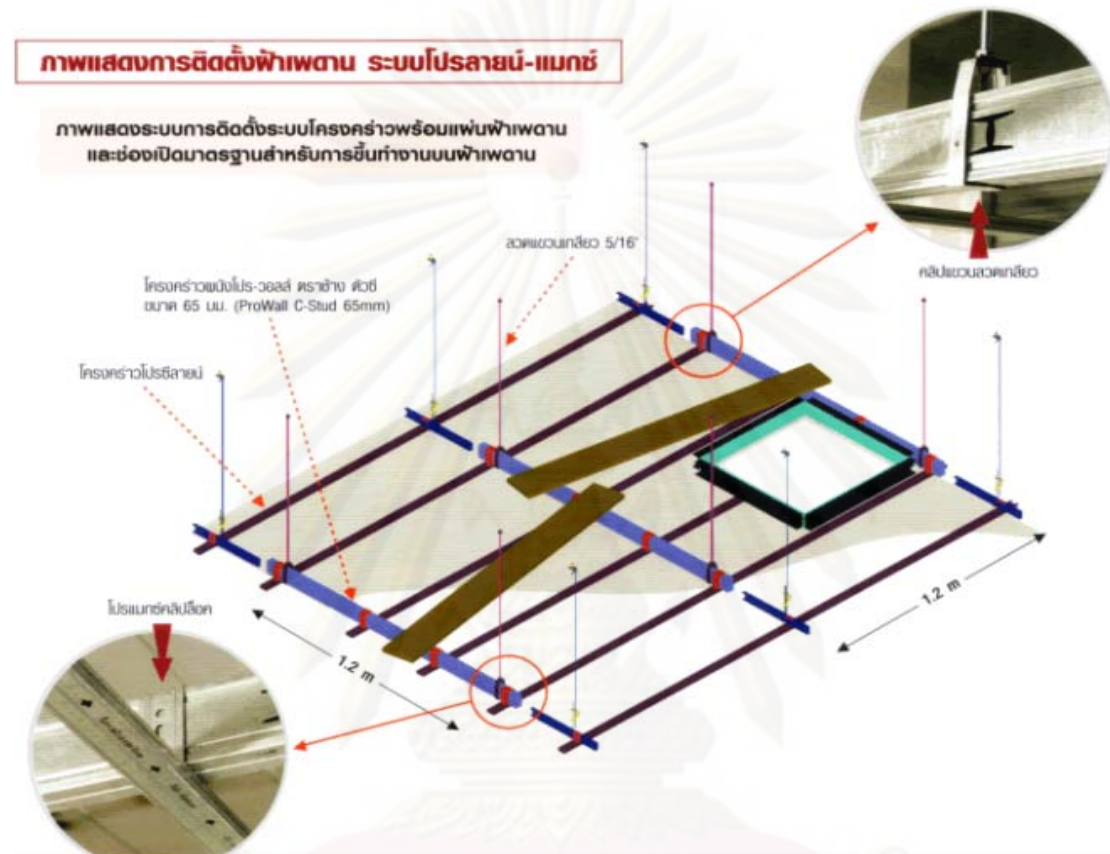


Figure 4.4 Isometric view of the ProLine MAX concealed ceiling system (Siam Gypsum Industry Co., Ltd.)

ศูนย์วิทยทรัพยากร
จุฬาลงกรณ์มหาวิทยาลัย

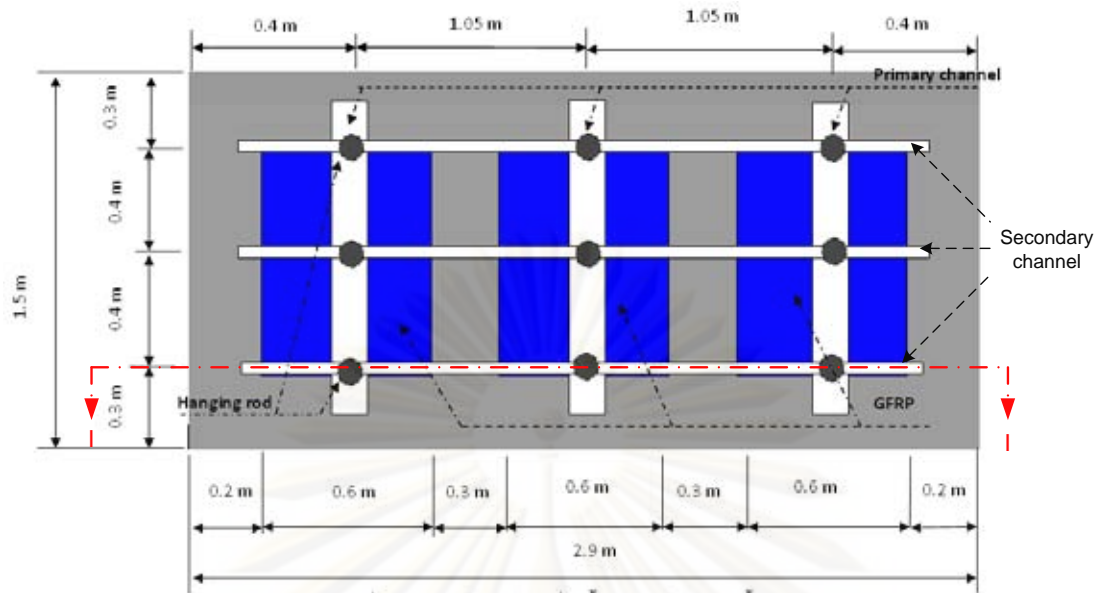


Figure 4.5 Bottom view of the specimen

Side gypsum boards and ceramic fiber blankets were used to insulate the specimen to avoid heat loss, to reduce the leakage between the furnace walls and the specimen, and to limit the heat exposure only at the bottom of the specimen. An acrylic-based firestop sealant was applied on the bottom of the gypsum board to prevent all possible heat penetration through the screws and nails. Typical cross sections as well as details of the steel profiles used in the assembly are illustrated in Figure 4.6. Details of the fasteners used in the gypsum board assembly are illustrated in Figure 4.7 and the assembly components are summarized in Table 4.1.

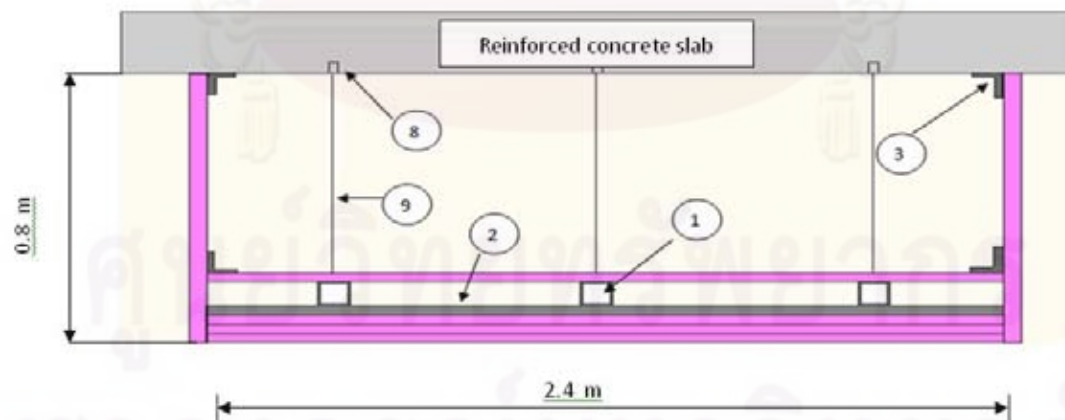


Figure 4.6 Cross section I-I of the gypsum board assembly

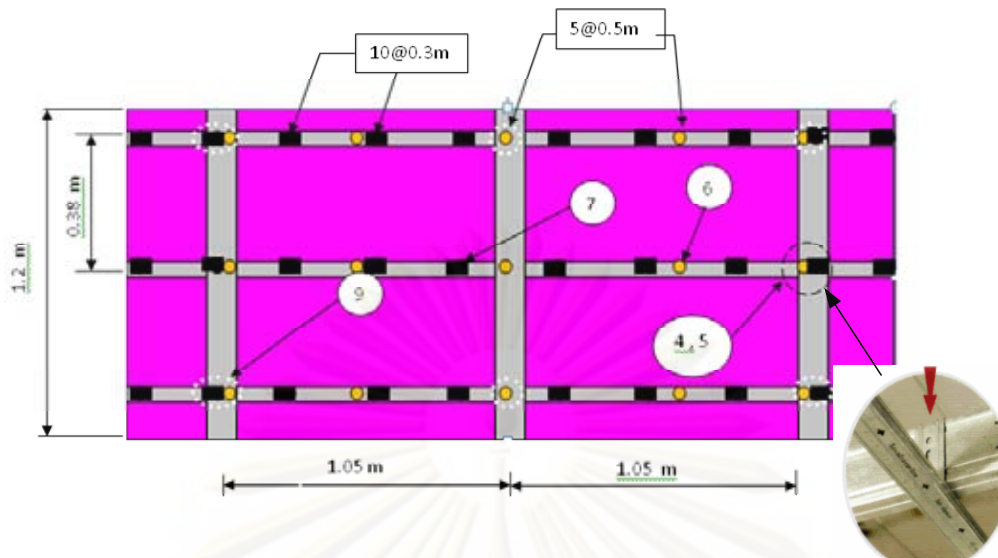
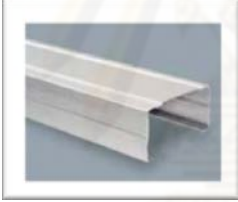








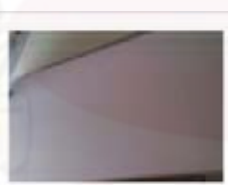






Figure 4.7 Details of the fasteners used in the gypsum board assembly

Table 4.1 Components of the gypsum board assembly

Number	Parts	Details
1		Primary channel ProWall C64 x 34 x 0.52 mm
2		Secondary channel Pro C-Line 37 x 15 x 0.52 mm
3		Side channel ProWall Angle 25 x 24 x 0.52 mm
4		Clip lock Pro MAX Connect clip 0.8mm-thick

5		Pro MAX Rigid hanger 0.1mm-thick
6		Nails 7-cm and 3-cm long for gypsum boards fasteners
7		Truss head screw size 10 mm
8		Cleat for fastening steel wire (Drop in anchor size 5/16")
9		Hanging wire (Thread rod size 5/16") with knots and vice ring (Nut and washer size 5/16")
10		Gypsum board type fire block Size: 1.2 m x 2.4 m x 15 mm Weight: 36.6 kg/sheet
11		An acrylic-based Firestop sealant

12		Gypsum board plaster for sealant materials
13		Cavity insulation material (rock wool) 50-mm thick
14		Ceramic fibers for outside insulation materials

4.1.4 Summary of Specimens Tested

Three types of gypsum board assemblies with ranging number of gypsum boards and cavity insulation were tested in this study. The description of each assembly is shown in the Table 4.2.

Table 4.2 Details of the tested gypsum board assemblies

Assembly number	Gypsum board thickness (mm)	Number of gypsum boards		Primary and secondary channels	Cavity insulation
		On the exposed side	On the unexposed side		
1	15	2	1	2-C64 x 34 x 0.52 mm 1-C34 x 15 x 0.52 mm	Rock wool
2	15	3	1	2-C64 x 34 x 0.52 mm 1-C34 x 15 x 0.52 mm	Rock wool
3	15	3	1	2-C64 x 34 x 0.52 mm 1-C34 x 15 x 0.52 mm	-

4.2 Testing Equipment

4.2.1 Instrumentation

To measure the temperature distribution within the gypsum board assembly, thermocouples were installed in various places. The thermocouples used in this study are of type K which is the most common general purpose thermocouple. This type of thermocouples is inexpensive and can measure temperatures up to 1350°C. The locations of the thermocouples are illustrated in Figure 4.8 – Figure 4.14.

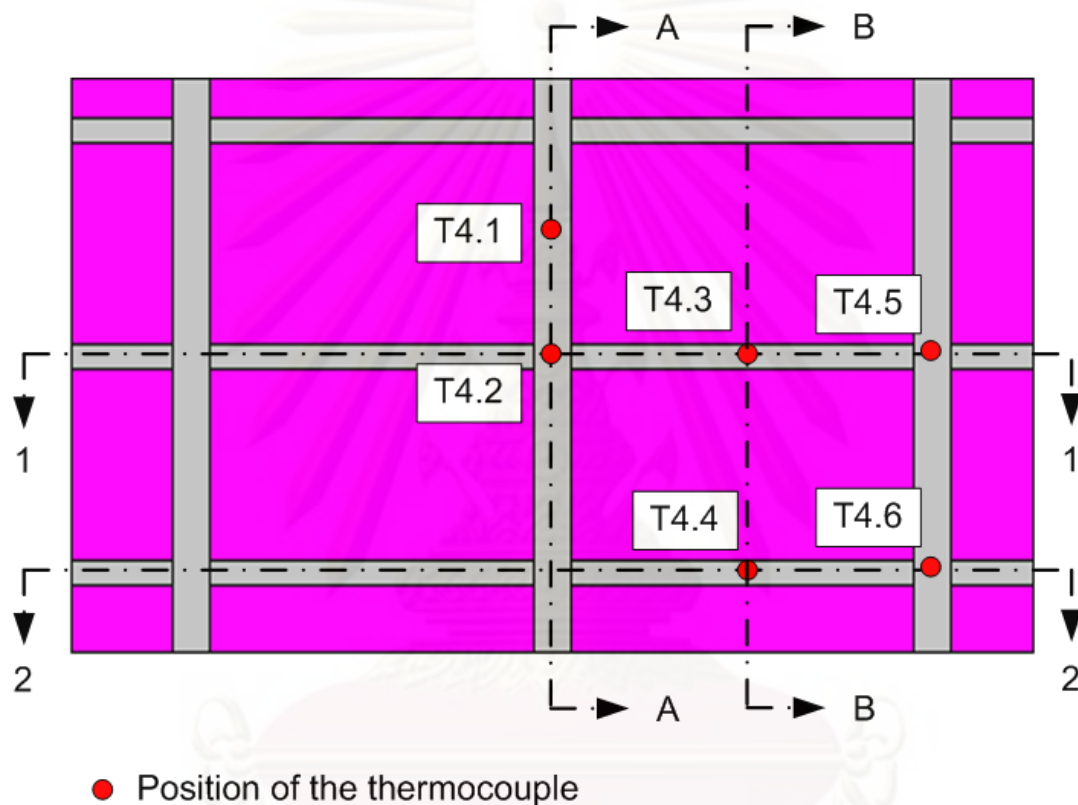


Figure 4.8 Locations of thermocouples at the unexposed face of the gypsum board assembly

ศูนย์วิทยทรัพยากร
จุฬาลงกรณ์มหาวิทยาลัย

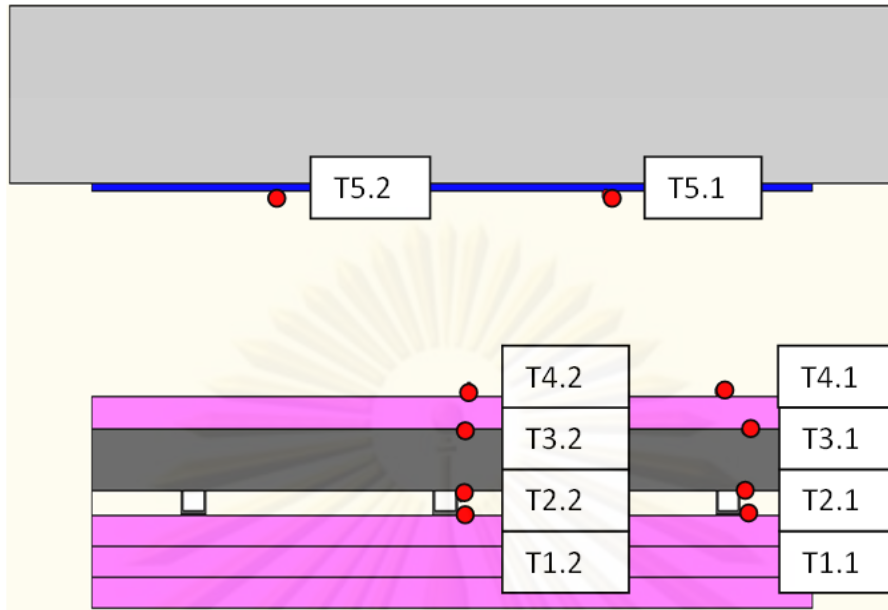


Figure 4.9 Locations of thermocouples within the cross section A-A

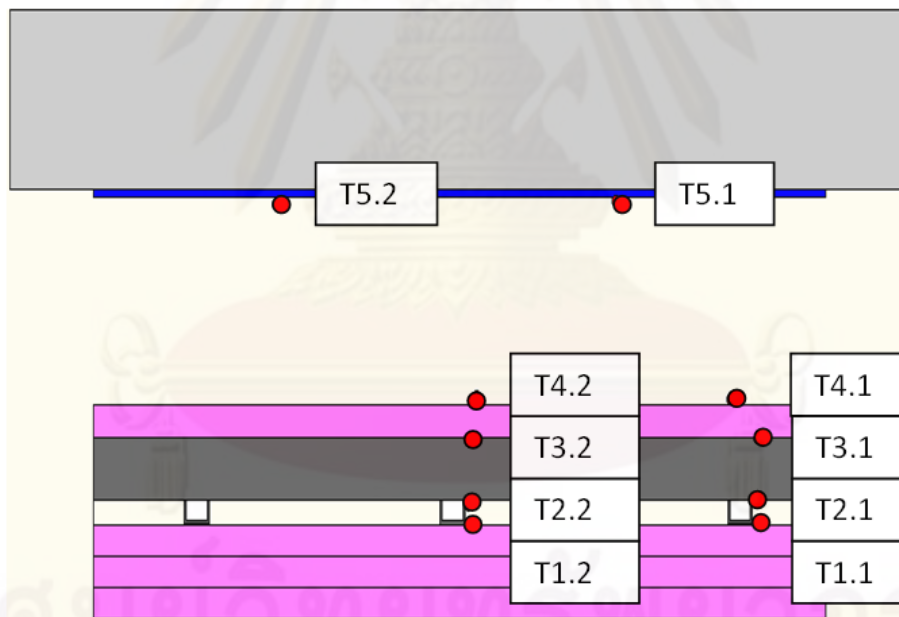


Figure 4.10 Locations of thermocouples within the cross section B-B

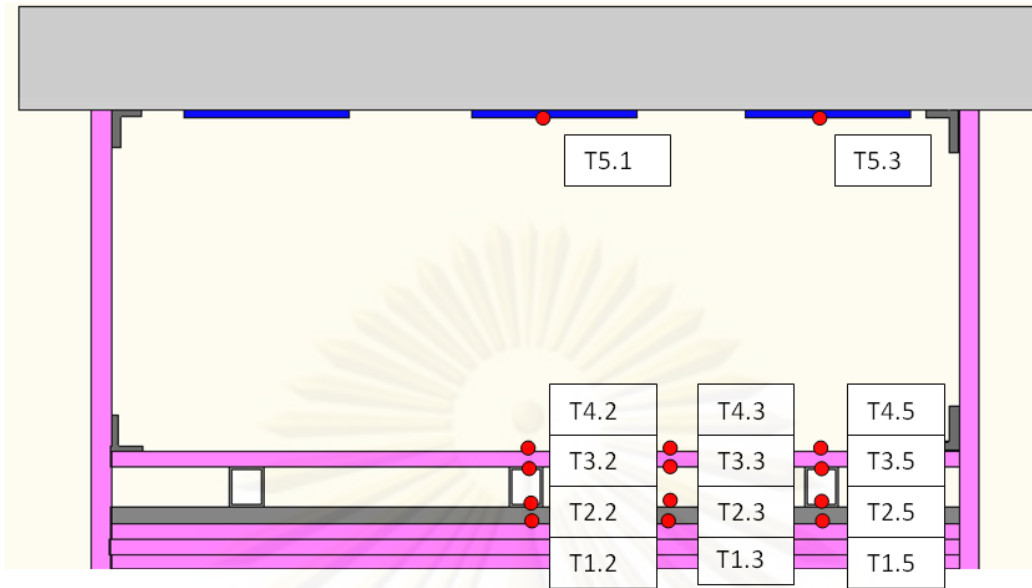


Figure 4.11 Locations of thermocouples within the cross section 1-1

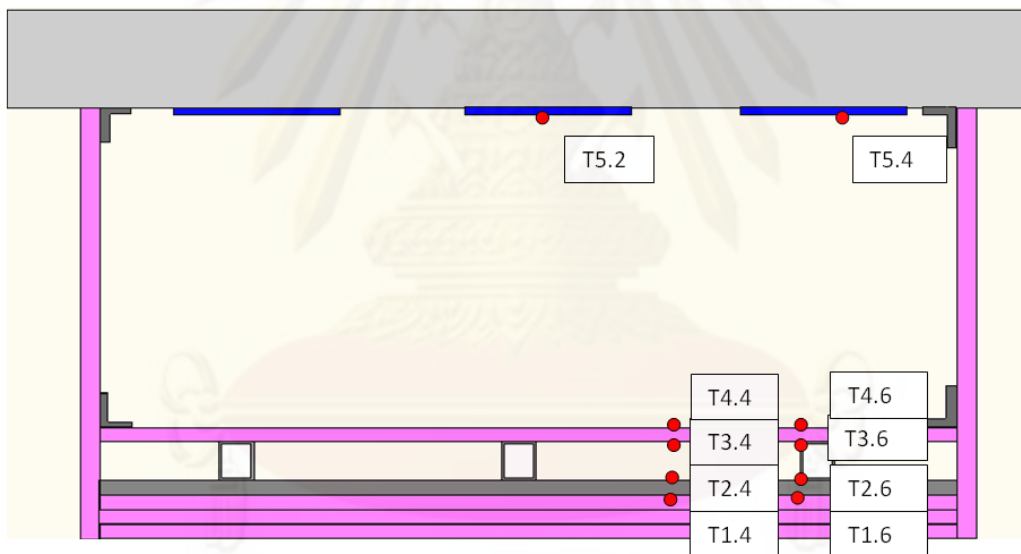


Figure 4.12 Locations of thermocouples within the cross section 2-2

ศูนย์วทยทรพยากร
จุฬาลงกรณ์มหาวิทยาลัย

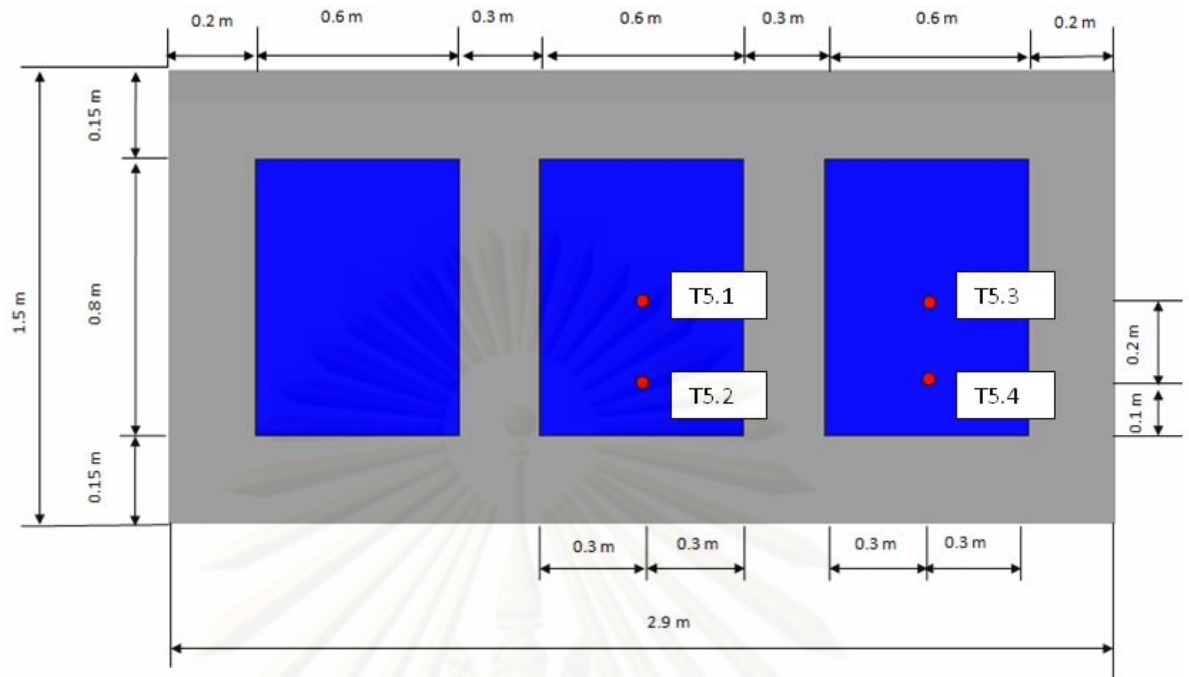


Figure 4.13 Locations of thermocouples at the FRP surfaces

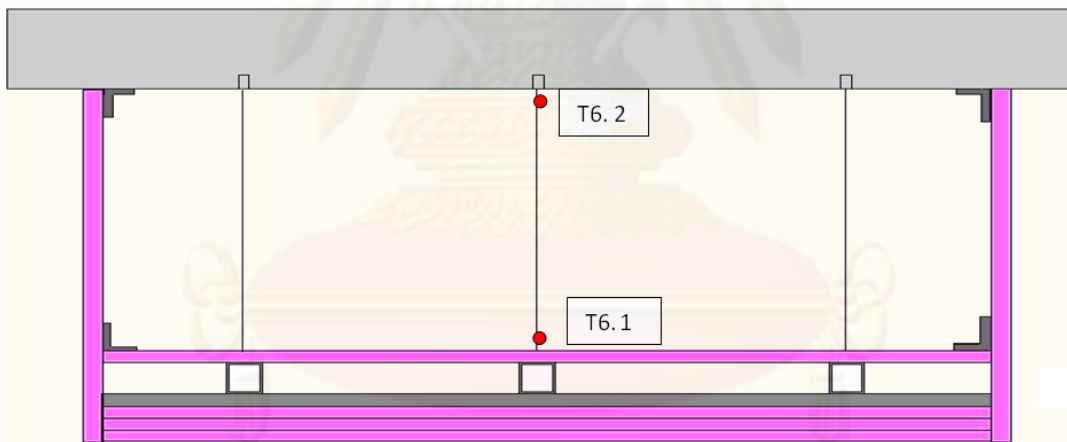


Figure 4.14 Locations of thermocouples at the hanging rods

ศูนย์วทยทรพยากร
จุฬาลงกรณ์มหาวิทยาลัย

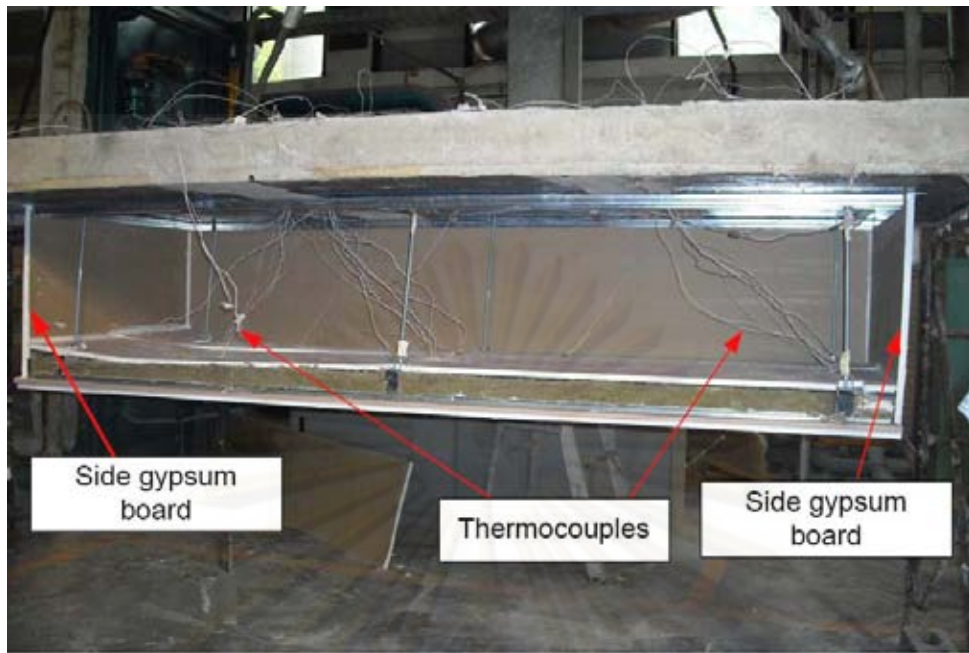


Figure 4.15 Specimen-1 with the thermocouples attached



Figure 4.16 Specimen prior to the fire test

จุฬาลงกรณ์มหาวิทยาลัย

4.2.2 Furnace

The fire resistance tests were conducted in the Fire Safety Research Center (FSRC) of Chulalongkorn University, Thailand. The furnace used in this study, as illustrated in Figure 4.17 and Figure 4.18, has six burners and six furnace thermocouples to control the furnace's temperatures during the tests. The furnace thermocouples along with the thermocouples attached across the gypsum board assembly were connected to the data logger. The data logger recorded the temperatures measured from the thermocouples during the fire test and sent data to the laboratory computer. These data were later analyzed and used to validate the computational model.

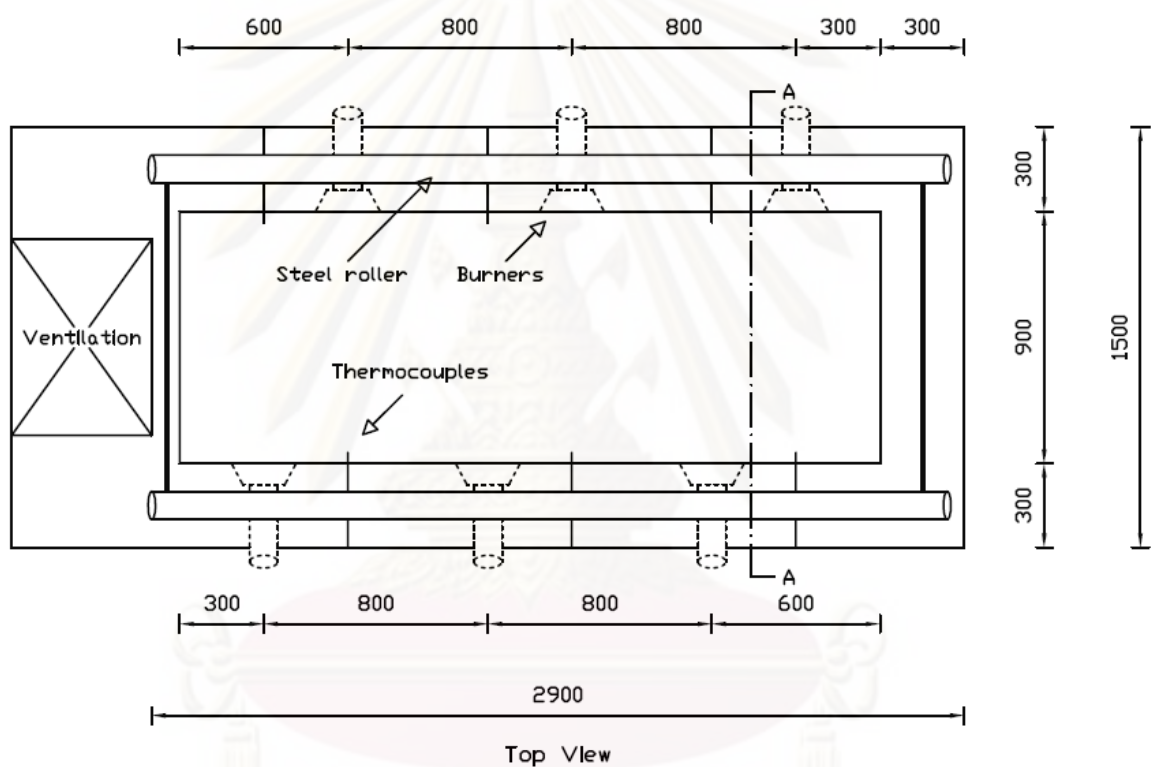


Figure 4.17 Top view of the furnace

ศูนย์วิทยทรัพยากร
จุฬาลงกรณ์มหาวิทยาลัย

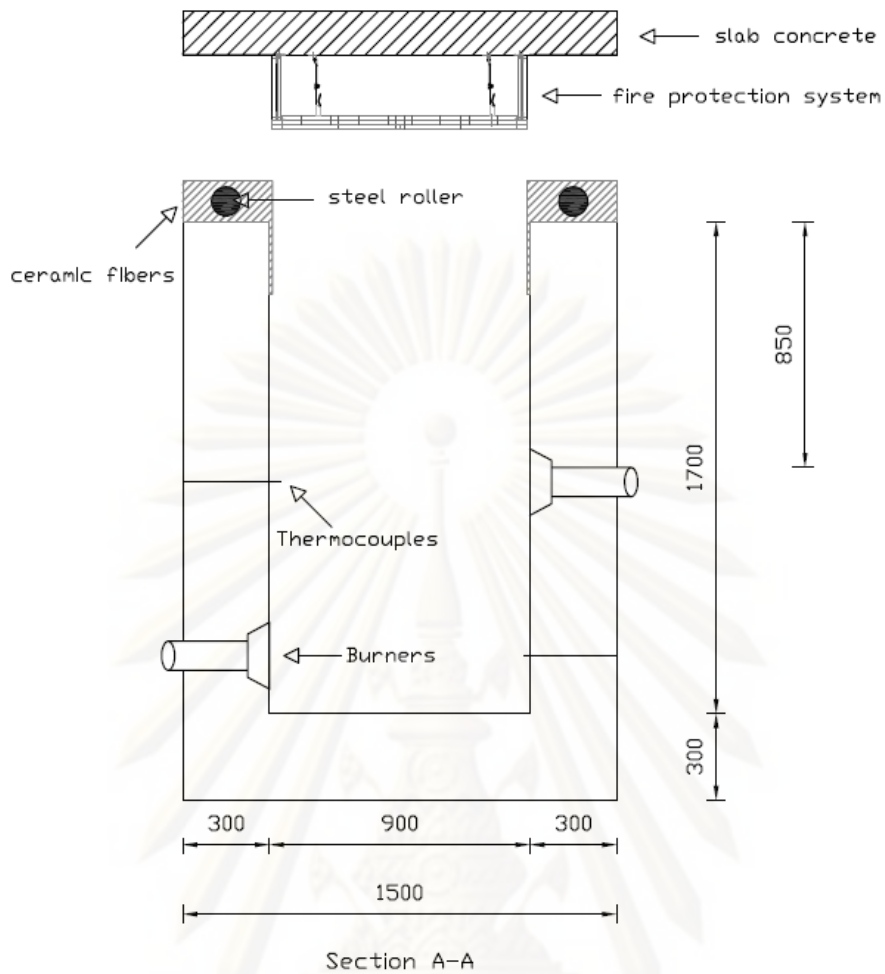


Figure 4.18 Furnace cross section

4.3 Testing Procedures

4.3.1 Fire Exposure

The conditions during testing were controlled in accordance with ISO 834 (2002) using two parameters: furnace temperatures and furnace pressure. The average temperature of the furnace was monitored and controlled such that it followed the relationship:

$$T = 345 \log_{10} (8t + 1) + 20 \quad (4.1)$$

where T is the average temperature within the furnace ($^{\circ}\text{C}$) and t is the time during the experiment (minute).

The 2-hour duration of the time-temperature curve based on Eq. (4.1) is illustrated in Figure 4.19

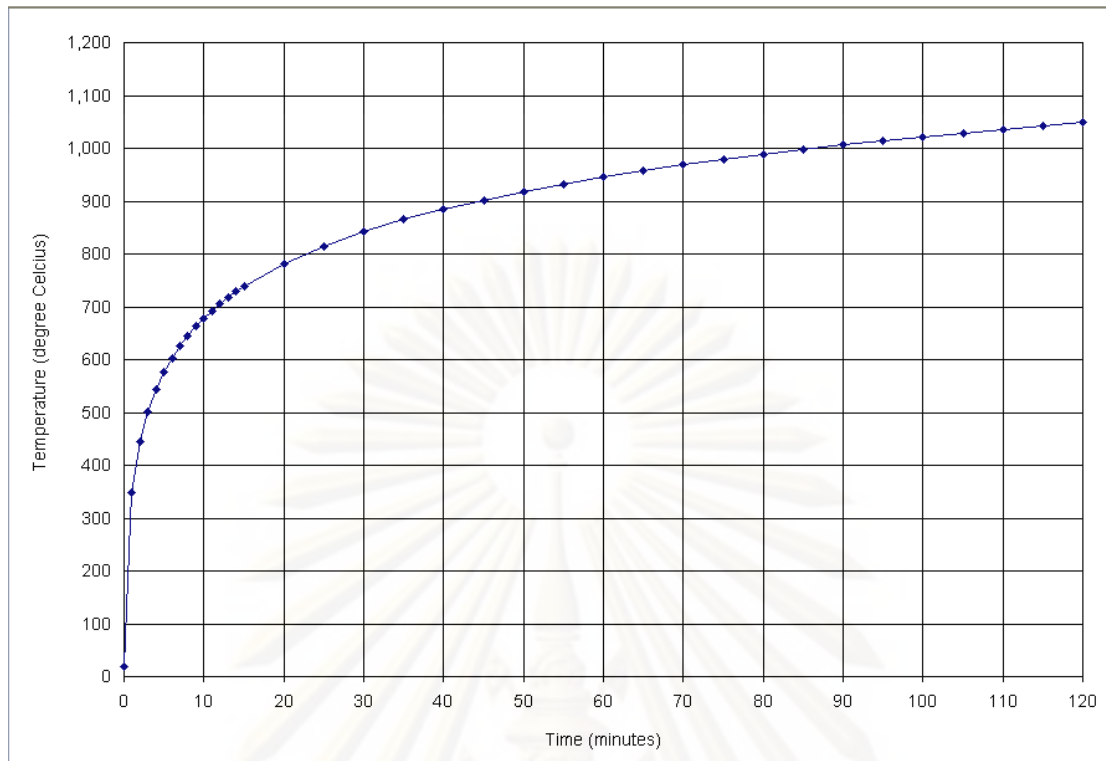


Figure 4.19 Standard Time-Temperature Curve (ISO 834 2002)

For the horizontal element, ISO 834 (2002) recommends that the furnace shall be operated such that a pressure of 20 Pa is established at the position 100 mm below the underside of the test specimen.

4.3.2 Performance Criteria

For the current study only the insulation criterion is considered. The insulation criterion is expressed in terms of a critical temperature at the epoxy adhesive to maintain the effectiveness of the FRP strengthening system. Based on the experimental works of Gamage *et al.* (2005), the critical temperature for determining the fire resistance rating of the gypsum board assembly is set to 70°C, the temperature at which the epoxy adhesive starts to debond.

4.4 Observations after the Fire Tests

Figure 4.20 shows the actual time-temperature curves produced within the furnace for the three fire tests in this study. Considering the difficulties involved in controlling the furnace, the operators achieved reasonable approximation of the desired curves, except for the test on assembly number 2. The temperature distributions within the gypsum board assembly during the fire resistance tests are presented in the next chapter. Each specimen was carefully observed and documented after each test. These observations are shown in Figure 4.21 – Figure 4.22.

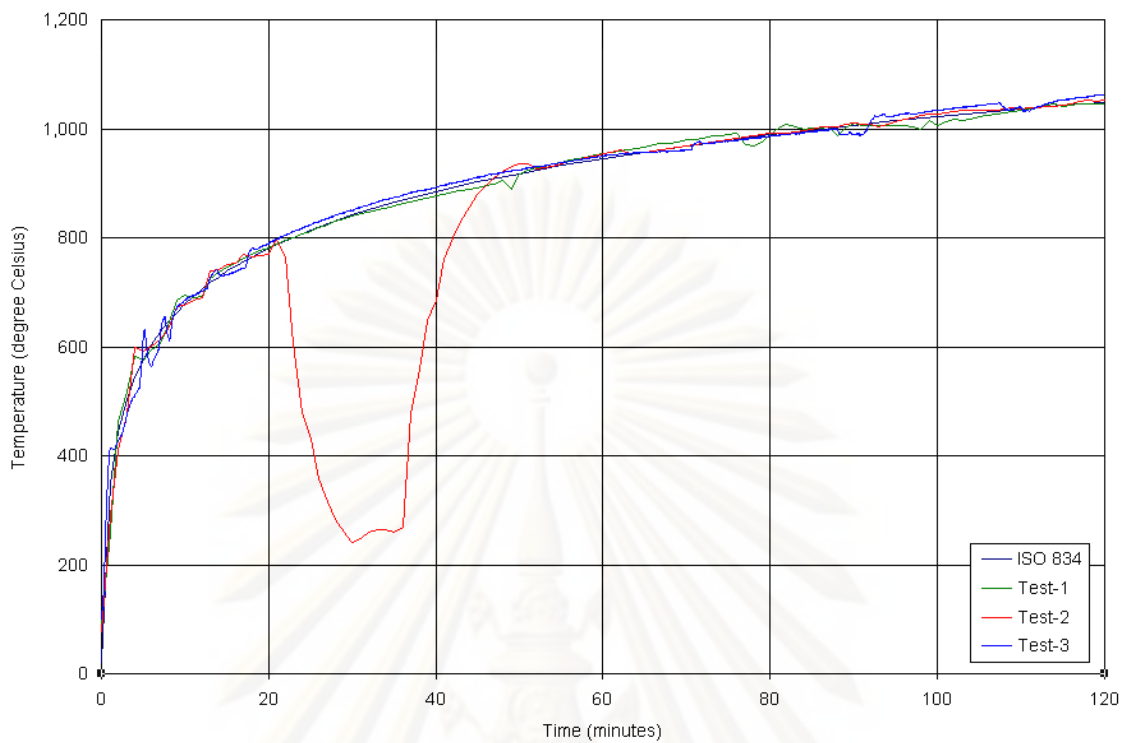


Figure 4.20 Actual time-temperature curves during the tests vs. standard ISO 834 time-temperature curve

4.4.1 Specimen-1

After the test, the specimen was cooled down for 24 hours before observation. As shown in Figure 4.21, it was observed that both of the gypsum board layers on the exposed surface had been completely fallen off. The steel channels, primary and secondary, were burnt but still intact. The secondary channel in the middle part was severely distorted and most of the insulation material was gone. One quarter of the gypsum board on the unexposed side fell off, causing the GFRP strengthening system to be exposed to fire. From the visual examination as documented in Figure 4.22, the GFRP was still intact and delamination was not observed in any part.

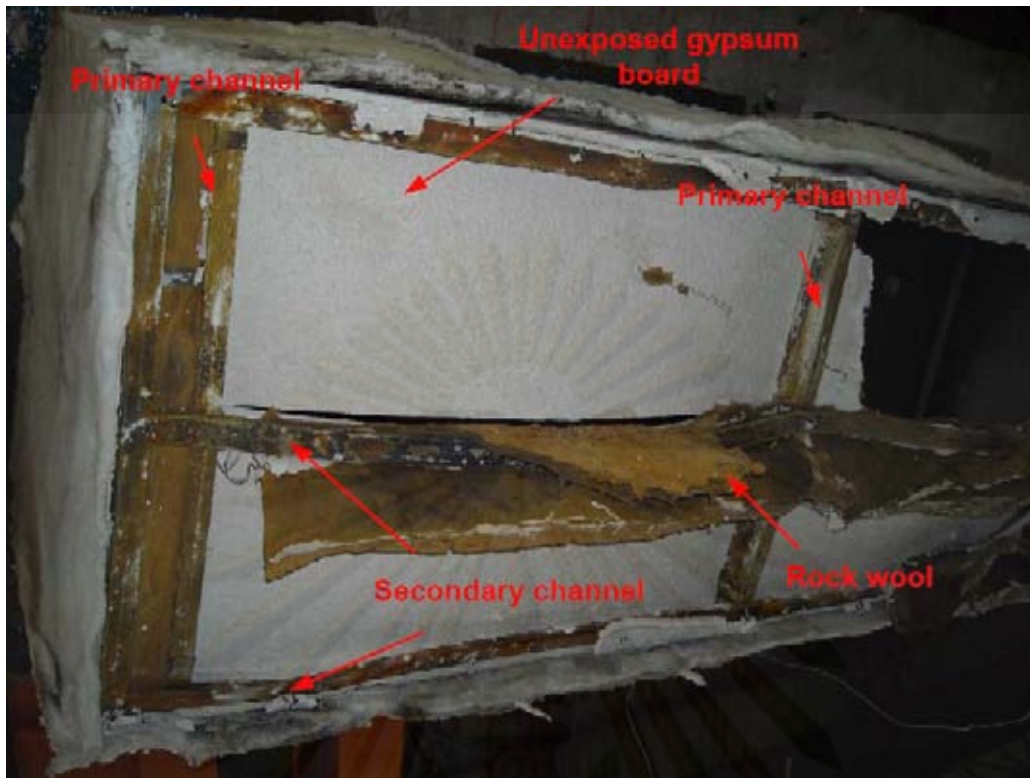


Figure 4.21 Specimen-1 after the fire test



Figure 4.22 The GFRP strengthening system in specimen-1 after the fire test

4.4.2 Specimen-2

Specimen-2 also was cooled down for 24 hours before visual examination. As shown in Figure 4.23, all three of the gypsum board layers on the exposed surface also fell off similar to specimen-1. But for specimen-2, some of the gypsum boards were still intact. Only half of the steel sections, either primary or secondary channel, appeared to be burnt off and none of them were distorted. The insulation material was still intact and only small cracks were observed in some parts of the material.

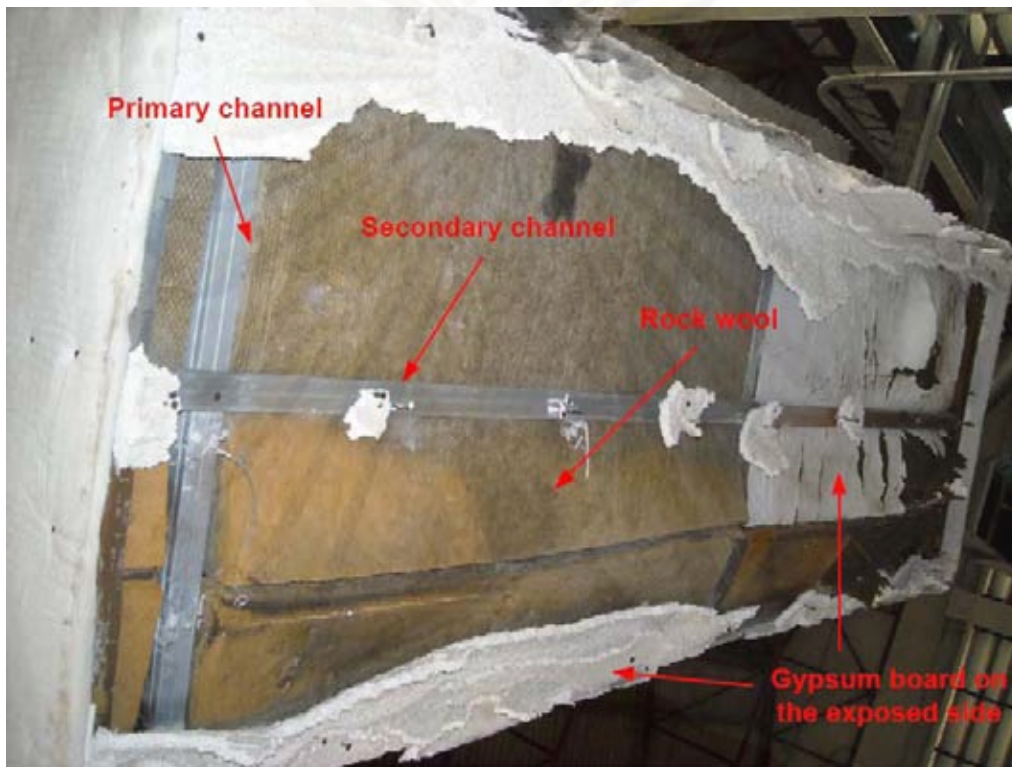


Figure 4.23 Specimen-2 after the fire test

4.4.3 Specimen-3

The condition of specimen-3 after fire test is shown in Figure 4.24. Some of the gypsum board layers on the exposed surface appeared to be still perfectly intact. Cracks on the gypsum board surface were observed, which were assumed to be due to the dehydration process of the gypsum boards.



Figure 4.24 Specimen-3 after the fire test

CHAPTER V

RESULTS AND DISCUSSION

5.1 Experimental Results

The temperature distributions within the gypsum board assemblies during the fire resistance tests are presented in this chapter. The measured temperatures were recorded from the thermocouples installed within each assembly at six different levels. The individual temperature readings from each of these levels were plotted for consistency check before further analyses in which spurious results were eliminated. The locations at which temperature readings were taken are illustrated on the upper left side of each graphic. Faulty temperature readings due to detachment of the thermocouples from the surface were also observed and the data from these thermocouples were omitted from the graphic.

5.1.1 Thermocouples at level 1

The thermocouples were placed at various locations on the surface of the exposed gypsum board facing the cavity (level 1). Some of these locations were at the interface between the exposed gypsum board and the secondary channel (T1.2, T1.3, T1.4, and T1.5) while others were at the interface between the exposed gypsum board and either the insulation material or the air cavity. The average temperatures from these thermocouples (T1) on assembly 1, assembly 2 and assembly 3 are illustrated in Figure 5.1, Figure 5.2 and Figure 5.3, respectively.

A long plateau at approximately 100°C can be observed for all assemblies, as shown in Figure 5.1, Figure 5.2 and Figure 5.3. This phenomenon, commonly referred to as the “time delay”, is due to the dehydration process of the gypsum board. When exposed to fire the free water and chemically combined water is gradually driven off at temperatures above approximately 100°C. The removal process of chemically combined water is called calcination or dehydration. The calcination begins on the exposed face and progressively works through the gypsum board. This process requires absorption of a large quantity of heat, thus causing heat transmission through gypsum to be retarded until calcination had been completed (Takeda and Mehaffey 1998). The average temperature on the surface of the exposed gypsum board facing the cavity (T1) was effectively limited to approximately 120°C, until the calcination process reached that surface. Once this occurred, the temperature T1 rose quickly. From Figure 5.1, Figure 5.2 and Figure 5.3, it can be observed that this phenomenon occurred at the 58th, 110th, and 107th minute for assembly 1, 2 and 3,

respectively. The length of this plateau generally depends on the density, composition and thickness of the gypsum board (Gerlich 1995).

Due to the dehydration process, the gypsum board may shrink causing it to pull away from nailed or screwed connections. Fire resisting gypsum boards, as used in this study, contain glass fibers that can control shrinkage by making a maze of fine cracks, instead of a single large crack as in regular gypsum boards, causing the delay on the fall off time of the boards. As the heating continues, the gypsum board undergoes chemical and physical changes and transforms into calcium sulphate anhydrite which has the appearance of dry cohesionless powder, resulting in the fall off of the board. The process by which consecutive thin layers of a material are shed as the material undergoes heating is called ablation (Thomas 2002). The duration between the dehydration process and the gypsum board fall off time depends on the glass fiber reinforcement that holds the board together. Buchanan (2001) has suggested that the fire resisting gypsum board will not fall off until the entire board reaches the temperature of about 700°C. Konig and Walleij (2000) and Sultan (1996) have reported that the critical falling-off temperatures are around 600°C for gypsum board ceiling linings.

Figure 5.1 illustrates that the average temperature on the surface of the exposed gypsum board facing the cavity (T1) of assembly 1 at the 120th minute is higher than 800°C, meaning that the ablation process had occurred and that the exposed gypsum boards had fallen off. This was confirmed by visual observation, as illustrated in Figure 4.22. Figure 5.2 illustrates that the average temperature T1 of assembly 2 at the 120th minute is 720°C, meaning that the exposed gypsum boards had also fallen off. From Figure 4.23 it can be seen that most of the exposed gypsum boards of assembly 2 had fallen off and only some were still intact. Figure 5.3 illustrates that the average temperature T1 of assembly 3 at the 120th minute is lower than 600°C, meaning that the exposed gypsum boards were still intact. From Figure 4.24 it is confirmed that the last layer of the exposed gypsum board was still intact. This means that the ablation process had occurred only for the first and second layer of the exposed gypsum boards. The maze cracks, indicating the shrinkage process on the gypsum board, could be observed on the surface of the remaining gypsum boards as seen in Figure 4.24.

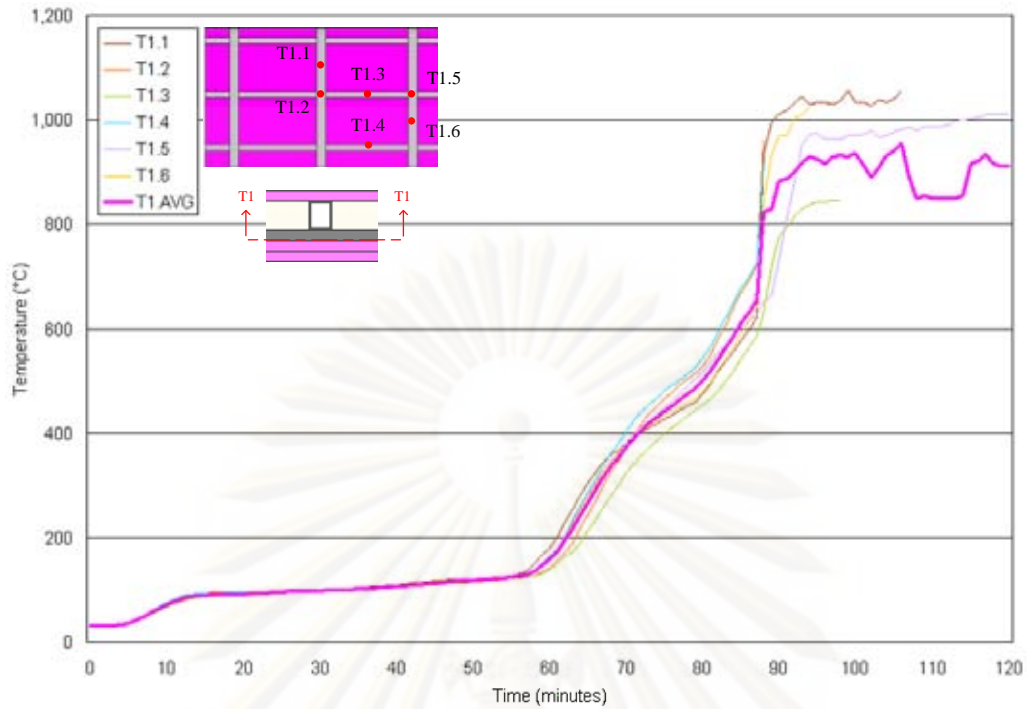


Figure 5.1 Time-temperature relationship at the surface of the exposed gypsum board facing cavity (T1) of assembly 1 during the fire test

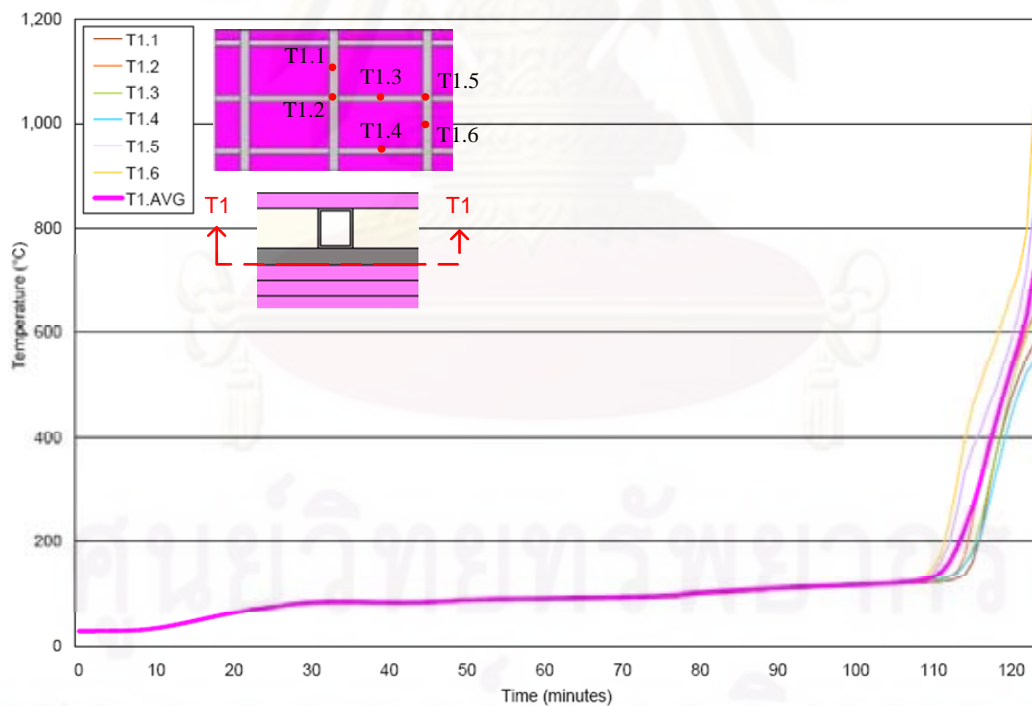


Figure 5.2 Time-temperature relationship at the surface of the exposed gypsum board facing cavity (T1) of assembly 2 during the fire test

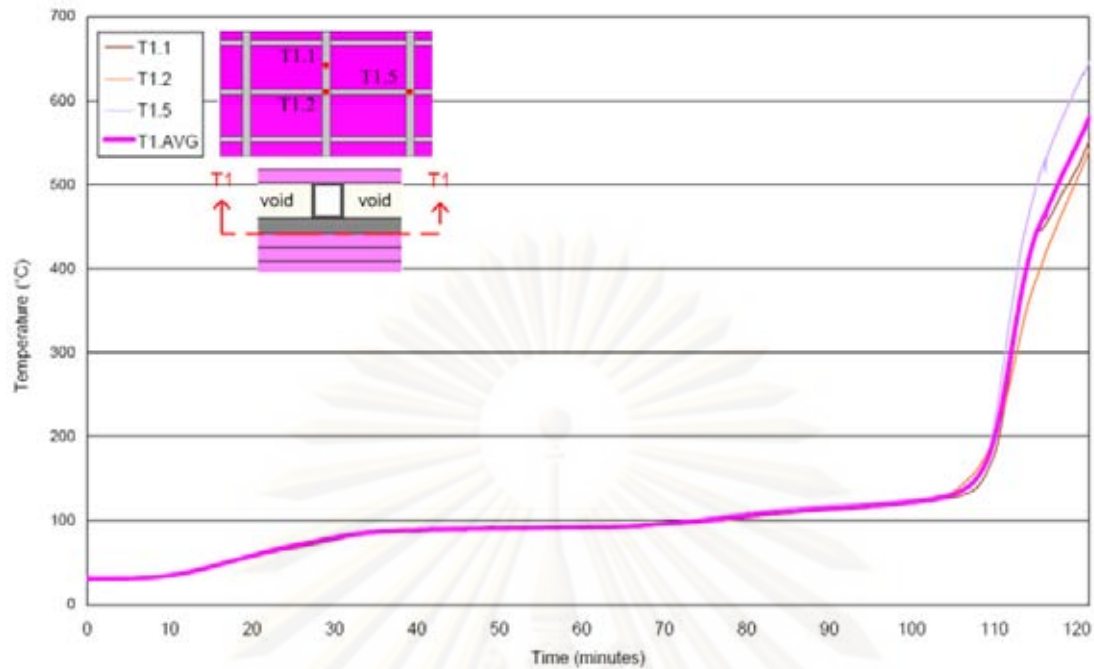


Figure 5.3 Time-temperature relationship at the surface of the exposed gypsum board facing cavity (T1) of assembly 3 during the fire test

5.1.2 Thermocouples at level 2

The thermocouples were also installed at various locations on the top of the secondary channels (level 2). Some of these locations were at the interface between the secondary channels and the primary channels (T2.2 and T2.5) while others were at the interface between the secondary channels and either the insulation material or the air cavity. The average temperature from these thermocouples (T2) on assembly 1, assembly 2 and assembly 3 are illustrated in Figure 5.4, Figure 5.5 and Figure 5.6, respectively.

The time-temperature relationship for T2 is identical to that for T1, but with slightly lower values, as long as the exposed gypsum boards were intact. Once the exposed gypsum boards were lost, the average temperature T2 increased rapidly with the furnace temperature. From Figure 5.4 it can be seen that this phenomenon occurred at the 87th minute. According to Gerlich (1995), the cold-formed steel which is normally used as steel channels in the gypsum board assembly loses its strength due to elevated temperatures. The current practice to ensure the performance of steel studs within the gypsum board assembly is by limiting the temperature of the steel studs to 400°C. This practice is to ensure that the steel yield strength is not reduced to less than about 60% due to the temperature effects. The cold-formed steel can be considered to lose all its strength when its temperature exceeds 700°C. As shown in Figure 5.4, the temperature T2 of assembly 1 exceeded 700°C at the end of the fire test. This means that the steel (the secondary channel) had yielded, as confirmed in Figure 4.22. Meanwhile, the average temperatures of the secondary channels for assembly 2 and assembly 3 are 560°C and 440°C, respectively.

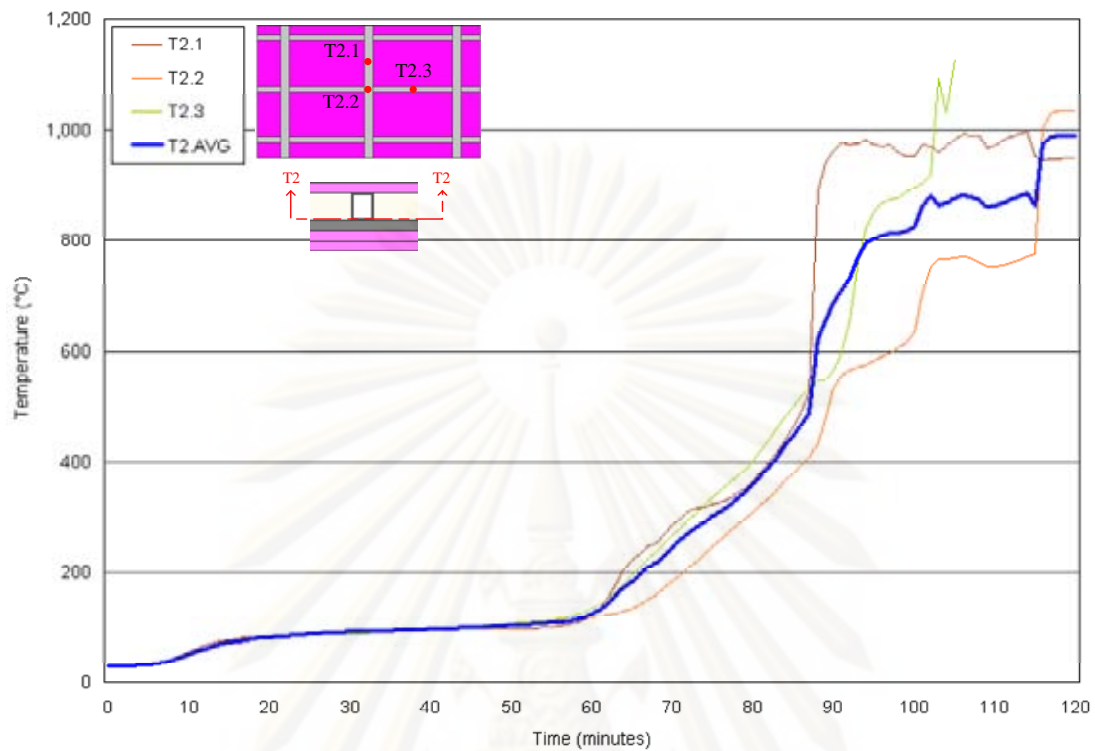


Figure 5.4 Time-temperature relationship at the interface between the secondary channel and the primary channel (T2) of assembly 1 during the fire test

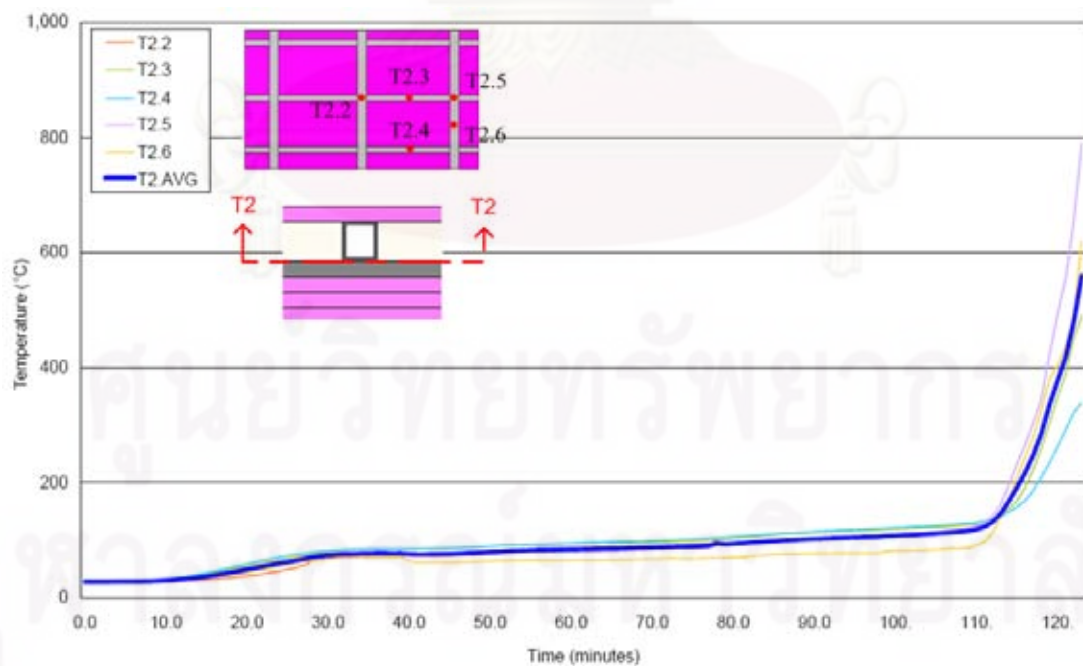


Figure 5.5 Time-temperature relationship at the interface between the secondary channel and the primary channel (T2) of assembly 2 during the fire test

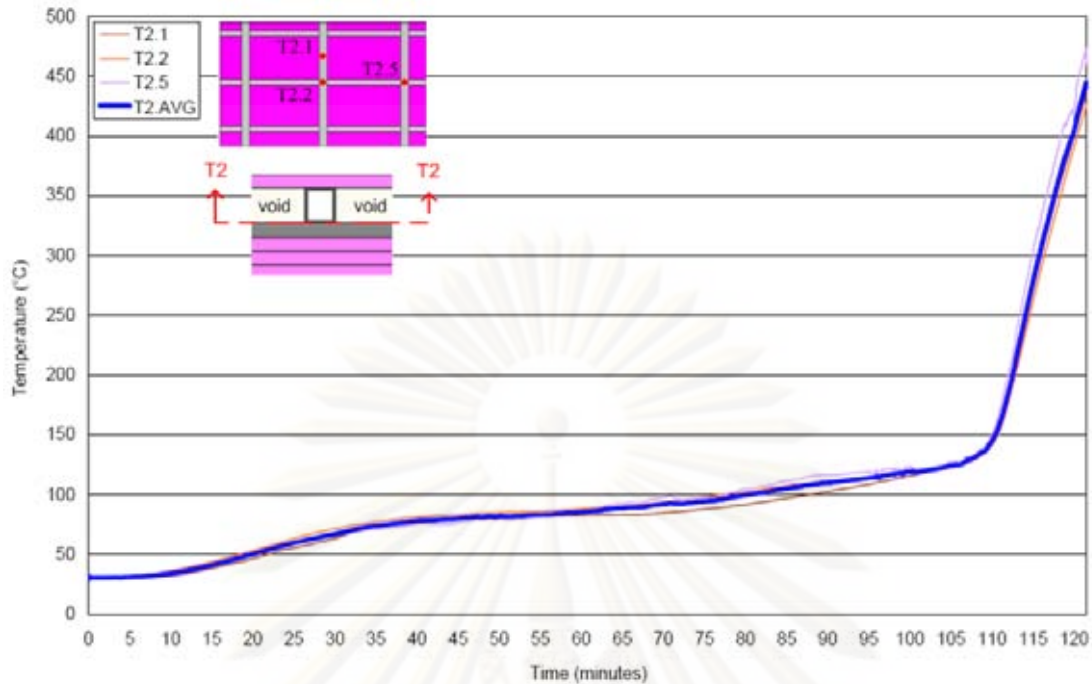


Figure 5.6 Time-temperature relationship at the interface between the secondary channel and the primary channel (T2) of assembly 3 during the fire test

5.1.3 Thermocouples at level 3

The thermocouples were installed at various locations on the top of the primary channels (level 3). These locations were at the interface between the primary channels and the surface of the unexposed gypsum board facing the cavity. The average temperature from these thermocouples (T3) on assembly 1, assembly 2 and assembly 3 are illustrated in Figure 5.7, Figure 5.8 and Figure 5.9, respectively.

The average temperatures on the primary channels (T3) at the end of the fire tests for assemblies 1, 2 and 3 are 964°C, 173°C and 218°C, respectively. The high value of T3 for assembly 1 was probably due to the fact that the exposed gypsum boards and the insulation material of this assembly had fallen off, thus exposing the steel directly to the furnace temperature. For assembly 2, even though the exposed gypsum boards had also fallen off but the secondary channels were not distorted, thus enabling the insulation material to stay intact and protect the primary channels.

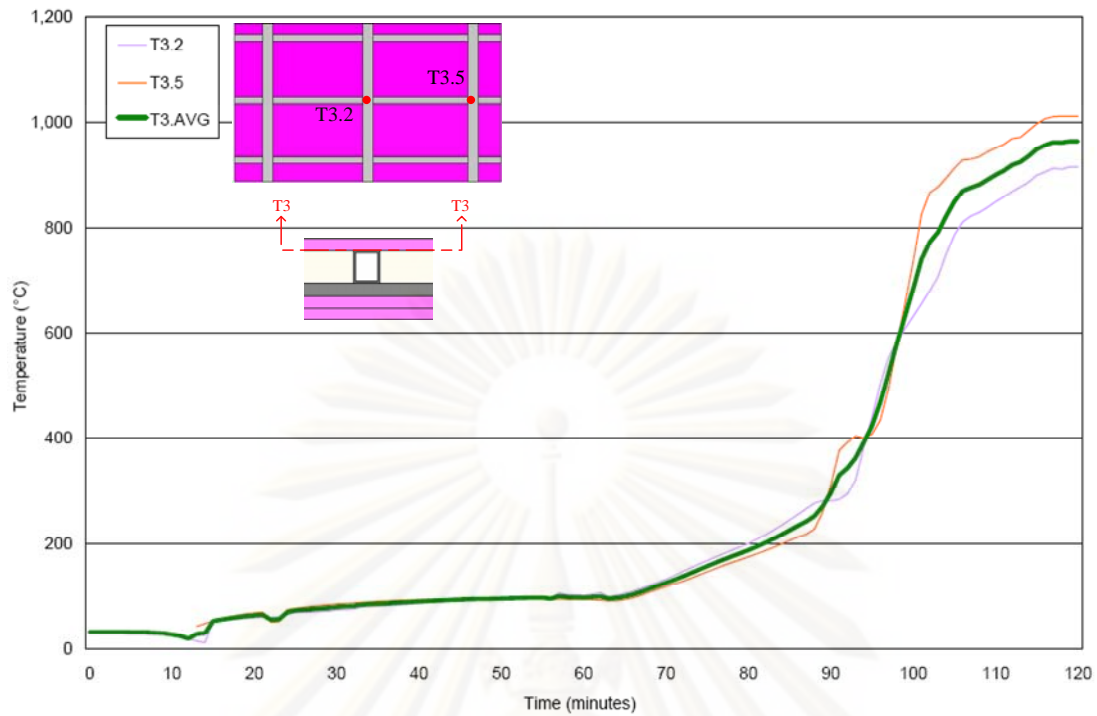


Figure 5.7 Time-temperature relationship at the interface between the primary channel and the unexposed gypsum board (T3) of assembly 1 during the fire test

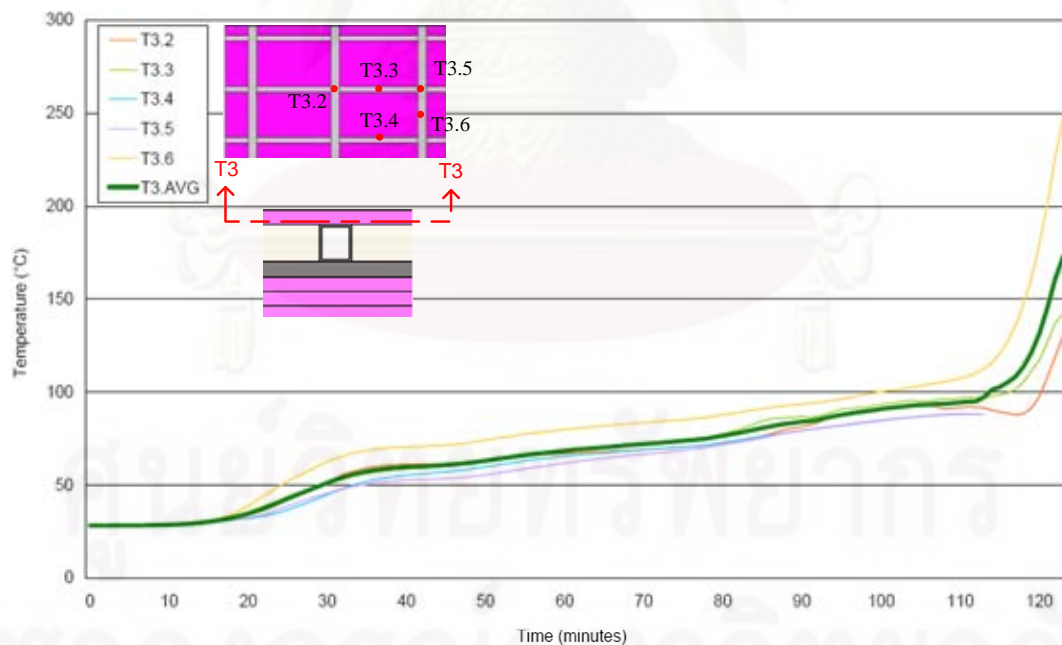


Figure 5.8 Time-temperature relationship at the interface between the primary channel and the unexposed gypsum board (T3) of assembly 2 during the fire test

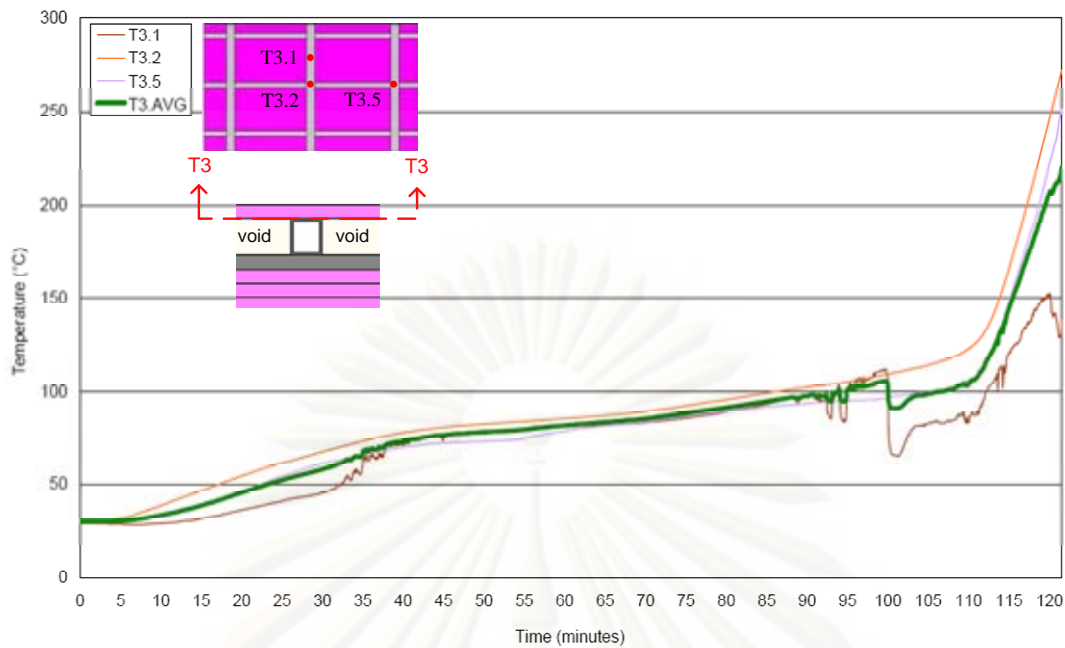


Figure 5.9 Time-temperature relationship at the interface between the primary channel and the unexposed gypsum board (T3) of assembly 3 during the fire test

5.1.4 Thermocouples at level 4

The thermocouples were installed at various locations on the top of the unexposed gypsum board (level 4). The average temperatures from these thermocouples (T4) on assembly 1, assembly 2 and assembly 3 are illustrated in Figure 5.10, Figure 5.11 and Figure 5.12, respectively. The average temperatures on the unexposed surface (T4) at the end of the fire tests for assemblies 1, 2 and 3 are 425°C, 81°C and 112°C, respectively. The reason for the high value of T4 for assembly 1 was probably due to the falling off of some part of the unexposed gypsum board, as shown in Figure 4.22. Once cracking of the unexposed lining occurred, the hot gases could pass into the cavity and increased the temperature on the unexposed surface.

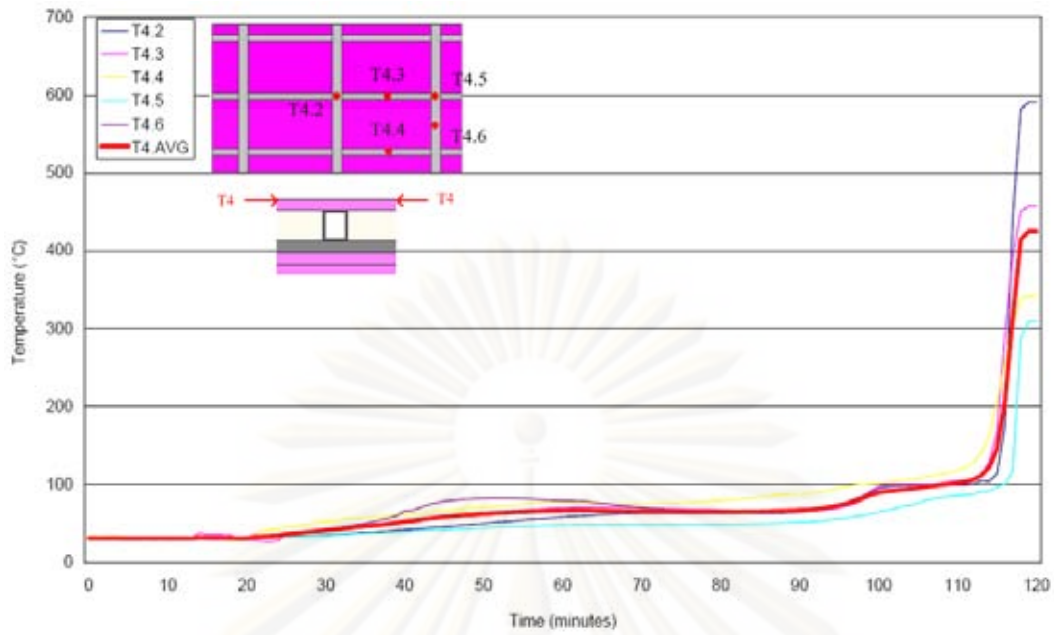


Figure 5.10 Time-temperature relationship at the top of the unexposed gypsum board (T4) of assembly 1 during the fire test

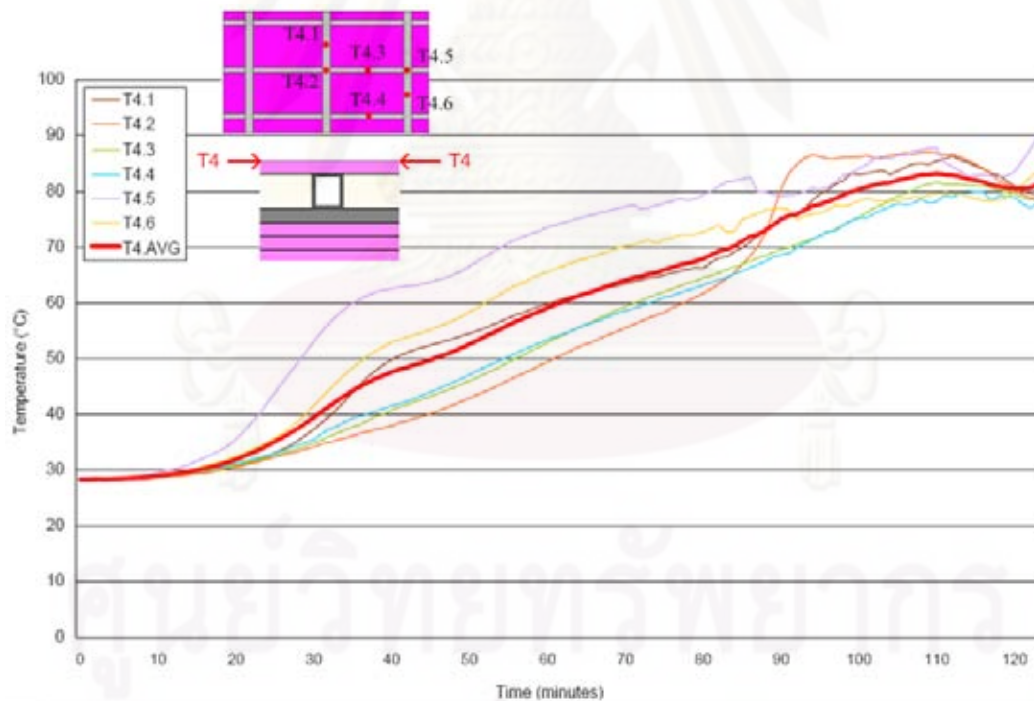


Figure 5.11 Time-temperature relationship at the top of the unexposed gypsum board (T4) of assembly 2 during the fire test

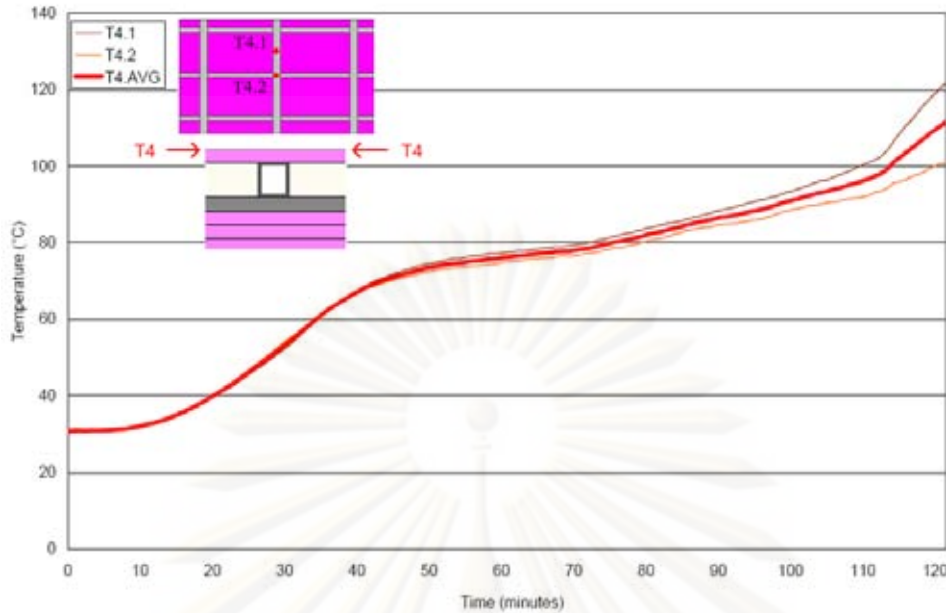


Figure 5.12 Time-temperature relationship at the top of the unexposed gypsum board (T4) of assembly 3 during the fire test

5.1.5 Thermocouples at level 5

The thermocouples are placed at various locations on the surface of the GFRP strengthening system (level 5). The measured temperatures from these thermocouples (T5) on assembly 1, assembly 2, and assembly 3 are illustrated in Figure 5.13, Figure 5.14, and Figure 5.15, respectively.

A failure criterion for determining the fire resistance rating in this study is that the temperature at the epoxy adhesive is less than 70°C. As shown in Figure 5.13, Figure 5.14 and Figure 5.15 the average temperatures at level 5 on assembly 1, assembly 2 and assembly 3 reached the value of 70°C at 104th minute, at 120th minute and at 83rd minute, respectively. However since there were some errors regarding the furnace control during testing of assembly 2, as shown in Figure 4.20, the fire resistance rating of this assembly is not conclusive. Even though the gypsum board assemblies (assembly 1 and assembly 3) could not satisfy the designated 2-hour fire resistance rating, these assemblies gave better performance in protecting FRP strengthening systems compared to the other fire protection systems used in the previous studies (Blontrock *et al.* 2001; Bisby *et al.* 2005; Gamage *et al.* 2005; Barnes and Fidel 2006; Williams *et al.* 2006; Kexu *et al.* 2007; Kodur *et al.* 2007; and Stratford *et al.* 2009). This means that the gypsum board assembly showed great performance in protecting the FRP strengthening system and is possible in providing the 2-hour fire resistance rating when it is properly designed.

The average temperatures at level 5 on assembly 1, assembly 2 and assembly 3 at the end of fire tests were 99°C, 68°C and 89°C, respectively. According to Gamage *et al.* (2005), when the epoxy temperature reaches 70°C the FRP

strengthening systems are assumed to have been debonded already. However, based on the visual observation at the end of the fire tests, the FRP strengthening systems in this study did not show any delamination behaviour. This indicates that the type of epoxy used in the current study may have a higher glass transition temperature (T_g) than that used in Gamage *et al* (2005). When the temperature of the epoxy in the FRP strengthening system exceeds T_g , the FRP strengthening system usually delaminates from the structure. Since the FRP strengthening system in this study had not shown any delamination, it is reasonable to assume that the epoxy temperature did not exceed its T_g and thus the effectiveness of the FRP strengthening system was still assured. However, further studies need to be done to determine whether the effectiveness of the FRP strengthening systems is directly related with the delamination of the systems.

From Figure 5.13 and Figure 5.15, it is noticed that the behaviour of gypsum board assembly 1 is similar to that of assembly 3 in terms of the ultimate temperatures at the end of the fire tests. However, note that the insulation failure criteria based on ISO 834 are that neither the average temperature on the unexposed surface increases by more than 140°C above the initial temperature nor the temperature at any point increases by more than 180°C. It was found that the average temperature on the unexposed surface for assembly 1 was 425°C, while the average temperature on the unexposed surface for assembly 3 was 112°C. Thus, assembly 1 can be considered failed based on the insulation criteria even though it could prevent the delamination process of the FRP strengthening system.

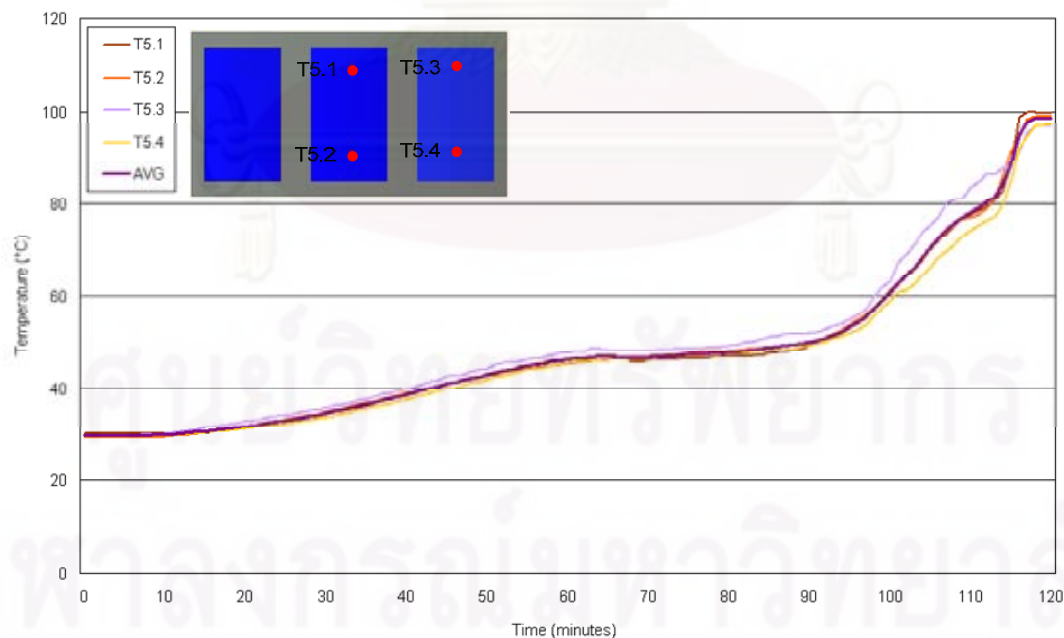


Figure 5.13 Time-temperature relationship at the surface of GFRP (T5) of assembly 1 during the fire test

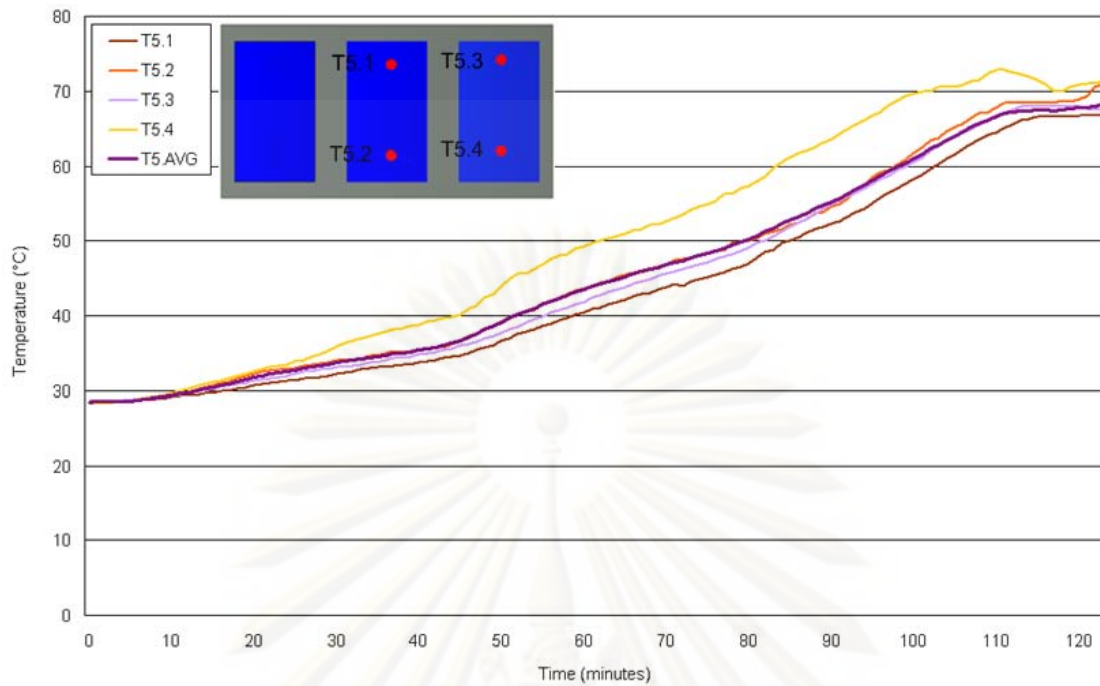


Figure 5.14 Time-temperature relationship at the surface of GFRP (T5) of assembly 2 during the fire test

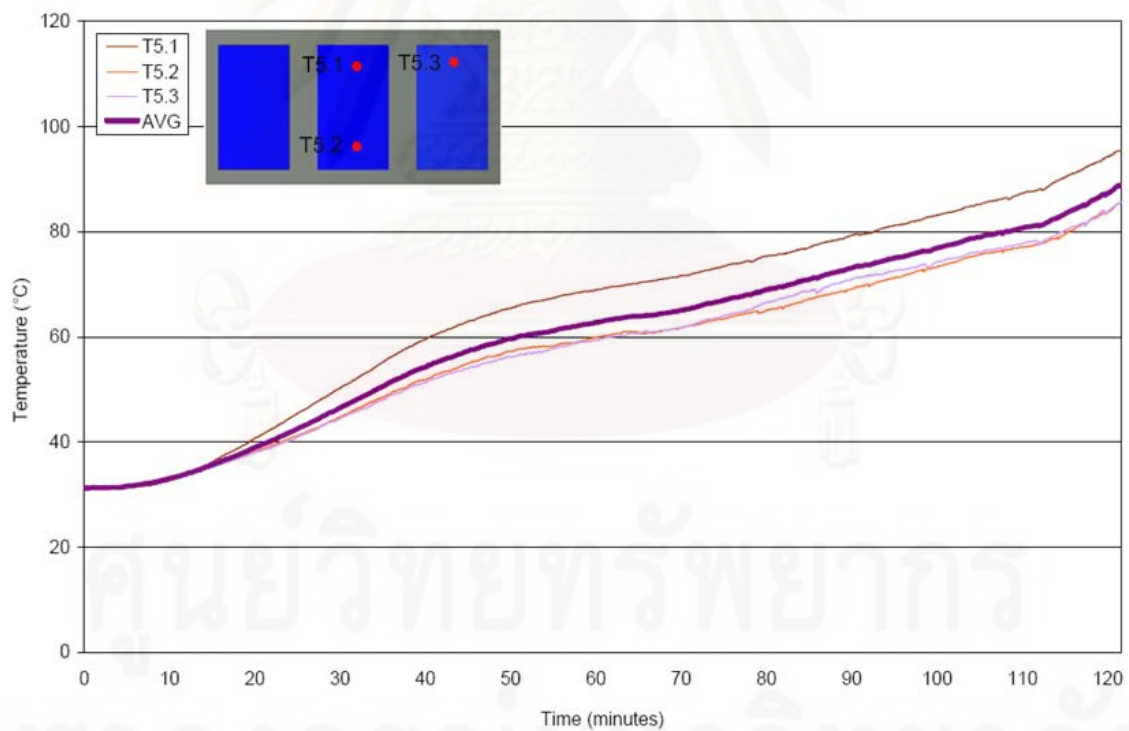


Figure 5.15 Time-temperature relationship at the surface of GFRP (T5) of assembly 3 during the fire test

5.1.6 Thermocouples at level 6

The thermocouples were installed at the bottom (T6.1) and also at the top (T6.2) of the hanging rod. The average temperatures from these thermocouples (T6) on assembly 1, assembly 2 and assembly 3 are illustrated in Figure 5.16, Figure 5.17 and Figure 5.18, respectively. The average temperatures of the steel rods for assemblies 1, 2 and 3 are 502°C, 92°C and 128°C, respectively. All the steel rods had not yielded and were capable of supporting the gypsum board assemblies until the end of the fire tests.

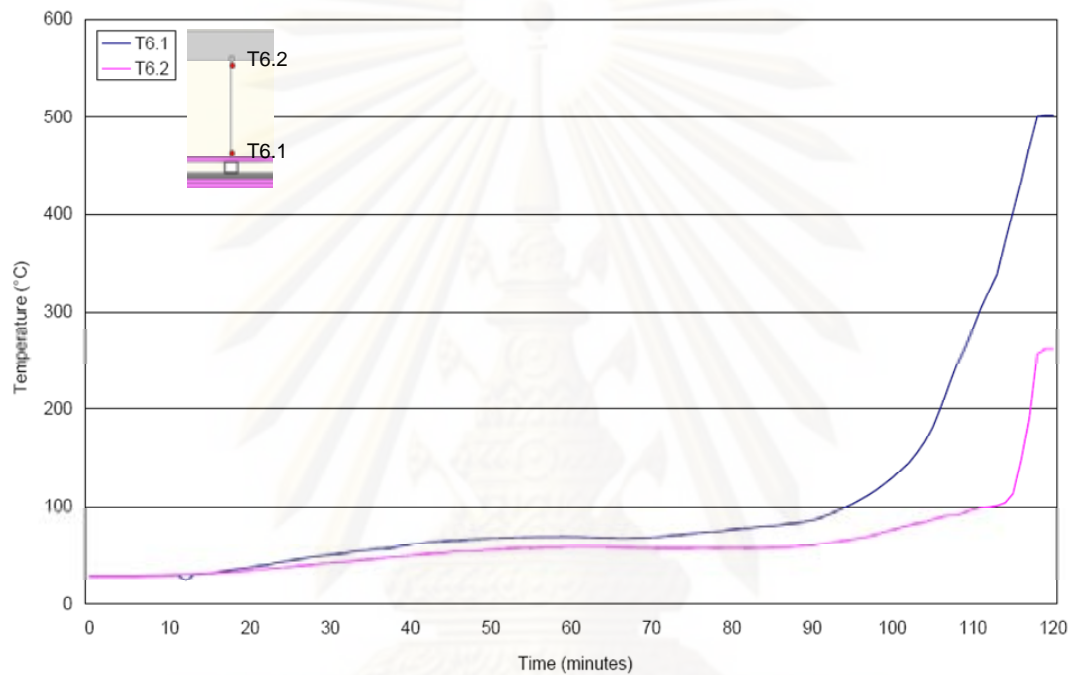


Figure 5.16 Time-temperature relationship at the hanging rod (T6) of assembly 1 during the fire test

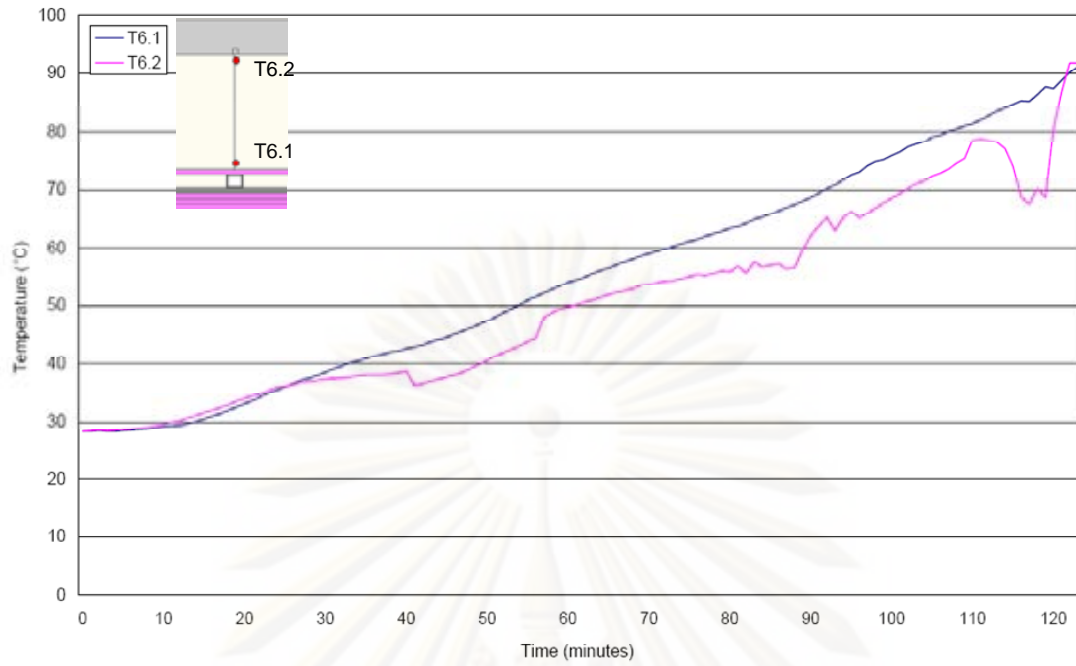


Figure 5.17 Time-temperature relationship at the hanging rod (T6) of assembly 2 during the fire test

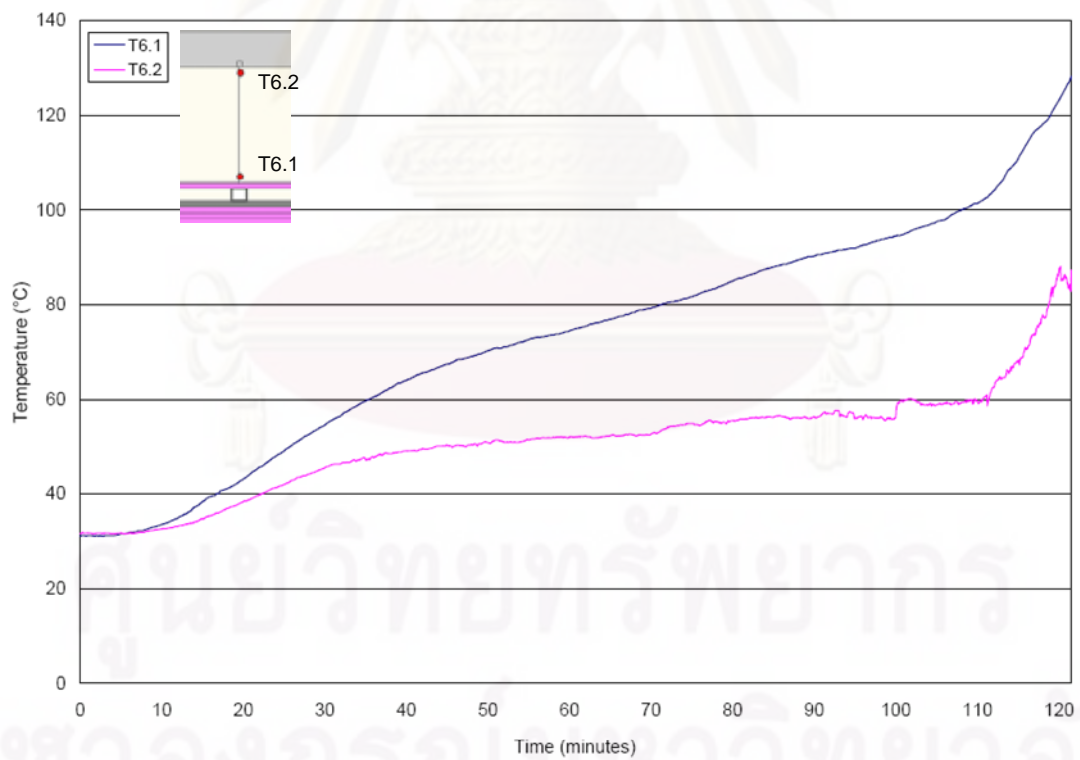


Figure 5.18 Time-temperature relationship at the hanging rod (T6) of assembly 3 during the fire test

5.1.7 Thermocouples at all levels

The average temperatures from thermocouples at level 1, level 2, level 3, level 4, level 5 and level 6 on assembly 1, assembly 2 and assembly 3 are illustrated in Figure 5.19, Figure 5.20 and Figure 5.21, respectively.

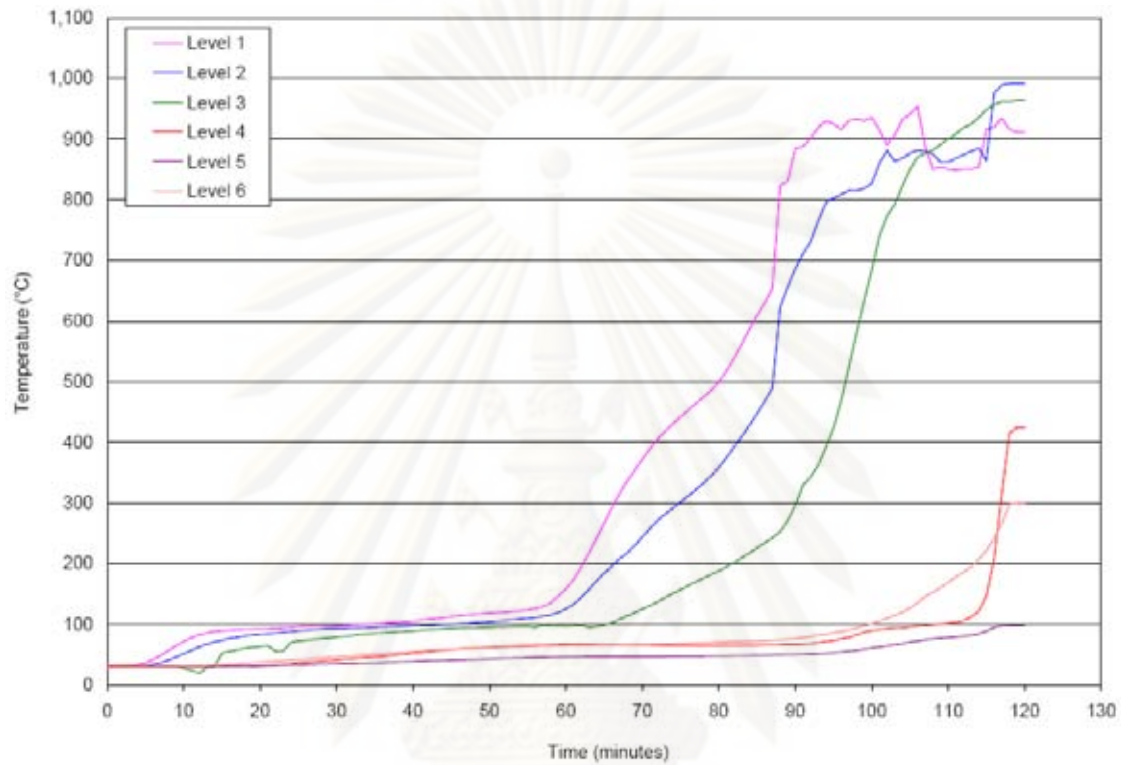


Figure 5.19 Time-temperature relationship at all levels on assembly 1 during the fire test

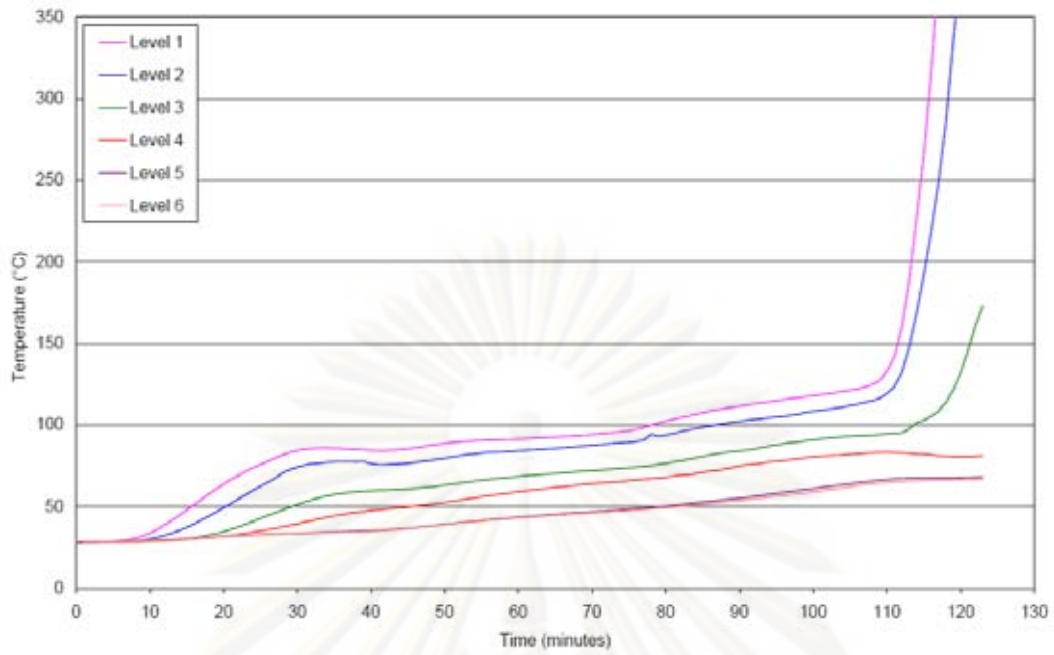


Figure 5.20 Time-temperature relationship at all levels on assembly 2 during the fire test

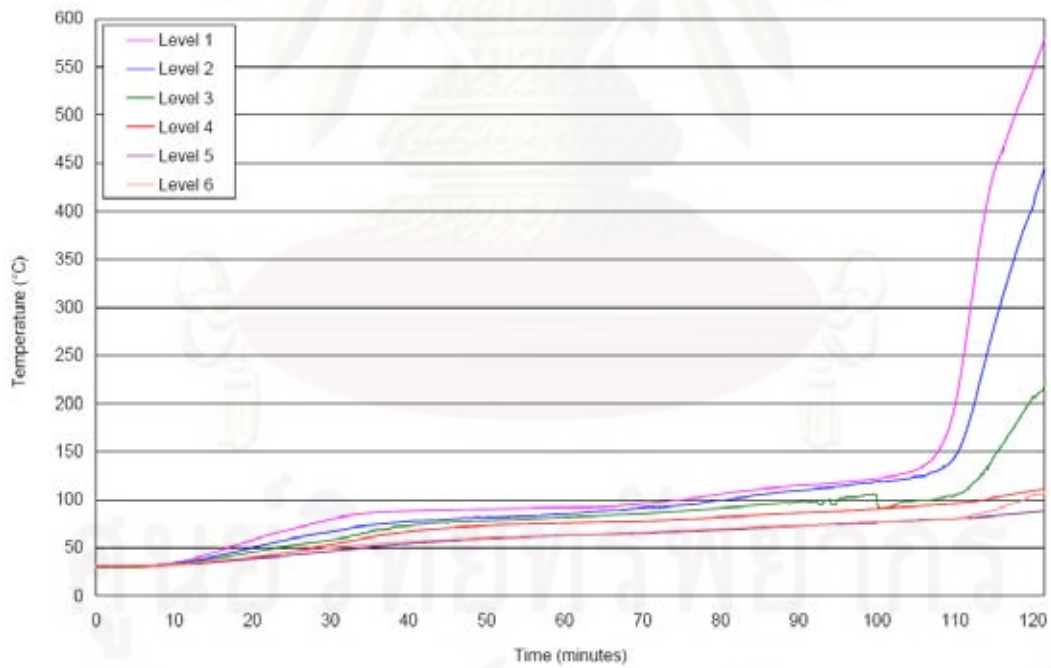


Figure 5.21 Time-temperature relationship at all levels on assembly 3 during the fire test

5.2 Computer Modeling Results

The results from the Abaqus/CAE computational models are presented in this section. The comparison of the experimental results and the Abaqus/CAE computational models are performed in order to check the validity of the computational models to simulate the heat transfer across the gypsum board assemblies. Temperature distributions across the gypsum board assemblies of computational models 1, 2 and 3 at the end of the fire tests are illustrated in Figure 5.22, Figure 5.24, and Figure 5.26, respectively. The comparison of the measured and predicted temperatures during the fire tests for assemblies 1, 2, and 3 are presented in Figure 5.23, Figure 5.25, and Figure 5.27, respectively.

As seen in Figure 5.23, Figure 5.25, and Figure 5.27, the predicted temperatures on the surface of the exposed gypsum board facing cavity (level 1) and on the top of the secondary channel (level 2) are in good agreement with the experimental results until the end of the dehydration phase, which is indicated by the sudden rise of the time-temperature curves. The models predict the end of the dehydration process earlier than the actual process during the fire test.

The average temperatures on the top of the primary channels (level 3) are under-predicted by the computational models. For assembly 1, this is probably due to the inaccurate values of the insulation material properties. As stated previously, the material properties of the insulation material are adopted from previous research works that is assumed to be testing a similar type of insulation material. While for assembly 2 and assembly 3, this is probably caused by the fact that the radiation effect in the cavity is neglected in the computational models.

The predicted temperatures on the unexposed gypsum board surface (level 4) of assembly 1 are in good agreement with the experimental results, until the gypsum board underwent calcination process which occurred at the 110th minute. The predicted temperatures for assembly 2 and assembly 3 are lower than the measured temperatures.

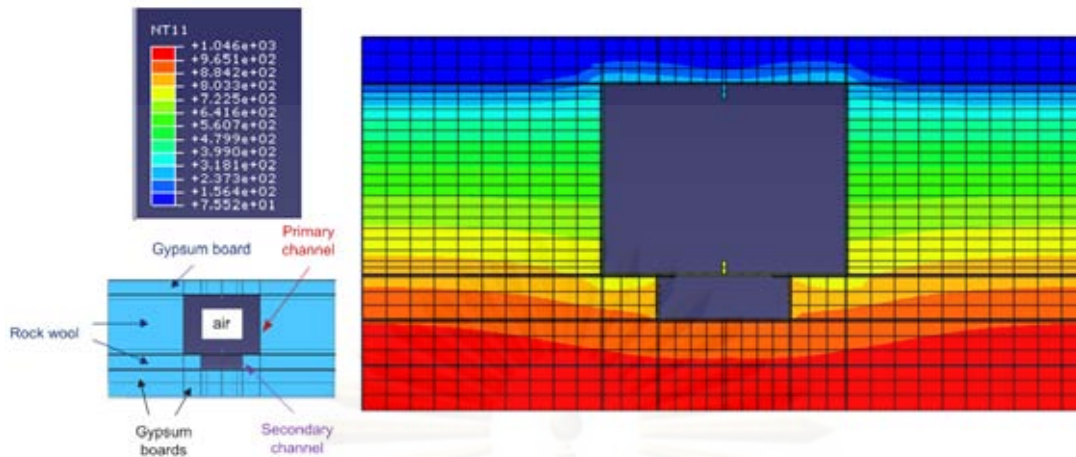


Figure 5.22 Temperature distribution across the gypsum board assembly of computational model 1 at the end of the fire test

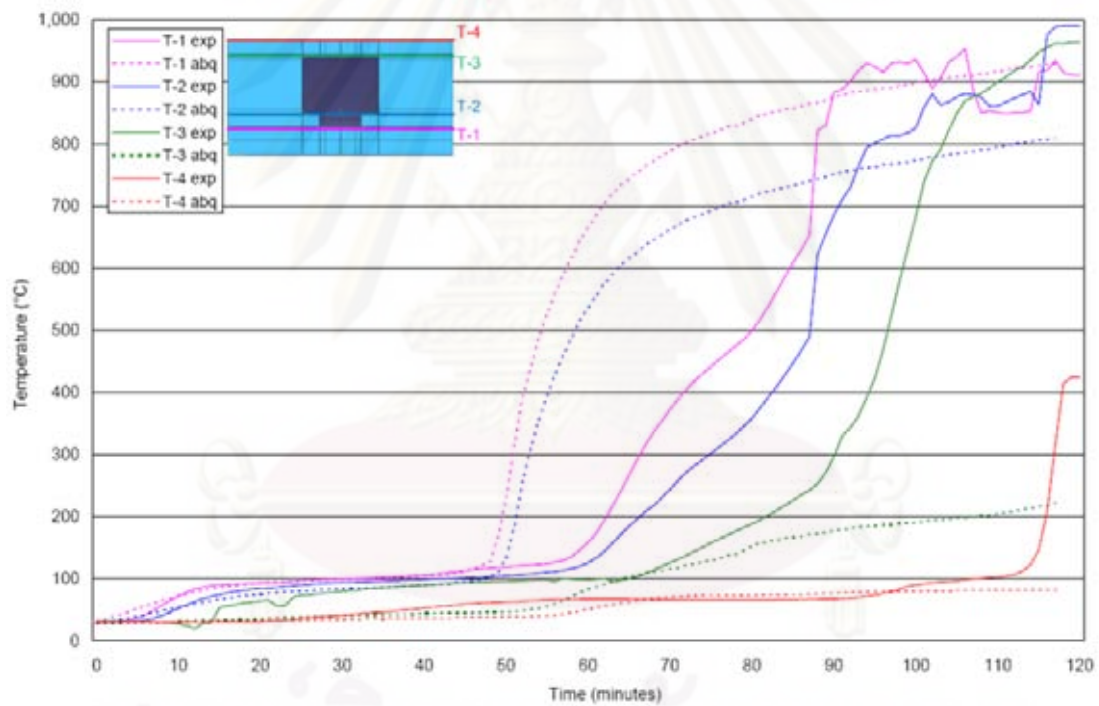


Figure 5.23 Comparison of results from the experiment and the computational model of assembly 1

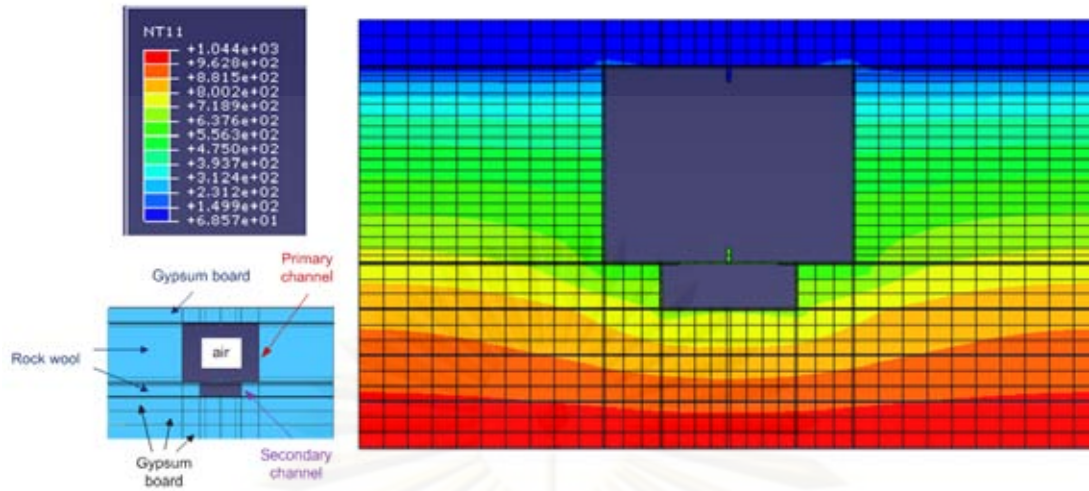


Figure 5.24 Temperature distribution across the gypsum board assembly of computational model 2 at the end of the fire test

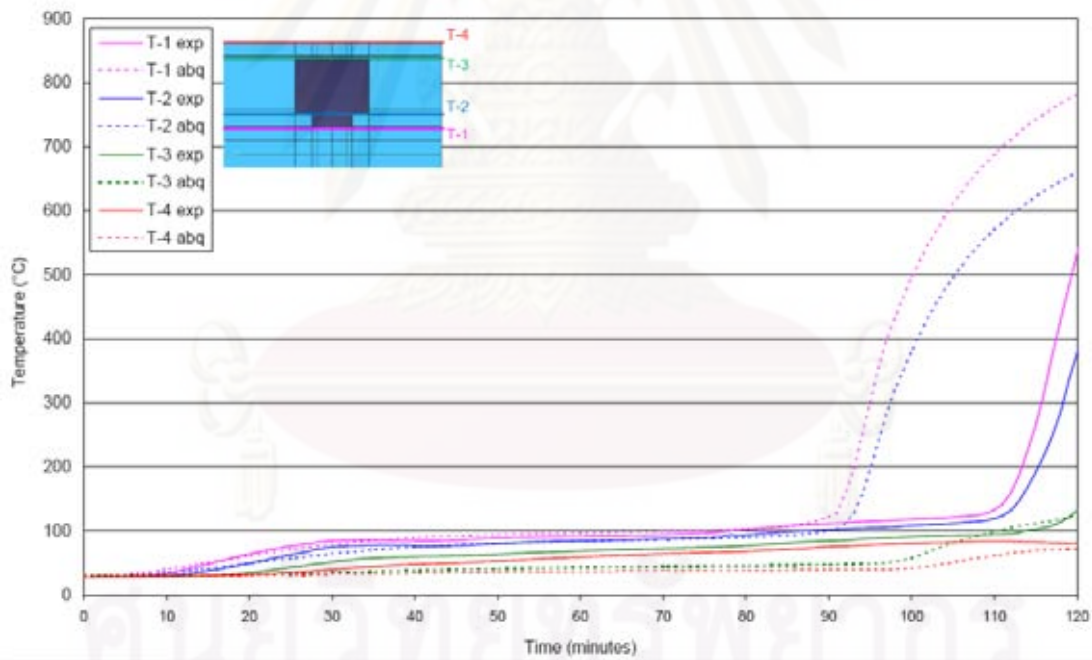


Figure 5.25 Comparison of results from the experiment and the computational model of assembly 2

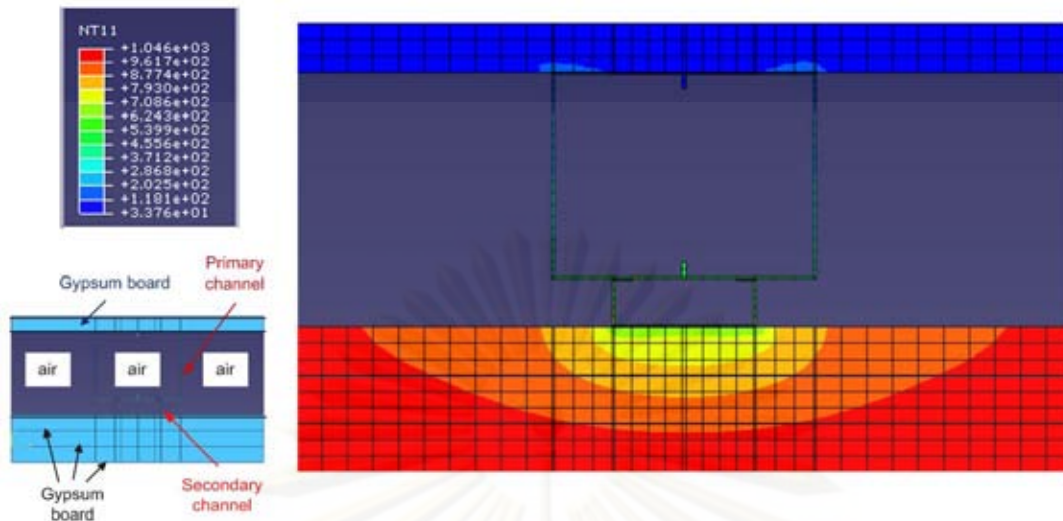


Figure 5.26 Temperature distribution across the gypsum board assembly of computational model 3 at the end of the fire test

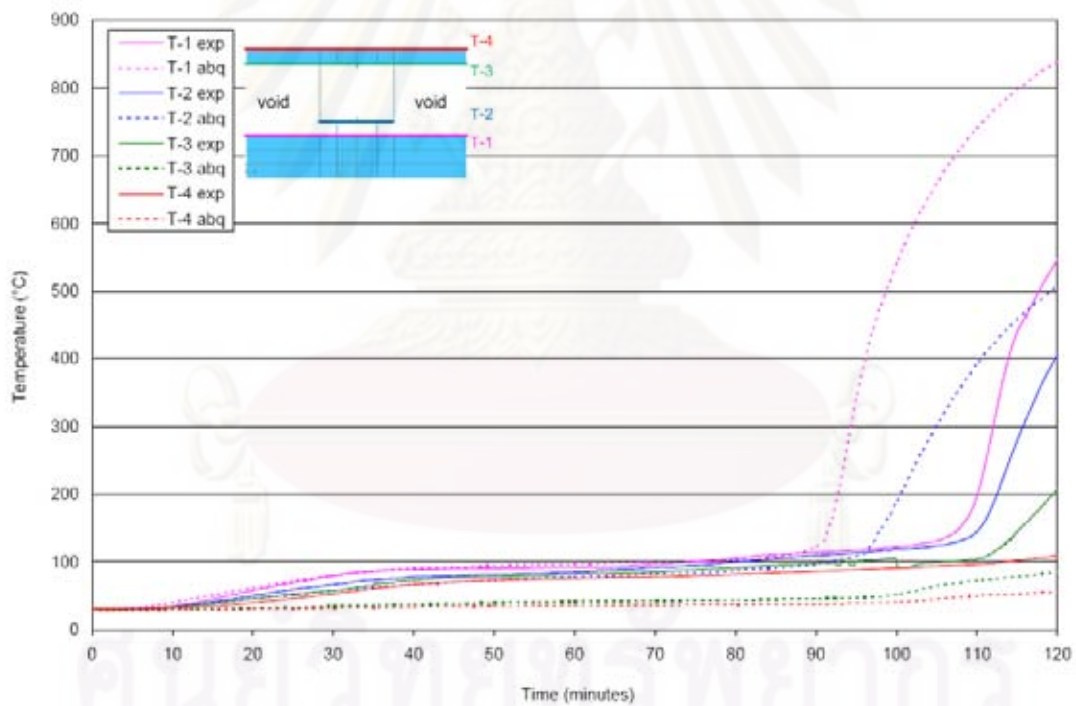


Figure 5.27 Comparison of results from the experiment and the computational model of assembly 3

5.3 Parametric study

5.3.1 Effect of gypsum board conductivity

In most studies, as explained in chapter 3, the thermal conductivity does not appear to vary much between 0°C and 600°C. It was therefore decided to reduce the thermal conductivity at 700°C. Simulations were performed with a 25% reduction and 50% reduction of the thermal conductivity. The comparison of results from the experiment (exp), the computational model of assembly 1 (J1) and either the computational model of assembly 1 using 25% gypsum board conductivity reduction (J2) or using 50% gypsum board conductivity reduction (J3) are illustrated in Figure 5.28 and Figure 5.29, respectively.

From the comparisons shown in Figure 5.28 and Figure 5.29, it can be observed that the reduction of the gypsum board conductivity at 700°C gives better predictions of the time-temperature relationships, especially those at level 1 and level 2. However, because the material properties of the insulation material are still the same, the time-temperature relationships at level 3 and level 4 are still similar to those from the previous computational model.

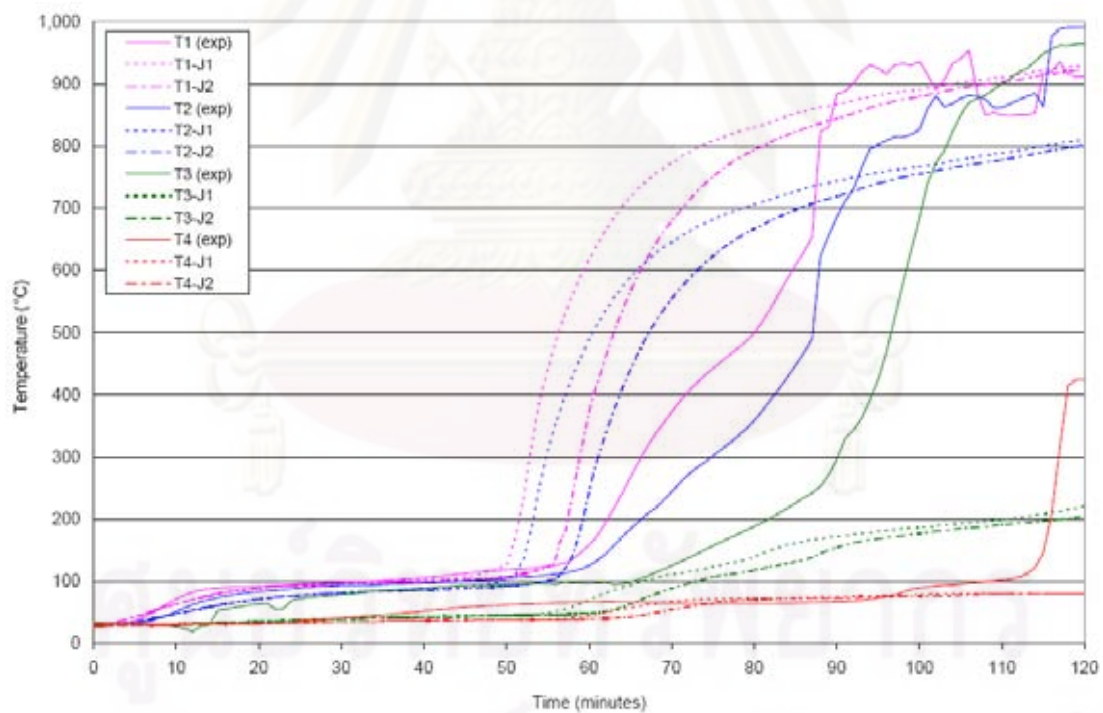


Figure 5.28 Comparison of results from the experiments, the computational model (J1) and computational model-2 (J2) of assembly 1

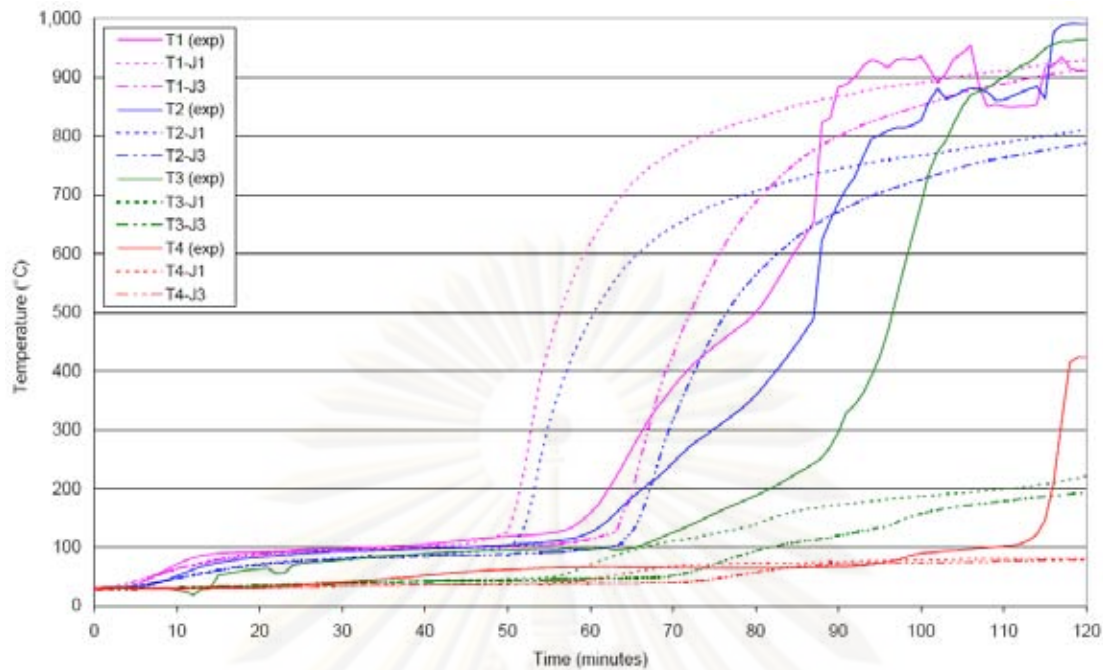


Figure 5.29 Comparison of results from the experiments, the computational model (J1) and computational model-3 (J3) of assembly 1

5.3.2 Effect of convective coefficient

The values of the convective coefficient of the unexposed surface of the gypsum board can vary (Jones 2001). Thus, to investigate the influence of the variation of the convective coefficient of the unexposed surface of the gypsum board two values of convective coefficient, $5 \text{ W/m}^2 \cdot \text{K}$ and $10 \text{ W/m}^2 \cdot \text{K}$, were used in the model. The comparison of results from the computational model using $5 \text{ W/m}^2 \cdot \text{K}$ -convective coefficient (J4) and from the computational model using $10 \text{ W/m}^2 \cdot \text{K}$ -convective coefficient (J3) is illustrated in Figure 5.30. From Figure 5.30, it can be concluded that changing the value of the convective coefficient of the unexposed gypsum board has negligible effect on the predicted temperatures.

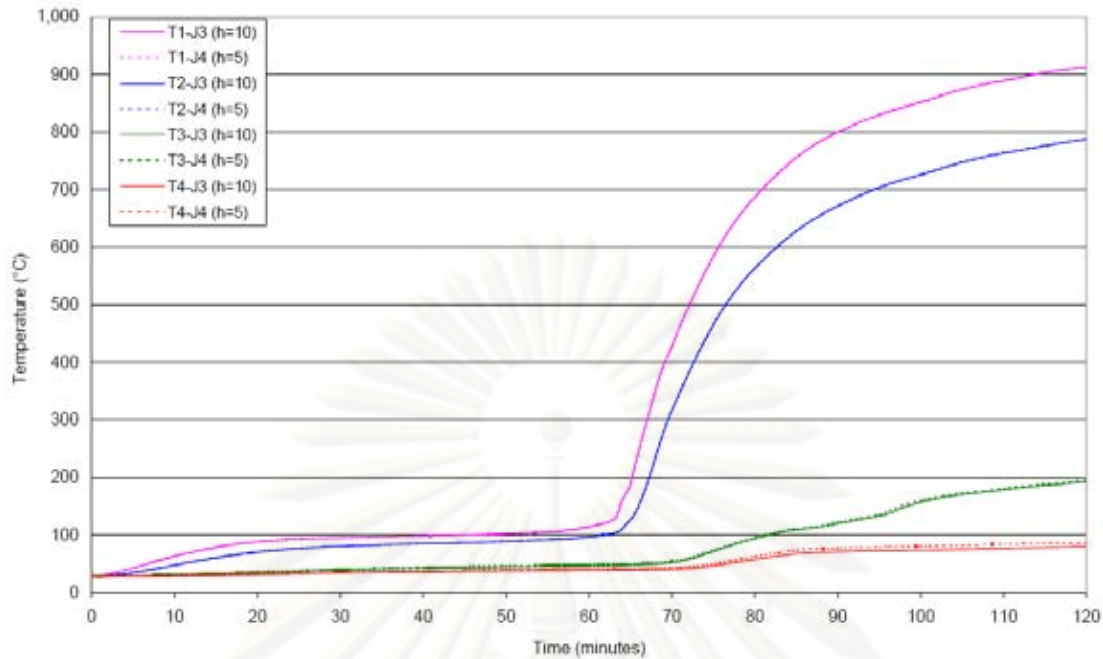


Figure 5.30 Comparison of results from the computational model-3 (J3) vs. the computational model-4 (J4)

5.3.3 Effect of the gap radiation

From Figure 5.25 and Figure 5.27, it can be concluded that the temperatures at level 3 are poorly simulated. This is probably caused by the negligence of the radiation effect on the cavity. In the computational model, the cavity was assumed to be small and was considered as a gap. Abaqus Analysis User's Manual (2008) states that normally in the gap, the heat flux from conduction is much larger than the radiative heat flux. Thus, in the current study it is assumed that gap radiation is being neglected. To investigate the effect of the cavity radiation to the predicted temperatures, another computational model that incorporated gap conduction and gap radiation was built.

According to Abaqus/Standard, the radiation heat transfer between the contact surfaces is defined by

$$q = C \left[(\theta_A - \theta^Z)^4 \right] - \left[(\theta_B - \theta^Z)^4 \right] \quad (5.1)$$

$$C = \frac{F \times \sigma}{\frac{1}{\xi_A} + \frac{1}{\xi_B} - 1} \quad (5.2)$$

where: θ^Z = the absolute zero on the temperature scale used = -273.15°C ,

- θ_A = temperature at the slave's surface,
 θ_B = temperature at the master's surface,
 F = effective view factor,
 σ = Stefan-Boltzmann constant = $5.67 \times 10^{-8} \text{ W m}^{-2} \text{ K}^{-4}$,
 ζ_A = emissivity on the slave's surface, and
 ζ_B = emissivity on the master's surface

According to Lienhard (2008), the view factor for two parallel surfaces can be defined by

$$F = \sqrt{1 + \left(\frac{h}{w}\right)^2} - \left(\frac{h}{w}\right) \quad (5.3)$$

where: h = the distance between the surfaces

w = the width of the surfaces

The comparison of results from the experiment (exp), from the computational model that incorporated gap conduction only (J1) and from the model that incorporated gap conduction and gap radiation (J4) is illustrated in Figure 5.31. From Figure 5.31 it can be concluded that the predicted temperatures from the computational model that incorporated gap conduction and gap radiation (J4) are better than that from the computational model that incorporated gap conduction only (J3). This means that the radiation heat transfer on the cavity of the gypsum board assembly gives significant effect on the temperature distribution of the unexposed gypsum board.

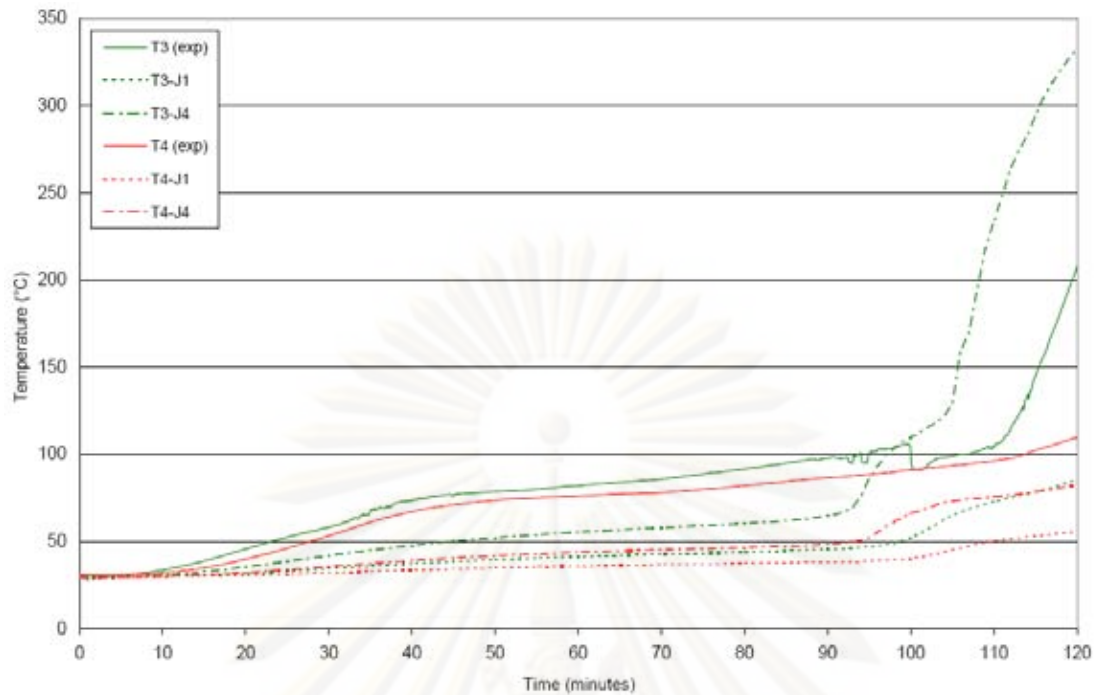


Figure 5.31 Comparison of results from the experiment (exp), from the computational model that incorporated gap conduction only (J1) and from the computational model that incorporated gap conduction and gap radiation (J4)

5.4 Conclusions and Recommendations

This research was carried out to determine the proper configuration of gypsum-board fire insulation systems for FRP that can satisfy a 2-hour fire resistance rating through numerical and experimental studies. To investigate the performance of the gypsum board assemblies in protecting the GFRP strengthened slab exposed to fire, three furnace tests were carried out. The strengthening system was installed using the wet-lay-up method to attach the GFRP sheets on the soffits of the concrete slab. Three gypsum board assemblies, including 2 x 1 assembly with rock wool installed at the cavity and 3 x 1 assembly with and without rock wool installed within the cavity, were used as the fire protection systems. Visual observations were performed at the end of the fire tests, after the specimens cooled down for 24 hours.

Using the temperature at the epoxy adhesive of the FRP strengthening system as the failure criterion ($T < 70^{\circ}\text{C}$), the fire resistance ratings for assembly 1, assembly 2, and assembly 3 were 104 minutes, 120 minutes and 83 minutes, respectively. However, since there were some errors regarding the furnace control during testing of assembly 2 the fire resistance rating of this assembly was not conclusive. Even though the gypsum board assemblies could not satisfy the designated 2-hour fire resistance rating, these assemblies gave better performance in protecting the FRP strengthening systems compared to the other fire protection systems used in the previous studies. The gypsum board assembly showed great performance in

protecting the FRP strengthening system and is possible in providing the 2-hour fire resistance rating when properly designed.

The average temperatures at level 5 for assembly 1, assembly 2 and assembly 3 at the end of fire tests were 99°C, 68°C and 89°C. Even though these temperatures were higher than the specified T_g that was used as the failure criterion in this study ($T_g=70^\circ\text{C}$), based on the visual observation at the end of the fire tests the FRP strengthening systems did not show any delamination behaviour. This indicates that the type of epoxy used in the current study may have higher glass transition temperature (T_g) than that used in the previous studies. Further testing needs to be done to determine the value of T_g of the epoxy adhesive used in this study.

Since delamination had not occurred, it is reasonable to assume that the FRP strengthening systems were still effective during the 2-hour testing period. However, further studies need to be done to determine whether the effectiveness of the FRP strengthening systems is directly related with the delamination of the systems.

From the experimental results, it is noticed that the behaviour of gypsum board assembly 1 is similar to that of assembly 3 in terms of the ultimate temperatures at the end of the fire tests. However, from Figure 5.13 and 5.15 it can be seen that the temperatures at the surface of the FRP strengthening system (level 5) for assembly 1 were lower than those for assembly 3 until the 110th minute during which the unexposed gypsum board and the insulation material on assembly 1 was presumed to have fallen-off (since visual observation was not possible during the test). Thus, it can be concluded that assembly 1 performed better in restraining the temperature at the surface of the FRP strengthening system below T_g compared to assembly 3. Based on these results, installing insulation material within the cavity of the gypsum board assembly is likely to increase its fire resistance rating as long as the insulation material remains in place. Based on this conclusion it is reasonable to state that if there was no equipment malfunction during the fire test of assembly 2, the assembly would have the best fire rating.

From the visual observation at the end of the fire test for assembly 1, it can be seen that some of the insulation materials that were still intact are those connected to the secondary channels. Securing the insulation materials on the secondary channels might also increase the performance of the gypsum board assembly. However, further studies need to be done to investigate the effect of installing the rock wool in the cavity and also adding the number of gypsum board layers on the fire resistance rating of the gypsum board assembly.

Heat transfer modeling using a commercially available finite element computer program, Abaqus/CAE, was carried out to predict the time-temperature history within the gypsum board assemblies. The experimental results are used to validate the Abaqus/CAE computational models. Three computational models were constructed to simulate the temperature distribution of the three tested specimens. The

predicted temperatures from the computational models are in good agreement with the experimental results, except for temperatures at the top of the primary channel and the cavity (level 3). This could be due to the inaccurate values of the rock wool material properties or due to the negligence of the gap radiation effect within the cavity of the gypsum board assembly. Including the gap radiation effect in the computational model gave better results. The parametric study on the gypsum board conductivity showed that choosing the correct thermal properties of the building materials is important in order to develop an accurate heat transfer model. When direct laboratory testing for determining the thermal properties of materials is not possible, the thermal properties based on the previous works could be adopted instead. By manipulating the thermal properties of these materials, the predicted time-temperature history within the gypsum board assembly can be done with reasonable accuracy.

The simulation studies reported in this thesis assume that there is no integrity failure of the gypsum board assemblies. The moisture movement, ablation and shrinkage within the gypsum board assembly during the fire test were not considered in this study. Even though heat transfer within the gypsum board assembly is highly dependent on the moisture content of the material, modeling the moisture movement across the assembly is a complex problem. Thus this phenomenon is generally neglected due to its complexity (Jones 2001). The ablation is the process when consecutive thin layers of gypsum shed from the lining, reducing the cross-sectional thickness of the gypsum board and therefore increasing the heat flux across the assembly. Abaqus/CAE does not allow the user to remove elements from the section to simulate ablation. Shrinkage makes the dimension of the material to alter. Abaqus/CAE does not allow the user to modify the dimensions of elements during calculation. Further research of these phenomena and their influences on computational results are recommended.

REFERENCES

- ACI Committee 216. **Guide for Determining the Fire Endurance of Concrete Elements**. Farmington Hills, Michigan: American Concrete Institute (ACI), 2006.
- ACI Committee 318. **Building Code Requirements for Structural Concrete**. Farmington Hills, Michigan: American Concrete Institute (ACI), 2005.
- ACI Committee 440. **ACI 440.2R-02 Guide for the design and construction of externally bonded FRP systems for strengthening concrete structures**. Farmington Hills, Michigan: American Concrete Institute (ACI), 2002.
- ACI Committee 440. **ACI 440.XR-07 Report on fiber-reinforced polymer (FRP) reinforcement for concrete structures**. Farmington Hills, Michigan: American Concrete Institute (ACI), 2007.
- Aguiar, J. B et al. Effect of temperature on RC elements strengthened with CFRP. **Materials and Structures**. (2007): 1–10.
- Alfawakhiri, F et al. Fire resistance of loadbearing steel-stud walls protected with gypsum board: A review. **Fire Technology** 35 (1999): 308-335.
- Alfawakhiri, F., and Sultan, M. A. Fire resistance of loadbearing LSF assemblies. **The 15th International Specialty Conference on Cold Formed Steel Structures: Proceedings of the conference**. St. Louis, MO: National Research Council of Canada, 2000.
- Al-Salloum, Y. A., and Almusallam, T. H. Rehabilitation of the infrastructure using composite materials: Overview and applications. **Journal of King Saud University, Engineering Sciences** 16 (2002): 1-13.
- Anders Carolin. **Carbon fibre reinforced polymers for strengthening of structural elements**. Doctoral Thesis, Department of Civil and Mining Engineering, Division of Structural Engineering, Lulea University of Technology, 2003.
- Ang, C. N., and Wang, Y. C. The effect of water movement on specific heat of gypsum plasterboard in heat transfer analysis under natural fire exposure. **Construction and Building Materials** 18 (2004): 505-515.
- Barnes, R., and Fidell, J. Performance in fire of small-scale CFRP strengthened concrete beams. **Journal of Composites for Construction** (November /December 2006):503-508.
- Benichou, N et al. **Thermal properties of wood, gypsum and insulation at elevated temperatures**. Internal report, Institute for Research in Construction, Fire Risk Management Program, National Research Council of Canada, 2001.

- Benichou, N., and Sultan, M. A. Fire resistance behaviour of lightweight-framed construction. **Structures in Fire: Proceedings of the 3rd International Workshop**, pp. 119-136. Ottawa: National Research Council of Canada, 2004.
- Benjeddou, O et al. Damaged RC beams repaired by bonding of CFRP laminates. **Construction and Building Materials** (2006): 1-11.
- Bevan H Jones. **Performance of gypsum plasterboard assemblies exposed to real building fires**. Master's Thesis. Department of Civil Engineering, University of Canterbury, 2001.
- Blontrock, H. Analyse en modellering van de brandweerstand van betonelementen uitwendig versterkt met opgelijmde composietlaminaten. In Klammer, E. L et al. The influence of temperature on RC beams strengthened with externally bonded CFRP reinforcement. **HERON Journal** 53 (2008).
- Blontrock, H et al. Fire testing of concrete slabs strengthened with fibre composite laminates. **Fiber Reinforced Polymer Reinforcement for Concrete Structures (FRPRCS-5) Symposium: Proceedings of the symposium**. London: Thomas Telford Ltd., 2001: 1-15.
- Buchanan, A. H. **Structural Design for Fire Safety**. New York: John Wiley & Sons, Ltd., 2001.
- Chowdhury, E. U et al. Investigation of insulated FRP-wrapped reinforced concrete columns in fire. **Fire Safety Journal** 42 (2007): 452-460.
- Committee of European Standardization (CEN) ENV 1993-1-2, **Eurocode 3; Design of steel structures, Part 1.2: General rules - Structural fire design**. 1995.
- Cooper, L. Y. **The thermal response of gypsum-panel/steel stud wall systems exposed to fire environments - A simulation for use in zone-type fire models**. Gaithersburg, MD: National Institute of Standards and Technology, 1997.
- Deuring, M. **Brandversuche an nachtraglich verstärkten tragern aus beton**. Research Report EMPA, Swiss Federal Laboratories for Material Testing and Research, 1994.
- Elewini, E et al. Gypsum board fall-off in floor assemblies exposed to a standard fire. **Fire and Materials, 10th International Conference: Proceedings of the conference**, pp. 1-15. San Francisco: National Research Council of Canada, 2007.
- Enochsson, O et al. CFRP strengthened openings in two-way concrete slabs-An experimental and numerical study. **Construction and Building Materials** 21 (2007): 810-826.

- Feng, M et al. Thermal performance of cold-formed thin-walled steel panel systems in fire. **Fire Safety Journal** 38 (2003): 365-394.
- Gamage, J. C. P. H et al. Performance of CFRP strengthened concrete members under elevated temperatures. **Proceedings of the International Symposium on Bond Behaviour of FRP in Structures (BBFS)**. Hongkong: International Institute for FRP in Construction, 2005.
- Gamage, J. C. P. H et al. Bond characteristics of CFRP plated concrete members under elevated temperatures. **Composite Structures** 75 (2006): 199-205.
- Hibbitt, Karlsson & Sorensen, Inc. **Abaqus/CAE User's Manual Version 6.8**. Providence: Hibbitt, Karlsson & Sorensen, Inc., 2008.
- Hibbitt, Karlsson & Sorensen, Inc. **Abaqus Analysis User's Manual Version 6.8**. Providence: Hibbitt, Karlsson & Sorensen, Inc., 2008.
- Hibbitt, Karlsson & Sorensen, Inc. **Abaqus Theory Manual Version 6.8**. Providence: Hibbitt, Karlsson & Sorensen, Inc., 2008.
- Hollaway, L. C., and Leeming, M. B. 1999. **Review of materials and techniques for plate bonding: Strengthening of reinforced concrete structures using externally-bonded FRP composites in structural and civil engineering**, edited by L. C. Hollaway and M. B. Leeming. Woodhead Publishing, Cambridge, UK.
- Hollaway, L. C., and Leeming, M. B. **Strengthening of reinforced concrete structures-using externally-bonded FRP composites in structural and civil engineering**. 2nded. Florida: CRC Press LLC, 2001.
- Hutchinson, A. Strengthening of existing concrete structures using fibre-reinforced composites. **Construction and Building Research Conference (COBRA): Proceedings of the conference**. Oxford: Oxford Brookes University, 1998.
- ISO 834. **Fire Resistance Tests – Elements of Building Construction**. Switzerland: International Organization for Standardization, 2002.
- J. T. Hans Gerlich. **Design of loadbearing light steel frame walls for fire resistance**. Master's Thesis, School of Engineering, University of Canterbury, 1995.
- Kachlakev, D., and McCurry, D. D. Behaviour of full-scale reinforced concrete beams retrofitted for shear and flexural with FRP laminates. **Composites: Part B** 31 (2000): 445-452.
- Kah Yong Tan. **Evaluation of externally bonded CFRP systems for the strengthening of RC slabs**. Master's Thesis, Center of Infrastructure Engineering Studies, Graduate School, University of Missouri-Rolla, 2003.

- Kexu, H. U et al. Experimental study on fire protection methods of reinforced concrete beams strengthened with carbon fire reinforced polymer. **Front. Archit. Civ. Eng. China** 1(4) (2007): 399-404.
- Klamer, E. L et al. The influence of temperature on RC beams strengthened with externally bonded CFRP reinforcement. **HERON Journal** 53 (2008).
- Kodur, V. K. R et al. Preliminary guidance for the design of FRP-strengthened concrete members exposed to fire. **Journal of Fire Protection Engineering** 17 (2007): 5-26.
- Leone, M et al. Effect of elevated service temperature on bond between FRP EBR systems and concrete. **Composites: Part B** 40 (2009): 85-93.
- Lienhard IV, J. H., and Lienhard V, J. H. **A Heat Transfer Textbook**. Cambridge, Massachusetts: Phlogiston Press, 2008.
- Liu, G. R., and Quek, S. S. **The Finite Element Method A Practical Course**. Burlington MA: Butterworth Heinemann, 2003.
- Mosallam, A. S., and Mosalam, K. M. Strengthening of two-way concrete slabs with FRP composite laminates. **Construction and Building Materials** 17 (2003): 43-54.
- Rahmanian, I., and Wang, Y. Thermal conductivity of gypsum at high temperatures: A combined experimental and numerical approach. **Acta Polytechnica** 49 (2009): 16-20.
- Sakumoto, Y et al. Fire resistance of walls and floors using light-gauge steel shapes. **Journal of Structural Engineering** (November 2003): 1522-1530.
- Sharp, M et al. Modeling the performance of non-loadbearing gypsum-protected steel-stud walls in furnace and room fire tests. **Proceedings of the Fifth International Conference on Structures in Fire (SiF)**, pp. 313-323 Singapore, 2008.
- Stratford, T. J et al. Bonded fibre reinforced polymer strengthening in a real fire. **Advances in Structural Engineering** 23 (2009): 867-878.
- Sultan, M. A. A model for predicting heat transfer through noninsulated unloaded steel-stud gypsum board wall assemblies exposed to fire. **Fire Technology Third Quarter** (1996): 239-259.
- Sultan, M. A., and Benichou, N. Fire resistance performance of lightweight floor assemblies. **Designing Structures for Fire Conference: Proceedings of the conference**, pp. 203-214. Baltimore, MD: National Research Council of Canada, 2003.

- Sultan, M. A., and Kodur, V. R. Light-weight frame wall assemblies: Parameters for consideration in fire resistance performance-based design. **Fire Technology** 36 (2000): 75-88.
- Tang, B. Fiber reinforced polymer composites application in USA. **The First Korea/U.S.A. Road Workshop Proceedings**. Washington, DC: Federal Highway Administration, 1997.
- Thailand's Ministry of Interior. **Thailand's Ministry of Interior Regulations** [Online]. (2006). Available from: <http://www.dpt.go.th/law/sublaw.html> [17 November 2008]
- Thomas, G. Thermal properties of gypsum plasterboard at high temperatures. **Fire Mater** 26 (2002): 37-45.
- Williams, B et al. Fire insulation schemes for FRP-strengthened concrete slabs. **Composites: Part A** 37 (2006): 1151-1160.
- Wakili, G. K et al. Gypsum board in fire-Modeling and experimental validation. **Journal of Fire Sciences** 25 (2007): 267-282.

BIOGRAPHY

Frieska Evita Ayurananda was born in Pati, a city in Central Java province, Indonesia on August 13th 1983. She was raised in Pati and graduated from SMU N 1 Pati in 2001. She moved to Jogjakarta in order to study at the Department of Civil Engineering, University of Gadjah Mada (UGM). She earned her Bachelor of Engineering's degree with cum laude in 2006.

She was awarded a scholarship from AUN/SEED-Net JICA to continue her study in master's degree program in the Civil Engineering Department at Chulalongkorn University, Thailand in 2006. Her research interests are in the usage of new materials, especially fiber reinforced polymer (FRP) in civil engineering field and also in the safety of the structures. She conducted her studies under the directions of Assoc. Prof. Thanyawat Pothisiri, Ph.D. and completed her master's studies in the second semester of 2009.

In 2009 she was presented her paper at The 1st ASEAN Civil Engineering Conference which was held in Pattaya, Thailand. The title of her paper was Finite Element Analysis of Gypsum-Board Fire Insulation Systems for Fiber Reinforced Polymer.

Publication:

T. Pothisiri and F.E. Ayurananda. Finite Element Analysis of Gypsum-Board Fire Insulation Systems for Fiber Reinforced Polymer. *The 1st ASEAN Civil Engineering Conference*. 12th – 13th of March 2009, Pattaya, Thailand.